Pre-breakdown electrical conductivity of nearly saturated mercury vapour at medium pressures

Ozveren, Guneyt Suheyl

PRE-BREAKDOWN ELECTRICAL CONDUCTIVITY of NEARLY SATURATED MERCURY VAPOUR at MEDIUM PRESSURES

by

Cuneyt Suheyl Ozveren

Thesis submitted for the Degree of Doctor of Philosophy in the Faculty of Science
University of Durham

May, 1981

SEVGILI ANNEME VE BABAMA

(to my dear Mother and Father)

and

To the beloved memory of M.K. Atatürk founder of modern Turkey for his belief in future generations and dedication to science; thus for a better understanding between our peoples.

ABSTRACT

Comprehensive measurements of the electrical conductivity of nearly saturated mercury vapour at medium pressures prior to the transition to glow discharge are shown to fit an analytical formula. The electrical conductivity exhibits an exponentially growing curve with values of electrical conductivity many orders of magnitude higher than the theoretically observed values. The electrical conductivity depends predominantly on the discharge pressure near saturation, but changes over to dependence mainly on discharge temperature as the degree of saturation is decreased. This behaviour is radically different from that which could be predicted from any known analysis, for example; Saha's thermal equilibrium analysis, and is thought to be a new phenomenon.

The literature on arc discharges in general and vapour arc cathode mechanisms in particular is extensively reviewed. Possible approaches to a model to account for the present measurements are discussed and proposals for future work, with the hindsight derived from the experience of the present investigations, are suggested. Similar behaviour has been observed in caesium vapour under similar conditions, and if the same effect is observed in other metallic vapours, such as copper and sodium, it will lead to an improved understanding of the phenomena taking place in industrial cold cathode discharges and arcs, which have been observed for many years and through many investigations without satisfactory explanation.

ACKNOWLEDGEMENTS

This thesis has been the outcome of the help of so many people, who have unreservedly extended their help, support and friendship in so many ways and in such numbers that the list seems endless.

With that in mind I would like to start thanking by expressing my infinite thanks and gratitude to Dr. V.G. Endean, for his invaluable guidance and supervision throughout this work, without his understanding, ever ready help and during patience this thesis would of course not have been realised. My thanks are also due to Dr. C. Christopoulos, for his kind encouragement in the beginning of this research, to Dr. E.C. Salthouse for always willi ng to help whenever a problem arose, to Professor G.R. Higginson for extended use of departmental facilities. To Mr. J. Peakin for his friendship and many hours of pleasurable discussion. To all involved in the construction of the experiments, especially to Mr. J. Greensmith to T. Nancarrow, P. Jackson and M. Fleetham. My thanks also to the Chief Technician Mr. C. Campbell.

I can never express in enough words my thanks to my family who have done everything in their power and more to encourage and support me, during these long years.

My thanks to the engineering department as a whole; to the English people in general, and to the people of the North in particular for making my stay a very pleasant one indeed. My thanks also to Lesley for her typing.

Lastly but not in the least to Maureen for her love and faith.

CONTENTS

LIST OF SYMBOLS

A	constant
A	Cross-sectional area (page 90)
α	Townsend's coefficient
$\int_o^d \alpha dx$	$\bar{\alpha} d_c$
b	static viscosity coefficient
C_1	
C_2	CONSTANTS
C_3	
C_r	heat capacity per unit mass
D_a	Ambipolar Diffusion Coefficient
D_i	Diffusion Coefficient for ions
D_e	Diffusion Coefficient for electrons
d	average distance between particles
d_c	cathode fall length
$d\ell$	differential length
E	Electric field
E_c	Electric field at the cathode surface
e	electron charge
F	Force
$g_{(...)}$	Statistical weight of species (...)
γ	secondary electron emission coefficient (by ions) (Townsend's)
h	Planck's constant
I	current
I.C	integration constant
j_c	current density at the cathode
j_e	electron current density

j_i	ion current density
j_s	Saturation Current density
K	Thermal Conductivity
k	Boltzmann's Constant
λ	mean free path
λ_i	ion mean free path
λ_e	electron mean free path
m	mass
m_e	mass of electrons
m_i	mass of ions
μ	mobility
μ_e	electron mobility
μ_i	ion mobility
N_A	Avorgadro's number
n_o	plasma number density
n_F	Fermi-level number density
n_a	neutral number density
n_d	number of droplets/unit volume
n_e	electron number density
n_i	ion number density
$(...)^n$	n is the power index
p	pressure
p_r	radiated power density
$Q(V_{th})$	momentum cross-section
q	degree of ionization
q_{cr}	collision cross-section
q_{cri}	collision cross-section for ions
q_e	negative charge
q_i	positive charge
φ	work function

R	radius
r	radius
r_d	droplet radius
ρ_e	negative charge density (electron)
ρ_i	positive charge density (ion)
Δr	infinitesimal change in the radial axis
s	surface area (Chapter I)
s	heat transfer function (Chapter II)
σ	electrical conductivity
σ_2	conductivity of mercury at critical point
T	temperature
T_L	liquid reservoir temperature
T_g	gas (vapour temperature)
T_o	constant
T_w	Temperature at the discharge walls
ΔT_g	Infinitesimal change in gas temperature
ξ	average time between collisions
$U(T)$	Parti tion function for atoms
$U^1(T)$	Parti tion function for ions
V	Voltage (Potential Difference)
VI	Voltage/Current Characteristics
V_a	Potential across the anode region
V_{ap}	Apparent Ionization Potential
V_c	Cathode fall potential
V_{evap}	Evaporation potential
V_o	Molar Volume
V_p	Voltage drop over the positive column
V_s	Volta ge drop across sheath
V_{th}	thermal velocity
v_c	electron velocity (drift)

v_i	ion velocity (drift)
v_{ir}	average random velocity of the ions
v_o	molecular volume

Symbols used with meanings other than as listed here have been so indicated in the text.

LIST OF FIGURES

CHAPTER ONE

1. INTRODUCTION

1.1 Electrical Discharges

1.2 Voltage Current Characteristics

1.3 The Glow Discharge

1.4 Electrical Arc Formation

1. INTRODUCTION

In its everyday use, a gas in its normal state is almost a perfect insulator. Recent developments in the technology of high voltage apparatus and installations of gaseous conductors, and the ever more pressing need for more powerful, efficient and reliable circuit breakers for power transmission (especially in d.c. power transmission) have created an immense interest in the transition of a gas from an insulating state to a conducting state.

1.1 Electrical Discharges.

When given conditions are so set that sufficient ionization has taken place; that is, when the number density of charged particles throughout the volume of the gas is brought up to a sufficient level, significant currents ranging from pico-amperes to mega-amperes can be made to pass through the gas by externally applied electric fields; either by using electrodes or via remote conductors, as in the case of high frequency, low pressure discharges. The gas is then said to be in its 'conducting' state, and is generally described as an electrical discharge.

The transition from an insulating state to a conducting state is called the 'electrical breakdown' of the gas. However one must approach the definition of electrical breakdown with caution because of the different criteria used for different discharge conditions. Although term plasma was originally introduced by I. Langmuir (1928), ref (1), to describe the state in the positive column of an electrical discharge, today it is universally applied to 'ionized gases'.

There are several types of electrical discharge. However they are all characterised by the presence of free charged particles in an electric field. An electrical discharge is usually started as a

result of particle collisions with initially present electrons, produced by external sources of ionization and excitation. The collisions create new ions and electrons until a maintenance mechanism which is sufficient for the discharge to become self-sustaining, sets in.

Charges can be produced either in the volume of the gas or at the surfaces of the electrodes and electric fields can be applied externally using electrodes located either inside or outside the discharge container. Charges produced by external sources such as heat, electromagnetic radiation or particle radiation can then multiply in the applied electric field and the current density increases as a result.

When production of free charged particles by an internal mechanism of some description becomes dominant over the production of free charged particles by external sources of ionization and excitation, then the discharge is said to be 'self-sustaining'. Non-self-sustaining discharges have no established internal charge production mechanisms and hence cannot exist without external sources of ionization and excitation. The pressure of the discharge gas is also a significant factor in electrical discharges and can alter the characteristics of the discharge considerably.

Since the electric arc represents one of the most important applications of electrical discharges in industry, extensive studies and investigations have been conducted into it. Nevertheless, most of our knowledge of arcs is still empirical and inconclusive. The definition of the electric arc presents a problem in itself, since the term has been used to describe several electrical discharges which look similar but lack a common mechanism. Hence, in the next section, without discussing specific mechanisms, an outline of gas discharges will be given and electrical discharges will be defined only in terms of their current and voltage characteristics. In the following sections it is shown that there must be a clear transition from the physical processes governing

dark and glow discharges to a new set of processes as the discharge passes into the electrical arc mode.

1.2 Voltage Current Characteristics

During the transition of a discharge from a non-conducting state to a highly conducting state, three distinct phases with different optical and electrical characteristics can be observed. These phases are called after their visual characteristics namely the dark, (because Townsend was the first to study such discharges, they are often called Townsend discharges), the glow and the arc discharge. Fig.(1) is a typical general VI characteristic of an electrical gas discharge.

Very generally we can say that when the applied voltage is increased from zero we observe a range in which the current is proportional to the applied voltage. After this the VI characteristic flattens out. In this range the current is said to have reached its 'saturation' value. The current is no longer proportional to the applied vol tage, and the latter may then be increased until a stage is reached at which a very small further increase in the applied voltage causes the current to increase by many orders of magnitude. If the voltage is further increased the gas almost immediately becomes a very good conductor of electrical current.

Conduction of electricity, starts at the lowest levels (conduction of current due to natural radiation etc.). Then Townsend currents begin to flow (pA to nA) as a result of multiplication mechanisms setting in (internal maintenance mechanisms). The discharge formed at current roughly between $\sim$ 1μA and 1A needs medium voltages to maintain it, and produces a glow. Hence discharges of this type are called "glow discharges". Most discharges carrying more than an ampere of electrical current with a very low maintaining voltage across their electrodes can

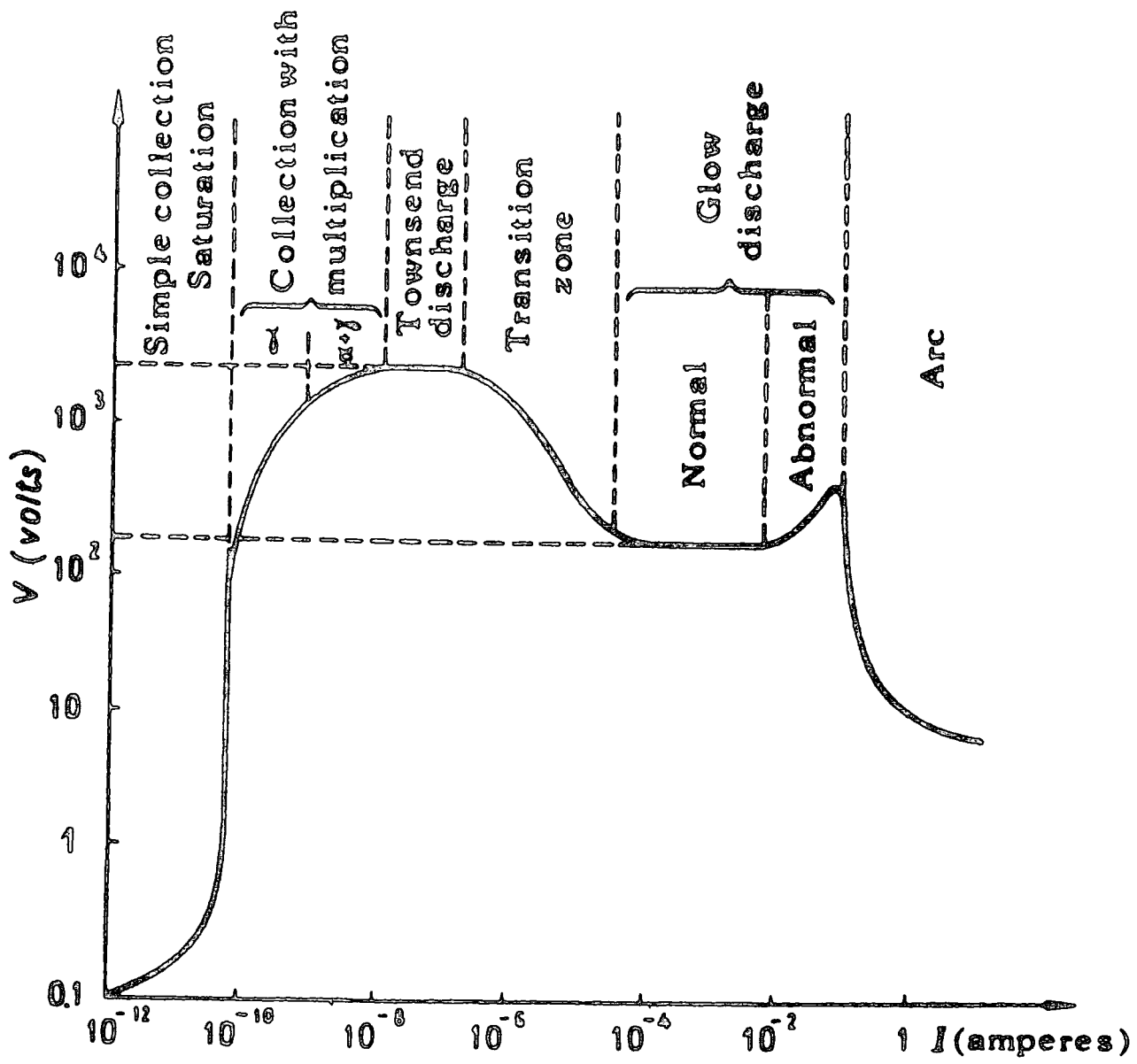

FIG. 1 V-I CHARACTERISTICS FOR A GASEOUS DISCHARGE

be called electric arcs. The VI characteristic of arcs can be divided into three sections, namely, negative slope, approximately zero slope and positive slope. The electric arc discharge goes through these phases as it approaches full ionization, where rapid changes in the conduction of electrical current are no longer possible.

Furthermore, as has been mentioned above, the pressure of the discharge changes the discharge characteristics radically. An electrical gas discharge takes different forms at different pressures, depending on the ratio of the electric field to pressure and the magnitude of the applied voltage. At low voltages, the field in the gap is inhomogeneous. Secondary ionization is negligible throughout the volume. Increase in the voltage applied between the electrodes strengthens the field near the cathode and leads to secondary ionization, which in turn reduces the potential drop at the cathode region. Thus structural changes in the cathode sheath and transition into a non-self sustaining glow discharge occur. At this point it is thought that the cathode sheath is dominated by ionization in collisions with electrons and by secondary emission at the cathode (as a result of ion bombardment of the cathode). Whereas ionization in the positive column is maintained by external ionization and excitation agents.

At strong fields (α/p) (where α is the Townsend coefficient, and p the pressure of the discharge) increases. Thus secondary ionization becomes more important and the discharge transforms into a self-sustaining discharge. Current amplification is realised more easily if E/p values reach tens of volts per torr (where E is the electric field). Thus the discharge passes progressively through dark and glow discharge states, until the glow cathode spots become arc spots mainly due to the phenomena occurring in the cathode region.

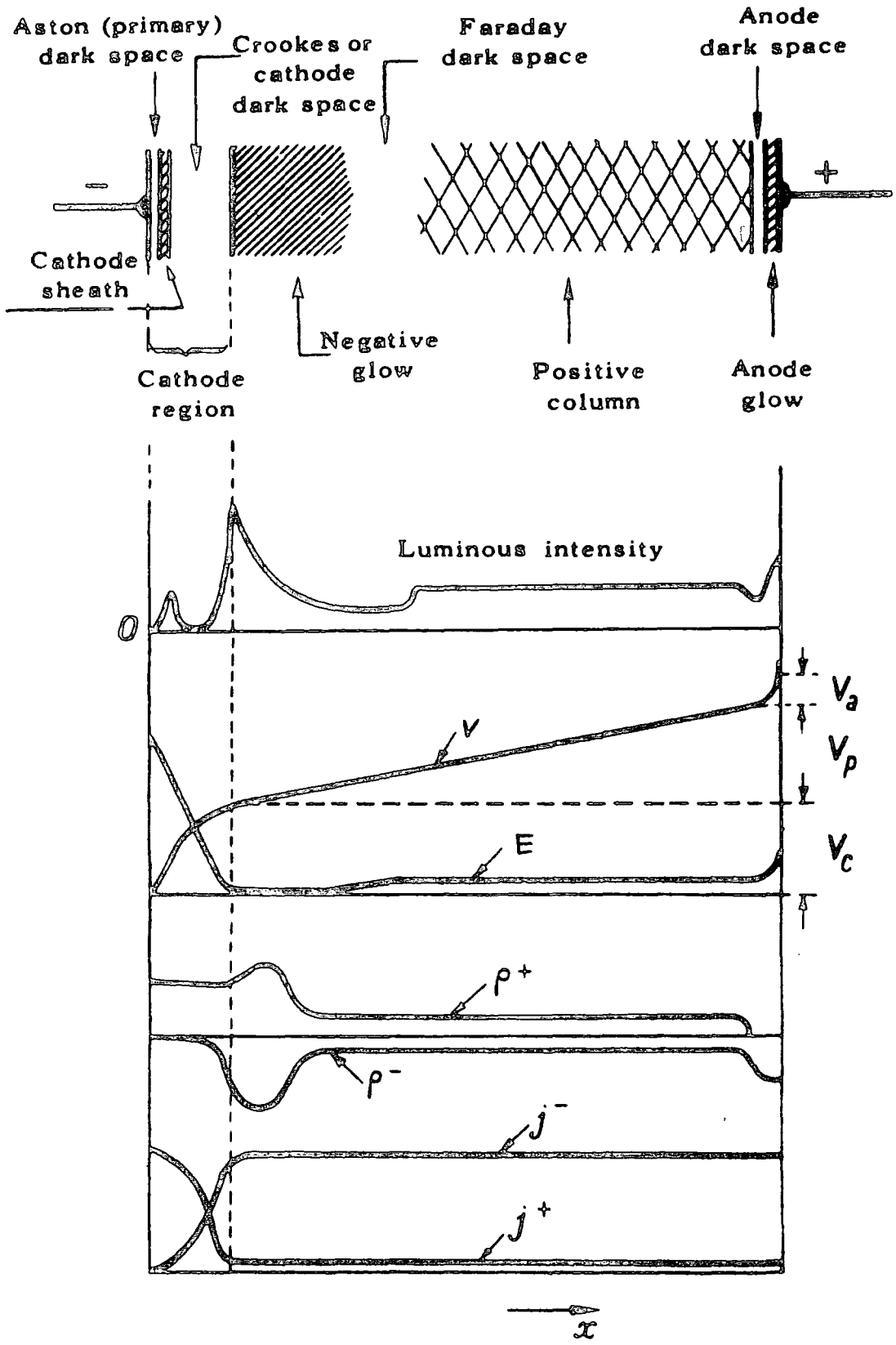

Fig. 2 Normal glow discharge. The shaded areas are luminous. (A. von ENGEL, *Ionized Gases*, Clarendon Press, 1957, p. 191)

1.3 The Glow Discharge

The glow discharge takes its name from the luminous section which appears near the cathode and is separated from it by a dark zone (Fig. 2). The glow discharge is characterised by its diffuse luminous zones and a constant potential difference between its electrodes. The relative dimensions of the zones depend on the pressure of the discharge and the inter-electrode distance.

As the pressure decreases the faraday dark space expands while the positive column contracts and may disappear altogether. On the other hand as the inter-electrode distance is decreased, the positive column contracts with it, i.e., the sizes of the other zones do not change. If the cathode is displaced, the zones up to the faraday dark space move with it. One final observation is that if the electrode system is mounted in a large spherical enclosure instead of a cylindrical tube, no positive column is observed.

Such observations and the theories on glow discharges make it possible to conclude that the positive column is not characteristic of the discharge as are the dark and luminous zones, in the vicinity of the cathode, and also that the potential across the discharge is a linear function of the distance from one of the electrodes. The potential difference at the boundaries of the tube is made up of

$$V = V_c + V_p + V_a \qquad (1.1)$$

where V_c the cathode fall potential, V_p is the drop over the positive column, and V_a is the potential across the anode. In a glow discharge, V_c is always much greater than $V_a + V_p$. Under certain conditions $V_a \cong 0$ otherwise it is approximately equal to the first ionization potential. V_c depends on the nature of the gas and the cathode material and changes little with the inter-electrode separation, pressure and current (as

long as the current is below a certain limiting value).

The electric charge density is only large in the cathode region (due to slow positive ion flow towards the cathode). The resultant space charge is practically zero over the whole length of the remainder of the discharge and the gas is in the form of plasma, the density of the plasma being much higher than in the cathode fall.

The resultant current density (applying the principle of conservation of charge) is the same over the length of the discharge.

The ion and electron contributions to the current are given by, respectively,

$$j_i = \rho_i V_i \quad ; \quad j_e = \rho_e V_e \tag{1.2}$$

In the positive column, $\rho_e = \rho_i$ but $V_e >> V_i$ since $\mu_e >> \mu_i$.

Therefore $j_e >> j_i$. At the anode $j_i = 0$. In the vicinity of the cathode $\rho_i >> \rho_e$. This compensates for the low mobility of the ions. Therefore $j_i >> j_e$ and at the cathode $j_e = 0$.

The Cathode Fall is the name given to the region which extends from the cathode surface to the negative glow. An approximate calculation for the normal cathode fall can be made if the following assumptions are made. First, all electrons from the cathode are emitted as a result of ion bombardment, that is to say that electron emission is a secondary emission process, and that the electric field in the vicinity of the cathode is a linear function of the distance. Secondly, a sufficient condition for the maintenance of the discharge is

$$\int_0^{d_c} \alpha \, dx = \ln(1 + 1/\gamma) \tag{1.3}$$

This can be seen as the same criterion as that for transition from the Townsend discharge to breakdown, but applied to the cathode region. Hence the assumption made is that the cathode region behaves like the

Townsend discharge.

Both these assumptions lead to following equations Ref. (2)

$$\int_0^{d_c} \alpha dx = \ln (1 + 1/\gamma) = \bar{\alpha}\, d_c = V_c/C_1 \qquad (1.4)$$

$$V_c = C_1 \ln (1 + 1/\gamma)$$

Assuming current is carried by positive ions

$$j_c/p^2 \simeq \mu_i p V_c^2 / (pd_c)^3 = C_2 \left(\frac{1 + \gamma}{\ln (1 + \frac{1}{\gamma})} \right) \qquad (1.6)$$

$$pd_c = \frac{1}{\alpha/p} \ln (1 + \frac{1}{\gamma}) = C_3 \ln (1 + \frac{1}{\gamma}) \qquad (1.7)$$

From the equations it can be concluded that V_c is independent of pressure, while current density is proportional to the square of the pressure 'p^2' (to p for cylindrical electrodes.) $j_c \geq I/s$ where s is the surface area of the electrodes, and that d_c is inversely proportional to pressure.

1.4 Electric Arc Formation

Figure (1) shows that if the current of the electrical discharge exceeds a certain limit, the voltage between the electrodes drops rapidly. The discharge is then said to have become an arc discharge. When an arc is established by transition from a glow discharge there is a significant change in current density at the cathode. It is already established (Ref. 3) that the current density of the normal glow discharge is constant as long as any part of the cathode remains uncovered by the cathode glow. Before going into the arc mode, the discharge passes through a phase in which the glow covers the total cathode surface as the discharge current is increased. At this stage the current can only

increase as a result of increasing current density, (Ref. 4). This involves a rise of voltage across the electrodes, hence the positive slope of the voltage-current characteristic in the glow region Fig. (1). This phase of the electrical discharge is called the abnormal glow. In this phase, the dark cathode space contracts and the voltage and the current of the discharge increase until the arcing potential is reached. In the case of a cold cathode the voltage across the discharge falls to several tens of volts, thus allowing practically unlimited increase of the current. The corresponding voltage in the voltage-ampere characteristic of the discharge is called the 'arc-ignition potential'. This change in the discharge characteristics must result from the appearance of a new mechanism which sustains the discharge. It should be possible to work out the qualitative dependence of the arc-ignition potential on pressure with the aid of the known dependence of the dark cathode region length 'd_c' as follows. For a given voltage pd_c = constant (similarity principle). For the abnormal glow, E/p also remains constant. As the pressure drops the size of the dark cathode region increases and the electric field decreases. Hence the ignition potential of the arc should increase rapidly if the transition is to take place at a definite magnitude of the field. The evidence for the above qualitative description is favourable (Ref. 5,6). It has been shown that in low pressures, when pd of the gas discharge is less than Paschen's minimum pd< pd min, (i.e., lies on the left hand branch of the Paschen's curve), the gas discharge does not pass through the glow discharge phase but, transfers directly from the dark discharge stage into the abnormal glow phase. This is characterised by a high maintaining voltage, and it is correspondingly more difficult for the glow discharge to pass into the arc mode.

The discussion up to this point has assumed a flat cathode. Since changes in the cathode configuration involve changes in the

width of the cathode dark space region as well as in the electric field intensity at the cathode, at a given discharge voltage the dependence of arc-ignition potential on gas pressure is also different.

Although this brings about interesting properties to a discharge with a hollow cathode (since the effect is pronounced at low pressures (Ref. 4)) it will not be elaborated on.

The current through an arc discharge could be limited by the resistance of the circuit, by the applied electric field and the nature of the gas, by the transfer of current from the volume of the gas to the cathode or by the transfer of current from the anode to the gas. Any theory of arc conduction should take into account at least the last three factors. As the results of investigations up to date have shown, the explanation of the current transfer to the cathode has proved to be the most difficult to explain. It is a problem as yet unsolved, and is the main reason why the present investigation was undertaken.

In dark and glow discharges, emission of electrons by the cathode is secondary emission. Since the conditions leading to the breakdown of the gas, and maintaining a glow discharge are practically the same it is reasonable to conclude that the nature of the phenomena taking place has not changed. On the other hand, since the discharge in an arc mode can be maintained at a very much lower voltage, some other phenomena must be taking over and causing additional ionization and therefore higher current densities.

The question that needs to be answered is where and how this additional mechanism takes over? It is possible to divide the discharge roughly into three regions, namely, the cathode region, the volume of the gas and the anode region. There is general agreement in the literature, however, that this additional mechanism must be in the cathode region.

CHAPTER TWO

2. REVIEW OF ARC COLUMNS AND RELATED THEORY

2.1 Equilibrium Theory

2.1.1 Temperatures of the gas, ions, and electrons

2.1.2 Local thermodynamic equilibrium

2.2 Simplified Models of the Positive Column

2.2.1 Temperature independent model

2.2.2 Temperature dependent model

2.2.3 Combined model

2.3 Ionization

2.3.1 Weakly ionised monatomic gases

2.3.2 Thermal ionization

2.4 Electrical and Thermal Conductivity

2. REVIEW OF ARC COLUMNS AND RELATED THEORY

In dealing with the physics of the electrical discharge, one is faced with a mixture of mechanical, thermal, radiative and electrical phenomena. Under such conditions, one might try to discuss the problem by first writing down the general equations, taking account of all these phenomena. Particular cases could then be dealt with by making the proper assumptions. This is an approach, which is, if not impossible, extremely difficult and lengthy. In a review chapter of this kind, the alternative is, by starting from a few simple and easily interpreted equations and basic concepts, to follow and develop the discussion, elaborating in detail where it is thought to be relevant to the present investigations. But this approach also presents its own difficulties. The results, conclusions and suggestions thus arrived at, because of the nature of the simplifying assumptions, are not final and are not always conclusive. The terms which have been neglected in the equations are not always negligible.

In the following sections and in the rest of the thesis, this pitfall will be avoided as far as possible by thorough discussion of the conditions and assumptions under which different simplified models and theories are valid, and also of the degrees of approximation involved. Among the models of the positive column of the electric arc, the one which is relevant to our investigation is the model of a positive column which is cylindrical in shape, and for simplicity, mathematically treated as if the electrodes were at an infinite distance. Under such conditions, all cross-sections are identical, and the partial differential equations become ordinary differential equations, in the steady state. These models, therefore, cannot be applied to industrial or experimental devices directly and indiscriminately, but rather should be taken as steps leading to the treatment of actual devices by the use of higher order approximations.

2.1 Equilibrium Theory

The idea of equilibrium is basic to the study of gas discharges since the validity of many indirect measurements depends on the assumption of equilibrium. By equilibrium is not usually meant simply a steady state equilibrium but rather an equilibrium within the gas as an isolated body insulated from outside effects. This is of course a state which is never fully realised in practice since the gas is generally losing energy to its environment which cannot be recovered, i.e. radiation, and receiving energy from the electrical circuit. Furthermore, due to the conduction of heat, there are going to be temperature gradients within the volume of the gas. Therefore the following conditions are set as necessary conditions for approximation to thermodynamical equilibrium within the volume of the gas

$$\lambda \, \Delta \, T_g/\Delta r \ll T_g \tag{2.1}$$

$$\lambda \, \Delta n/\Delta r \ll n \tag{2.2}$$

$$e \, E \, \lambda \ll \frac{1}{2} \, m \, V^2_{th} \tag{2.3}$$

Relation (2.1) is the condition for small temperature gradients where T_g is the temperature of the gas in question. Relation (2.2) is the condition for infinitesmally small density gradients thus making the implicit assumption that there should be small energy transport by diffusion. Relation (2.3) is the condition that there should also be small energy transport due to the electric field, which implicitly also means low electric fields and short mean free paths, that is, medium to high gas pressures. The equilibrium is ultimately brought about by continuous interchange of energy by means of collisions and radiation.

2.1.1 Temperatures of the gas, ions, and electrons:

Since the ions and the neutral particles of the gas have almost the same mass, they readily exchange their energies in collisions. Also, due to the high neutral number density and high collision cross-sections, these collisions occur frequently. Thus a state of thermal equilibrium is readily established between them. That is to say, $T_g \simeq T_i$ although it should be pointed out that due to acceleration of ions in the electric field T_i is slightly higher than T_g .

The higher mobility of electrons causes them to absorb a higher proportion of energy from the electric field. Part of this energy is passed on to the neutral particles and ions through inelastic and elastic collisions. The energy thus transferred via elastic collisions increases the temperature of the gas while the inelastic collisions excite and ionise it. Frequency of the collisions depends on the electron temperature T_e . Increasing the pressure of the gas decreases the electron temperature since the number of ionising collisions increases. This increases the amount of energy transferred to the neutral particles and ions, which means that $T_g = T_i$ is increased. This interchange of energy continues until $T_e \simeq T_i \simeq T_g$. When the temperatures of the particles are thus equalised it is said that there is an equilibrium between these particles in the thermodynamical sense.

The principal processes in which the plasma in the positive column is involved are collisions between particles and interactions with electric and magnetic fields of external and self-induced origin. The former lead to the thermodynamic equilibrium between the particles, while the later give rise to the electrical neutrality of the plasma due to the strong electrostatic forces created when $n_i \neq n_e$. The state of equilibrium of the ionised gas is characterised by the absolute temperature 'T', the number density of charge carriers, "n" = $n_e = n_i$ and the degree of ionization q . In the state of thermodynamic equilibrium, these

variables are not independent of each other. If the ionization is determined by temperature and density, (see Saha's equation below) the gas is then said to be in an equilibrium state of thermal ionization. When the ionization is due to an external field and the gas is not in equilibrium, the discharge will often reach a steady state which can be defined by variables T_i, T_e, T_g, q .

2.1.2 Local Thermodynamic equilibrium

In a plasma, if a state of thermodynamic equilibrium is approximately attained within each small volume element of plasma, the plasma is then said to be in a state of local thermodynamic equilibrium (LTE). Since the plasma temperature is a slowly varying function of the space coordinates the dimensions of the small volume element must be chosen to be large in comparison with the mean free path but small enough so that the temperature may be assumed to be constant within it Ref. (7).

All simplified models of the positive column in the high pressure arc are based on the assumption of a state of LTE in the column. Although whether or not this is true is a subject of dispute, the following facts are pertinent.

a) In the majority of cases the conditions do not strictly speaking meet all the requirements for the attainment of LTE, electrons playing the major role in violating the conditions.

An electron drifting in the direction of the electric field with a drift velocity v_e ; in the average time ξ between collisions, receives an energy equal to $e E v_e \xi$. Since the drift velocity is equal to $v_e = \mu E$, where the mobility $\mu = e \xi / m$, The energy received is

$$\frac{e^2 E^2 \xi^2}{m_e} \qquad (2.4)$$

If we take the average electron kinetic energy as $\frac{3}{2} KT_e$ and that of a neutral gas atom as $\frac{3}{2} KT_g$, and assume that in the steady state a fraction (Y)

of the energy received in the collision is given up in the next collision with the neutral gas atom, then energy lost is

$$\frac{3}{2} k(Y) (T_e - T_g) \qquad (2.5)$$

Balancing gains and losses,

$$\frac{e^2E^2\xi^2}{m_e} = \frac{3}{2} k(Y) (T_e - T_g) \qquad (2.6)$$

We could replace ξ by λ/v_{th} ; where λ is the mean free path and v_{th} is the average thermal speed. Since this is a rough approximation, we do not differentiate between the average speed and the root mean square speed

so that $$\frac{\xi^2}{m_e} = \frac{\lambda^2}{m v_{th}^2} \qquad (2.7)$$

since $\frac{1}{2} m_e v_{th}^2 = \frac{3}{2} kT_e$ combining equation (2.7) and equation (2.6)

We thus obtain

$$\frac{(T_e - T_g)}{T_e} = \frac{2}{9} \left(\frac{1}{(Y)}\right) \left(\frac{eE\lambda}{kT_e}\right)^2$$

In high pressure arcs with very small mean free paths $\lambda_e E/kT$ turns out to be considerably less than unity, but for elastic collisions (Y) is equal to $\frac{2m_e}{M}$ where M is the mass of the relevant neutral particle, so $(T_e - T_g)/T_e$ is therefore not necessarily small. For inelastic collisions (Y) is considerably above the (Y) for elastic collisions. With these higher values of Y, $(T_e - T_g)/T_e$ for typical cases is of the order of a few percent close to the axis, Ref (2) but energetically inelastic collisions are only possible for a minority of fast electrons.

It should be noted, however, that since these temperatures enter generally into the equations as exponential functions, small differences could introduce large changes in reality.

b) Despite these objections, the conclusions drawn from the assumption of LTE should be reasonably valid in most cases. Current methods in plasma physics accept theories and models with ± 20% prediction rate as valid if only because most of the diagnostic methods operate between these limits.

2.2. Simplified Models of the Positive Column:-

The positive column of the d.c. discharge forms a plasma which, though never perfectly uniform, can be studied experimentally, and in an idealised form theoretically. At low pressures the positive column of the arc discharge is not unlike that of the glow discharge, and furthermore is not necessary for the maintenance of the discharge.

The high pressure arc column ($p \gtrsim$ 50mm Hg) Ref. (8) is different mainly with respect to its higher gas temperatures ($\gtrsim$ 5000 K). At these high temperatures the ionization is thought to be mainly of thermal origin.

Certain types of arc around atmospheric pressure and below radiate only a few percent of their total power. The rest is thought to be dissipated as heat which is conducted to the walls. In this kind of model it is further assumed that the neutral gas is immobile, which implicitly neglects any forced motion as well as any kind of natural convection. It is also assumed that the electric field gradient generates only an electric current density and the temperature gradient (radial) introduces only the heat flux.

Therefore, following the above assumptions, one can write a general equation which balances the heat generated via joule effect and the heat transfer due to the thermal conductivity,

$$\sigma E^2 = \left(\frac{1}{r}\right) \frac{d}{dr} \left(rK \frac{dT}{dr}\right) \qquad (2.9)$$

This equation is known as the Elenbaas-Heller equation Ref. (9), where σ is the electrical conductivity K is the thermal conductivity. In this equation E is assumed uniform throughout the column, and the temperature T is assumed to be a function of the radial distance 'r' only.

The solution of the above equation is not simple, since σ and K depend on plasma temperature and pressure. This functional dependence cannot realistically be neglected. However equation (2.9) can be further refined by approximating the dependence of σ and K on the plasma temperature using analytical expressions.

2.2.1. Temperature independent model:-

With this model σ and K are assumed to be independent of the plasma temperature. This of course is a very drastic approximation, because σ depends on the degree of ionization which may vary radically with a slight incremental difference in T. This also suggests that σ should have a significant maximum at the axis of the discharge. However, if the assumption is valid equation (2.9) is easily integrated to yield

$$T = T_o - ar^2 \quad \text{where} \quad a = \frac{\sigma E^2}{4K} \tag{2.10}$$

The constant T_o may be estimated by the condition that at the wall, r = R the radius of the discharge, and the temperature converges to that of the wall, 'T_w' therefore we should have

$$T_o = T_w + a R^2 = T_w + \frac{\sigma E^2 R^2}{4K} \tag{2.11}$$

Although the assumption made in deriving the above relation is not a valid one, since the expression defines what seems to be a reasonable radial distribution of T, it could be used as a first approximation on which to base a further approximation.

This could be realised by calculating the thermal conductivity and electrical conductivity from this radial distribution using Saha's equation.

2.2.2. Temperature dependent Model

We could, on the other hand, make the opposite extreme assumption; that is we could assume σ is very strongly dependent on the plasma temperature. Accordingly σ should be zero anywhere but along the axis of the discharge. The radial temperature distribution, therefore, would be,

$$\left(\frac{1}{r}\right)\frac{d}{dr}\left(rK\frac{dT}{dr}\right) = 0 \qquad (2.12)$$

for $r \neq 0$ since it would be physically meaningless if it was otherwise, we should have

$$rK\frac{dT}{dr} = -A \qquad (2.13)$$

Where the constant would have a suitable value depending on the thermal power per unit length. To further our discussion we should make one more assumption at this point concerning the dependency of K on the plasma temperature. The simplest one would be to assume that K does not depend on the plasma temperature T at all. Accordingly we can carry on with the same relation

$$\frac{dT}{dr} = -\frac{A}{rK} \qquad (2.14)$$

With the same boundary conditions that were set on the temperature independent model, the above relation integrates into

$$T-T_w = \left(\frac{A}{K}\right) \ln\left(\frac{r}{R}\right) \tag{2.15}$$

As can be seen; the above relation leads to an infinite temperature at the axis; and therefore if the assumptions made in arriving at this relation were valid, it would be true only for regions not too far away from the walls of the discharge.

On the other hand, if instead of assuming that K was independent of the plasma temperature 'T', we had made the assumption that

$$K = BT^n \tag{2.16}$$

in that case, equation (2.14) would be

$$r\, BT^n \frac{dT}{dr} = -A \tag{2.17}$$

This relation, after integration, would give

$$T^{n+1} - T_w^{n+1} = -\frac{n+1}{B}(A) \ln\frac{r}{R} \tag{2.18}$$

This further assumption, as can be seen, does not bring any further improvement on the model, since it also leads to infinite temperatures along the axis.

Although a useful relation for the radial temperature distribution was derived from the temperature independent model, clearly it was based on a questionable assumption, namely, that the σ and K were temperature independent. In the second model, it was not so much that the assumptions made in trying to derive the relations, were wrong. The relations thus obtained only held for regions not too far away from the discharge walls. This suggests a compromise or rather, a

combination of the two different sets of assumptions that were made.

2.2.3 Combined Model:

Instead of the implicit assumption that was made in the previous model, namely, that the current is strictly along the axis of the discharge, let us assume that there is an ionised channel along the axis, cylindrical in shape, and symmetrical about the axis of the discharge. Let us assume further that the temperature and electrical and thermal conductivity of the ionised channel are constants.

Now we can combine the two models with the temperature independent model governing inside this ionised channel and the temperature dependent model governing outside the channel. The values of T must be equal at the boundary 'r_c', where r_c is the radius of the channel

Let $\sigma = \sigma_c$ when $r < r_c$ and $\sigma = 0$ for $r_c < r < R_c$ and let $K = K_c$ for $r < r_c$ and $K = K$ for $r_c < r < R$; where R is the radius of the discharge σ is the channel electrical conductivity. Then for

$r < r_c$ from equation (2.10)

$$T = T_o - \left(\frac{\sigma E^2}{4K_c}\right) r^2 \qquad (2.19)$$

and from equation (2.15)

$$T - T_w = - \left(\frac{A}{K}\right) \ln \left(\frac{r}{R}\right) \text{ for } r_c < r < R$$

at $r=r_c$ from continuity of heat flux

$$A = \sigma E^2 \frac{r_c^2}{2K_c}$$

This last expression would yield the value of the constant A if the value for r_c was known, but this model provides us with no provisions for the

value of r_c. At this point, to find a value for r_c, in the literature, Steenback's minimum principle is referred to, Ref (9); which, although it is said to be successful has very debatable validity. According to this method one chooses arbitrary values for r_c. The corresponding radial distributions of temperature are found and σ, K and K_c values are determined. Then an assumption is made to the effect that the actual value for r_c is the one which leads to a minimum value of E for a given total pressure, total radius and total current.

Further improvements to these basic models are possible by using several other means. Introduction of the heat transfer function 's' is one example. Since σ and s are both functions of T, σ can be seen as a function of s . Therefore one can plot curves giving σ versus s . But such curves are not necessarily simple in most of practical cases. Chemical decomposition and ionization always introduce irregularities in the curves, which can only be obtained by experimental measurements or by detailed and long calculations based on solutions of Saha's equation.

2.3 Ionization

If the current density of the discharge is very high the degree of ionization may also become sufficiently high for properties of fully ionised gases to be applicable. Because of the slowly decreasing effect of the coulombforce, the effective scattering cross-section of a positive ion is about two orders of magnitude higher than that of a neutral atom Ref. (10). The 'fully-ionised' behaviour therefore appears at approximately $q = 0.01$ and not when $q \to 1$, (9).

We shall not discuss further the case of strongly ionised gases, but will concentrate on the case relevant to the present investigation namely that of weakly ionised monatomic gases.

2.3.1 Weakly ionised monatomic Gases:

The ionization of atoms and molecules requires energy which usually originates from electron, positive ion and/or neutral particle encounters with an atom or a molecule. It can also originate from adsorbtion of quanta of radiation. The processes in which these mechanisms can occur are numerous but one widely considered mechanism is equilibrium thermal ionization.

In the case of weakly ionised monatomic gases such as mercury vapour, most metallic vapours and noble gases, a simplification arises because the phenomena of ionization occurs without the accompanying complexities of chemical decomposition.

2.3.2 Thermal ionization

The theory of thermal ionization was first treated by Saha Ref(11). He describes the effect of heating on matter as a gradual loosening process of the sub-molecular or sub-atomic particles. The addition of heat to matter takes it through fusion, vaporization, molecular dissociation, excitation and finally ionization states. The thermal vibration, particle encounters and radiation process take the molecules from an orderly crystallographic array in a solid to discrete atoms in which the loosely bound outer layer (valence) electrons are removed leaving ionised particles of the initial atoms.

The actual amount of energy required to excite or ionise an atom or a molecule is defined as the resonance or ionization energy of that species and is the energy required to raise an electron from a lower to a higher energy level, or to remove an electron from an atom or a molecule to an infinite distance. Thus it is possible for ionization processes to proceed in stages. Successive additions of energy may first excite the particle and then ionize it.

In order to calculate the conductivity of the gas it is necessary to estimate the degree of ionization of the gas and thus its plasma

number density. If thermal equilibrium and thermal ionization conditions apply, this may be done by using Saha's equation.

The general form of Saha's equations is

$$\frac{n_e\, n_i}{n_a} = 2\,\frac{(2\pi mk)}{h^3}\;T^{3/2}\;\;\frac{U^1(T)}{U(T)}\;\exp\left(-\frac{eVi}{kT}\right) \qquad (2.21)$$

where V_i is the ionization potential h Plank's constant, n_i the density of ions and n_a the density of atoms.

$$U(T) = \sum_k g_k \exp\left(-\frac{eV_{ek}}{kT}\right) \qquad (2.22)$$

$$U^1(T) = \sum_l g_l \exp\left(-\frac{eV_{el}}{kT}\right) \qquad (2.23)$$

are the partition functions for the atoms and ions. The first sum is for all the excited states of atoms. The second sum is for all the excited states of ions. Higher ionised states are neglected. In the case of weakly ionised monatomic gas we could consider only the unexcited atom of statistical weight g_a and unexcited ion of statistical weight g_1. Furthermore the electron density n_e and the ion density n_i are equal to each other in a plasma. Therefore

$$n \;\alpha\; n_a^{\frac{1}{2}}\;T^{3/4}\;\exp\left(-\frac{eV_i}{2kT}\right) \qquad (2.24)$$

Using the above approximate equation, an expression for the current density may easily be derived. Given that

$$j = en\mu E = \sigma E \qquad (2.25)$$

where, e is the electronic charge, n is the plasma number density and

and μ the mobility. Then from simple kinetic theory of gases, results (see Appendix I)

$$\mu_e = \frac{e\lambda}{m_e v_{th}} \tag{2.26}$$

where v_{th} is the average thermal velocity, λ the mean free path and m_e the electron mass. Experimental evidence confirms to a first approximation that

$$\mu = \text{constant } (\lambda / v_{th}) \tag{2.27}$$

Now $\lambda \alpha 1/n_a$, since $p = n_a kT$, then $\lambda \alpha (T/p)$, also $\bar{v}_{th} \alpha (T^{\frac{1}{2}})$. Therefore

$$\mu = \text{constant } (p^{-1}) (T)^{\frac{1}{2}} \tag{2.28}$$

Combining eq. (2.28) and eq. (2.24) with eq. (2.25)

$$j = \text{constant } (p^{-\frac{1}{2}}) (T^{5/4}) E \exp\left(-\frac{eV_i}{2kT}\right) \tag{2.29}$$

To substitute into the Elenbaas-Heller equation both sides of the eq. (2.29) are multiplied by E. Thus

$$jE = \sigma E^2 \qquad \text{and therefore,}$$

$$\sigma E^2 = \text{constant } (p^{-\frac{1}{2}}) (T^{5/4}) \exp\left(-\frac{eV_i}{2kT}\right) E^2 \tag{2.30}$$

where E is taken as uniform, it may be introduced in the constant.

The approximation for K, the thermal conductivity, could be the same

as the one used in the temperature dependent model, that is

$$K = \text{constant } (T^n) \tag{2.31}$$

where n is an empirical exponent and its value could be taken as $n < 1$ for most weakly ionised monoatomic gases. These equations with corrections for radiation losses have been treated rigorously in the literature. The results in literature show that the curve of temperature versus radius decreases parabolically from the center to the wall of the discharge.

2.4 Electrical and Thermal Conductivity

Electrical conductivity is related to the concept of mobility by the relation

$$\sigma = \mu_e en \tag{2.32}$$

the relevant mobility is that of electrons in the plasma as a whole. The contribution of the positive ions to the electrical conductivity is neglected in practice. Mobility is defined by the relation

$$\mu = \frac{e\lambda}{m\, v_{th}} \tag{2.33}$$

where

$$\lambda = {}^{1}/_{nq_{cr}} \tag{2.34}$$

n is the number density of the relevant species and q_{cr} their collision cross-section. If there is more than one species of collision targets

$$\lambda = 1/\sum n_i q_{cri} \qquad (2.35)$$

two types of collision targets (for electrons) should be considered, namely ions and neutrals. The latter could be taken to behave as hard spheres except that q_{cr} varies with the speed of the impact electron. Ions, on the other hand, have long distance action through the Coulomb force. That is why a plasma only 2 - 5% ionised will behave in practice like a fully ionised gas.

The relation

$$K = b\, C_r \qquad (2.36)$$

gives the thermal conductivity of the gas, where b is the static viscosity and C_r is the heat capacity per unit mass. C_r is calculated from the derivative of the internal energy

$$KE_{(av)} = {}^3/_2 \quad \frac{kT}{m} \qquad (3.37)$$

Ref. (12).

The viscosity coefficient is given by

$$b = {}^1/_3 \quad n\, m\, V_{th}\, \lambda \qquad (2.38)$$

Ref. (13).

CHAPTER THREE

3. WALL AND ELECTRODE PHE NOMENA

3.1 Wall Sheaths

3.1.1 Ambipolar diffusion to the wall

3.1.2 Calculations for the wall sheath

3.2 The Cathode Region

3.2.1 Cathodic Sheath Phe nomena

3. WALL AND ELECTRODE PHENOMENA

In the theory of the positive column, for both high and low pressures, there is a body of knowledge on which there is general agreement in the literature. No such agreement exists for surface phenomena. Although contact between solids and gases or liquids and gases occurs frequently in the universe, for example, in the atmospheres of stars and planets, our knowledge about such contacts, that is, about wall and electrode phenomena, has remained limited.

The surface layer of the solid state of matter is the least well-defined part of it. From a mechanical point of view, it is very difficult to obtain and maintain a surface polished to better than 1μ. Also, from a chemical point of view, it is difficult to prevent absorbtion of 'stray' molecules which modify the structure of the surface, and often prevent oxidation. In the case of electrical arc discharges, there is also the question of the much higher currents and current densities involved, whereby the interaction between the discharge and the walls become much stronger than in all other types of discharge.

Although all the other types of electrical discharges in gases may be studied using the assumption of ideal walls and/or electrodes, the arc discharge cannot be subjected to the same assumption. Since an 'ideal cathode', which would not erode, would not be able to supply the high current densities of the arc discharge, it should be possible to think of the electrode erosion and electron emission as two different products of the same phenomenon, or at least, not to consider them to be independent of each other. This contrasts with the other types of discharge, where it seems that, generally, electrode erosion is a by-product, of limited importance, of plasma processes which are not strongly related to cathode electron emission processes.

There are several ways in which the surfaces of liquid or solid bodies in contact with gases can behave:-

a) Primary emission: Evaporation, which is the emission of neutral particles due to the effect of heating, and emission of charged particles, which can broadly be divided into two types, emission due to the effect of the heat (thermionic emission) and emission due to the effect of an electric field.

b) Secondary emission: of neutral or charged particles by bombardment of the surface by charged or neutral particles of matter and/or photons.

c) Adsorbtion: of charged particles, neutral particles and/or photons.

d) Reflection: of charged particles, neutral particles and photons; ions and molecules can be reflected without being neutralised or ionised.

Before discussing what happens in the vicinity of electrodes, in the following sections we shall first discuss the phenomena taking place at an 'inert' wall, that is, a wall which does not exchange current with the plasma. This can be a good approximation to reality when proper 'outgassing' procedures have been applied to the system in question. Indeed, the concept maybe extended to the 'ideal' wall from which, for all practical purposes, no gas or vapour is released.

Although, from the plasma physics point of view, wall phenomena are basically the same in both high and low pressure arcs, at very high pressures, because of the much shorter mean free paths and therefore much smaller ambipolar diffusion coefficients, the plasma physics phenomena are ultimately dominated by the role of the wall acting as a heat sink. This role could be discussed by using classical thermodynamic methods. Since it is not relevant to the present investigations,

however, it will not be followed up in any detail. In the following sections, therefore, the very high pressure arc is implicitly excluded.

3.1 Wall Sheaths

Consider a plasma inside a metal box, and let the whole assembly be heated to an absolute temperature T. Since electrons travel faster than ions even under L.T.E. conditions, it follows that, in the absence of a wall sheath, they would hit the wall more frequently. As a result, inert walls have a general tendancy to become negative with respect to the plasma. Thus near the wall charge separation takes place, resulting in a boundary layer with a large electric field within it, and a potential difference between the wall and the plasma. The voltage drop across the wall sheath, when established, slows down the movement of electrons towards the wall and accelerates ions in the same direction, until both current densities become equal. When an ion hits the wall, it is reasonable to assume that there is a finite probability 'α' of it gaining an electron and then bouncing off the wall as a neutral. For a conducting wall, the electron picked up would be one of the electrons in the Fermisea of the metal and the energy release would be roughly equal to the difference between the work function of the metal wall and the ionization potential of the ion. On the other hand, for an insulating wall, the picked-up electron would have been one of the electrons which was adsorbed into the surface layer of the wall. The existence of adsorbed layers of electrons is consistent with the fact that the wall is at a negative potential with respect to the plasma.

3.1.1. Ambipolar diffusion to the wall.

When ions and electrons are present in equal concentrations at a point, they will diffuse with their respective velocities. Since electrons diffuse more quickly than ions, thus leaving the positive ions behind, this in turn sets up a field which decelerates the electrons,

and accelerates the ions, until, in the steady state, particles of both signs diffuse with the same velocity. If the mean free path is much smaller than the dimensions of the box, we can assume this kind of diffusion, called 'ambipolar' diffusion, which brings to the boundary of the sheath an equal (or almost equal - since we are dealing with a one-dimensional model and assuming uniform temperatures) supply of ions and electrons. We shall consider only two types of particles, since a review of the literature showed that more complicated cases do not bring out any significant changes.

3.1.2 Calculations for the wall sheath

From an ambipolar diffusion point of view, once the sheath is formed, most of the electrons will be reflected and will not hit the wall (generally the energy required for them to overcome retarding field will be greater than their kinetic energy). On the other hand, since the ions are accelerated in the sheath, the current density of the ions arriving from the plasma will be equal to the current density of the ions at the edge of the sheath, which in turn will be equal to the current density of the ions captured by the wall. Therefore, we can write, from standard results in kinetic theory of gases Ref. (15).

$$-D_a \mid \bar{\nabla} n \mid = \alpha_p (n v_{ir}/4) \qquad (3.1)$$

where D_a is the ambipolar diffusion coefficient $\mid \bar{\nabla} n \mid$ is the absolute value of the density gradient at the edge of the sheath, V_{ir} is the average random velocity of the ions. Again using the well known relations of the transport theory Ref. (14)

$$D_a = - \frac{D_i \mu_e + D_e \mu_e}{\mu_e + \mu_i} \qquad (3.2)$$

α_p the probability that the positive ion is neutralised.

or, if $\mu_e >> \mu_i$

$$D_a = (k/e)\ \mu_i\ (T_e + T_i) \tag{3.3}$$

where μ_e and μ_i are the electron and ion mobilities respectively. Now

$$\mu_i = \frac{e\lambda i}{nv_{ir}} \qquad \text{so that, with} \quad T_e >> T_i$$

and combining eq (3.1) and eq.(3.2),

$$\frac{\lambda_i}{d} = \left(\frac{\alpha}{4}\right)\ \left(\frac{nv_{ir}^2}{kT_e}\right) \tag{3.4}$$

where, in this equation 'd' physically stands for the length at which the density of the charge carriers goes to zero at an "extrapolated wall" and is mathematically defined by

$$|\ \bar{\nabla} n\ | = \frac{n}{d} \tag{3.5}$$

The voltage drop across the sheath may be calculated as follows: The effect of a sheath voltage is to reduce the random electron current density by the ratio $\exp(-eV_s/kT_e)$, Ref. (16). Thus,

$$(n\ v_{er})\ \exp(-eV_s/kT_e) = nv_{ir} \tag{3.6}$$

If purely random motion of the ions is assumed this relation gives

$$\exp(-eVs/kT_e) = (T_i/T_e)^{\frac{1}{2}}\ (m_i/m_e)^{-\frac{1}{2}} \tag{3.7}$$

A rough approximation would be that the ion temperature in the vicinity of the wall increased to one half of the electron temperature. Then

$$\exp\ (-eV_s/kT_e) \ = \ \frac{1}{\sqrt{2}}\ (m_i/m_e)^{-\frac{1}{2}} \qquad (3.8)$$

An alternative approach is to write down Boltzman's relation for both ions and electrons,

$$n_i \ = \ n_o \ \exp\ (eV/kT) \ ; \ n_e = n_o \exp\ (-eV/kT)$$

where n_o is the plasma number density well inside the box where the electric potential V due to the charge separation would be zero. Then applying Poisson's equation, we would get

$$\frac{d^2V}{dx^2} \ = \ - \rho/\varepsilon_o \qquad (3.9)$$

where ρ is the charge density and is equal to

$$e\ (n_i - n_e) \qquad (3.10)$$

therefore eq. (3.9) becomes

$$\frac{d^2V}{dx^2} \ = \ - \ \frac{e(n_i - n_e)}{\varepsilon_o} \qquad (3.11)$$

or,

$$\frac{d^2V}{dx^2} \ = \ \frac{2n_o e}{\varepsilon_o}\ [\ \frac{1}{2}\ \exp\ (\frac{eV}{kT}) \ - \ \frac{1}{2}\exp(\frac{eV}{kT})\ ]$$

$$= \ \frac{2n_o e}{\varepsilon_o} \ \sinh \ (\frac{eV}{kT}) \qquad (3.12)$$

or if we expand the Boltzman's relation with the exponential series

formula and keep the first order approximation

$$n_e = n_o \exp(-\frac{eV}{kT}) = n_o (1 - \frac{eV}{kT}) \tag{3.13}$$

$$n_i = n_o \exp (\frac{eV}{kT}) = n_o (1 + \frac{eV}{kT}) \tag{3.14}$$

then eq. (3.11) would be

$$\frac{d^2V}{dx^2} = \frac{2n_o e^2 V}{\varepsilon_o kT} \tag{3.15}$$

it would be convenient to introduce dimensionless variables, such as

$$\theta = \frac{eV}{kT} \qquad \text{and} \qquad U = \frac{x}{\lambda_D}$$

where

$$\lambda_D = (kT\varepsilon_o/2n_o e^2)^{\frac{1}{2}} \tag{3.16}$$

then eq. (3.15) would be of the form (dimensionless)

$$\frac{d^2\theta}{dU^2} = - \theta \tag{3.17}$$

relating the potential to the distance across the sheath. Characteristic length of the sheath λ_D is often called the Debye length or the screening distance where kT/e is the characteristic unit of the potential. Inside the sheath plasma equations are no longer valid; the basic condition that $n_e = n_i$ breaks down.

3.2 The Cathode Region

For the cathode mechanisms of discharges other than arcs, satisfactory models in terms of known processes can be set up. Even if they have not been fully calculated quantitatively there is unanimous agreement that they are essentially correct. In the glow discharge, positive ion bombardment of the cathode is responsible for the electron emission (Von-Engel - Steenbeck theory of the normal-glow cathodic fall Ref. (9)). In some cases, good numerical agreement was reached by supplementing this basic process, with electron release at the cathode by photons, metastable atoms and excited atoms from the discharge itself.

In the range of the abnormal glow and in the transition from the glow to the arc, the theory by Von-Engel and Steenbeck explains the basic facts. It adds to the above processes and eventually replaces them by thermionic emission from the cathode, which becomes hotter as the current increases, as a result of positive ion bombardment. This mechanism is not the same as positive ion bombardment on its own, in which individual interactions are dealt with and a positive ion may or may not release an electron from the cathode, the relevant coefficient always being less than one. The thermionic mechanism is a collective contribution to the formation of a hot spot on the cathode which then emits electrons as a result of its temperature. In such conditions there is no restriction to the effect that the electron current density may not exceed the positive ion current density of the bombarding ions.

The laws governing thermionic emission are well known, Ref. (17), quantitatively. However, only arcs with highly refractory cathodes seem to be relevant to Von-Engel's and Steenbeck's theory. Generally, in most of the other cases the Richardson thermionic emission current density corresponding to the cathode material boiling point falls short of the observed high current densities. Alternative mechanisms based

on field emission, metastable atoms and excited atoms have been proposed without achieving consensus in the literature.

Theoretically, the supply of the emitted electrons must be the semi-free electrons in the Fermisea and the concept of work function should be governing the liberation of these electrons. If it did, such current densities would not be possible for most of the arc spots. On the other hand, we also know from solid state physics, that values of current density of the order of 10^{11} A/cm^2 , some orders of magnitude higher than those published for cathode spot current densities, (up to 10^8 A/cm^2; = 10^6 A/cm for H_g), are possible. Therefore the inevitable conclusion is that there must exist a process leading to some kind of 'hole' through which electrons in the Fermisea are let loose.

3.2.1 Cathodic Sheath Phe nomena

A simplified model for the cathodic sheath phe nomena of the glow discharge, in which the plasma edge is regarded as emitter of positive ions and the electrons emitted from the cathode move as a parallel beam explains the facts satisfactorily. There seems to be no reason why the passage from relatively low current densities and high voltage drops, to high current densities and much lower voltage drops should impose any qualititative changes in the basic model. However there are quantitative discrepancies. Not only is the number of positive ions striking the cathode surface not sufficient to extract the correct number of electrons, but also the electrons themselves cannot create sufficient ions in the discharge, because they appear to acquire an energy corresponding to a voltage between the resonance potential and ionization potential, but not exceeding the ionization potential, of the discharge gas.

Possible explanations, are either that stepwise ionization is dominant in the sheath, or that somekind of randomization mechanism, may be related to the mechanisms of plasma electrostatic oscillations,

leading to the situation that only the kinetic energy acquired by the electrons is related to the voltage drop. Then some of the individual electrons distributed on both sides of this average value could acquire energies exceeding the ionization potential. If the first explanation was correct, it would not in any case hold for high pressure arcs or for vapours which have no metastable states, since these would exhibit some special features in the cathode region, which are not in fact observed.

Let us assume that the plasma edge which is supplying positive ions, to the sheath, and the cathode surface which is emitting electrons, are plane parallel surfaces. Also the initial directed particle velocities will be taken as zero and the particles will be assumed to be accelerated as a result of the potential difference across the sheath.

The total current density will be

$$j_{total} = j_e + j_i = \text{constant} \qquad (3.18)$$

where the electron current density j_e is

$$j_e = en_e v_e = \text{constant}_1 \qquad (3.19)$$

and the ionic current density j_i is

$$j_i = en_i v_i = \text{constant}_2 \qquad (3.20)$$

where n_i, n_e, e, v_i and v_e are ion number density, electron number density, electronic charge drift velocity of ions and electrons respectively. If V is the voltage drop between a point in the sheath at a distance x away from the cathode surface and the cathode surface itself, then the drift velocities are given by

$$v_e = (2e/m_e)^{\frac{1}{2}} V^{\frac{1}{2}} \quad ; \quad v_i = (2e/m_i)^{\frac{1}{2}} (V_c - V)^{\frac{1}{2}}$$

where V_c, m_e and m_i are the total voltage drop across the sheath, electron mass and ionic mass. Poisson's equation for one dimension, is,

$$\frac{d^2V}{dx^2} = \left(\frac{e}{\varepsilon_o}\right)(n_i - n_e) \tag{3.21}$$

$$\frac{d^2V}{dx^2} =$$

$$-\frac{1}{\varepsilon_o}\left[\left(\frac{j_i}{(2e/m_i)^{\frac{1}{2}}(V_c - V)^{\frac{1}{2}}}\right) - \left(\frac{j_e}{(2e/m)^{\frac{1}{2}} V^{\frac{1}{2}}}\right)\right]$$

multiplying by dv and noting that $\frac{d^2V}{dx^2} = \frac{1}{2}\frac{d}{dV}\left(\frac{dV}{dx}\right)^2$ and integrating,

$$\frac{1}{2}\left(\frac{dV}{dx}\right)^2 = \left(\frac{j_i}{\varepsilon_o}\right)\left(\frac{2m_i}{e}\right)^{\frac{1}{2}}(V_c - V)^{\frac{1}{2}} + \left(\frac{j_e}{\varepsilon_o}\right)\left(\frac{2m_e}{e}\right)^{\frac{1}{2}}(V)^{\frac{1}{2}} + I.C \tag{3.22}$$

This equation is similar to the Child-Langmuir equation for the calculation of space-charge limited current. In the derivation of the integration constant, interesting conclusions arise. If we assume that there is an ample supply of electrons and ions at both sides of the sheath. Then the electric field is zero at both $V = V_c$ and $V = 0$ with;

$$\lim_{V \to 0} \frac{dV}{dx} = 0$$

we would have for I.C.

$$I.C = -\left(j_i/\varepsilon_o\right)\left(\frac{2m_i}{e}\right)^{1/2} V_c^{1/2} \qquad (3.23)$$

where as;

$$\lim_{V \to V_c} \left(\frac{dV}{dx}\right) = C$$

then we would have

$$I.C. = -\left(j_e/\varepsilon_o\right)\left(\frac{2m_e}{e}\right) V_c^{1/2} \qquad (3.24)$$

The two are non-trivial if and only if

$$j_e (m_e)^{1/2} = j_i (m_i)^{1/2} \qquad \text{that is}$$

$$\frac{j_i}{j_e} = \left(\frac{m_e}{m_i}\right)^{1/2} \qquad (3.25)$$

Assuming (3.24) is valid whereas a field $E_c \neq 0$ exists at the cathode surface, results in

$$\frac{1}{2} E_c^2 \varepsilon (2V_c/e\varepsilon_o^2)^{1/2} [j_i (m_i)^{1/2} - j_e (m_e)^{1/2}] \qquad (3.26)$$

known as McKeown's equation. For complete solution a second relation between E_c and j_i/j_e is needed.

CHAPTER FOUR

4. REVIEW OF CATHODE EMISSION MECHANISMS

4.1 Anomalous Electrodynamic Ion Acceleration

4.2 Thermionic and Field Emission of Electrons

4.3 The Effect of Protrusions and Oxide Layers

4.4 Metal Vapour Effects

4.5 Dynamic Field Emission

4.6 Continuous Transition from Solid/Liquid to Plasma

4. REVIEW OF CATHODE EMISSION MECHANISMS

In chapter 3 an expression for the ratio of ion current density to electron current density in a cathodic sheath was derived in eq. (3.25). Theoretical and experimental quantitative comparisons of this ratio show large discrepancies. There seems to be little doubt that ion current densities are mainly due to the ions emitted from the plasma edge due to the thermal ionization in the volume of the plasma. Calculation of the theoretical electron current density emitted from the cathode surface, however is a matter of controversy and does not yield the right order of magnitude to satisfy the relation

$$\frac{j_i}{j_e} = \left(\frac{m_e}{m_i} \right)^{\frac{1}{2}} \tag{4.1}$$

The ratio $(m_e/m_i)^{\frac{1}{2}}$ calculated for mercury is 1.6×10^{-3}. To check the left hand side of the expression, we need to calculate the j_i and j_e values for mercury as well. j_i could be calculated by following the popular supposition that the ions which are being emitted from the plasma edge are created by thermal ionization of the plasma. Using Saha's equation for the plasma number density

$$n = (n_F \, n_a)^{\frac{1}{2}} \exp. \left(-\frac{eV_i}{2kT} \right) \tag{4.2}$$

and taking the plasma temperature T as 5000 K (generally accepted temperatures for the positive column) so that

$$N_F = \frac{2(2\pi \, mkT)^{3/2}}{h^3} = 2.7 \times 10^{26}/m^3$$

(m, k, T and h are mass of the electron, Boltzmann's constant, plasma temperature and Plank's constant respectively),

from ideal gas laws n_a is

$$n_a = P/kT = 2.2 \times 10^{25}/m^3$$

from Saha's equation eq. (4.2) n_o is

$$n = 7.2 \times 10^{20}/m^3$$

$$n \simeq 10^{14}/cm^3$$

the plasma number density n will be $\sim 10^{14}/cm^3$ Assuming that the speed of the ions at the plasma edge was purely thermal due to their kinetic energy, and estimating the mass of mercury ions from the relation

(mass of H_g ion) = (Atomic weight of H_g) (mass of Hydrogen)

that is M_i (Hg) = A(Hg) (M_H)

where $(M_H) = (1838)$(mass of electron) and $A(H_g) = 200$, the thermal speed of the ions may be estimated from

$$\frac{1}{2} m v_{th}^2 = \frac{3}{2} kT$$

that is,

$$v_{th} = \left(\frac{3\ kT}{m}\right)^{\frac{1}{2}} = 7.9 \times 10^2 \text{ m/sec.}$$

As a result, using the well known relation for the current density

$$j = env_{th} \qquad (4.3)$$

j_i for mercury would be $1.2\ A/cm^2$. After ascertaining this value of j_i it is clear that in order to obtain the right values for the left hand side of the equation (4.1) we would need electron current densities of the order of $10^4\ A/cm^2$, and this is where the problem lies. The electron current density due to the thermionic emission mechanism is approximately $10^{-18} A/cm^2$ giving a value for j_i/j_e many orders of magnitude larger than the expected value. On the other hand if random current densities in the solid state, which are of the order of $10^{11}\ A/cm^2$, are put into the ratio, the result is several orders of magnitude smaller than the required ratio. Of course the assumption that the random current density yielded by solid state physics is all available for emission from the cathode is a very drastic one.

These comparisons, of course, do not necessarily mean that the model for the cathodic sheath is completely wrong. Support for this view, can be drawn from the reported experimental observations. Current densities up to $\simeq 10^8\ A/cm^2$ have been observed in the cathode spots, Ref. (19), ($\simeq 10^6\ A/cm^2$ for the case of mercury, Ref. (20)). If these current densities were totally due to electron emission, the j_i/j_e ratio would be 10^{-5} for mercury. There would still be a discrepancy but not so large as to justify disregarding the model completely, provided that an efficient emission mechanism for the electrons could be established.

In the face of these discrepancies, we need to revise our assumptions. There seems to be nothing wrong in assuming that there is an ample supply of ions at the plasma edge. The only weak point in calculating j_i using this assumption concerns the velocities of ions, that is, in assuming random thermal velocities. However assuming zero directed velocities at the edge and then calculating the drift velocities due to the electric field in the sheath does not change the order of magnitude of the ion current. Therefore the energy transferred to the cathode per

unit time is still not sufficient to extract the correct number of electrons from the cathode. Having said this we have to point out that this argument is based on the energy input to the system. However, energy, regardless of its mode, could be amplified as well as being transferred and/or transformed, although for amplification another source of energy is needed. This source could be the potential energy of the system. That is to say, if the velocities of the ions were amplified above the levels calculated in terms of the energy input to the system, that would bring more ions to the cathode surface per unit time and thus lead to more electrons being extracted from the cathode.

Nevertheless, the answer to this problem does not necessarily lie in classical extraction and/or emission mechanisms. As is widely supported and argued in the literature, these mechanisms, might have to be modified, supplemented or replaced by more energy-efficient physical mechanisms. In the following sections various suggested mechanisms and approaches to the problem will be discussed.

4.1 Anomalous Electrodynamic Ion Acceleration

The force $d\bar{F}$ on a current carrying element dl in a uniform magnetic field is

$$d\bar{F} = I\,(\overline{dl} \times \bar{B})$$
$$I(dl) = en\bar{v}Adl$$

where $\bar{v}$ is the velocity A is area and $enAdl = dq$ in a length dl Therefore,

$$d\bar{F} = enA\,\overrightarrow{dl}\times \bar{B} \qquad (4.6)$$

$$d\bar{F} = dq\,(\bar{v} \times \bar{B}) \qquad (4.7)$$

and for a single particle we have

$$\bar{F} = e(\bar{v} \times \bar{B}) \tag{4.8}$$

When this law is applied to a current in a completely closed circuit, integration over the circuit shows that there can be no resultant forces on the circuit. However, net forces and torques can arise in parts of the circuit. In arc discharge systems charge carriers are not always electrons following in close loops. Ions could also carry the current in a part of the circuit. H. Aspden Ref. (21), has argued that since the electron and ion masses are vastly different, application of Newton's third law shows that there should be a torque balancing force on the ions. Following the above reasoning Aspden suggests that ions will be accelerated according to a force which is in scalar terms

$$F = \left(\frac{m_i}{m_e}\right)\frac{\mu_0 q_i q_e v_e v_i}{4\pi r^2} \qquad [N.] \tag{4.9}$$

taking $v_e \simeq 10^8$ cm/sec. and $v_i \simeq 10^4$ cm/sec.
$r \simeq 10^2$ cm. and using the $\frac{m_i}{me}$ ratio for mercury F would be $\simeq 10^9$ dyne. With a reasonable sheath thickness, and using the relation $F \times s = \frac{1}{2} m v_i^2$ $(s = d_c)$, the ion speed will be $v_i \simeq 10^8$ cm/sec. With this order of magnitude $j_i/j_e \simeq 10^{-2}$ for $j_e \simeq 10^6$ A/cm^2 (a typical observed current density for Hg arcs).

This clearly is a controversial suggestion. Without putting a case for or against the suggestion, the following considerations which are thought to be pertinent will be mentioned.

The suggestion is not so much controversial in the sense that it assumes coulomb interaction between the charged particles at vast distances at atomic level as will be seen from the equation because it is the

m_i/m_e ratio which amplifies the force. Nor is it contentious that instantaneity of action at a distance is implicitly assumed, and that the geometrical configuration of the electron path (metallic circuit) is important whether or not it is a closed circuit. The critical point is whether or not the criterion that self-action of charged particles in a closed circuit can produce no net resultant forces is more fundamental than the criterion of torque-balance based on Newton's laws of motion. Although it is fair to say that the laws of motion have stood the test of the time in a non-relativistic world, they should be applied with great caution in this sense.

4.2 Thermionic and Field Emission of Electrons

In a glow discharge, the Townsend coefficient γ for removal of electrons from the cathode by the bombardment of positive ions with kinetic energies of the order of $\sim eV_c$ gives satisfactory values for the ratio j_i/j_e . Thus the second relation eq. (3.25) in the case of glow discharge is

$$j_i/j_e \approx 1/(\gamma)_{eq}. \tag{4.10}$$

where $(\gamma)_{eq}$ is the sum of the secondary processes aiding ionic bombardment in electron production.

Unfortunately, quantitative values for the above relation in the case of arc discharges are far away from satisfying the condition set in eq. (3.25). Von-Engel and Steenbeck suggested Ref. (9), that the electronic emission is a result of ion bombardment not in the way described by Townsend but rather due to thermionic emission which in turn is due to the heat released by positive ion impact on the cathode. This mechanism is not possible in many cases. With mercury and copper, for example, thermionic emission at the boiling temperatures ($\approx$ 600K

in the case of the former and $\simeq$ 2570K in the case of the latter) falls short of the required values. Clearly this mechanism is possible only for arc discharges with high boiling point or melting point (thermionic) cathodes, also called 'spotless' arcs. Therefore the inevitable inference is that some significant and effective changes in the operation of the work function potential barrier are necessary.

Thermionic emission was first discovered by Edison in 1883. Following various workers Richardson first published a thermodynamical theory of electron emission from hot metals (Ref. (17)., which was later modified by H.A. Wilson and Richardson and then completed by Dushman in 1923. That is why the following relation is sometimes called Dushman's equation, but mostly is known as Richardson's law for thermionic emission.

$$j_s = AT^2 \exp\left(-\frac{e\phi}{kT}\right) \tag{4.11}$$

j_s is called the saturation current density although in fact there is never complete saturation. It is now known that the presence of an electric field E results in an effective reduction of the work function . This effect, known as the Schottky effect, results in an equation of the form

$$j \simeq j_s \exp\left(e\,(eE)^{\frac{1}{2}}/kT \right)$$

$$j \simeq AT^2 \exp\left(-\phi_e + e(eE)^{\frac{1}{2}}/kT\right) \tag{4.12}$$

This result may be derived using quantum statistical methods and also as a consequence of simple electrostatic laws (the image charge

theorem). The formula remains valid up to field strengths of $\sim 10^6$ v/cm Ref (2). The current density is still temperature limited however and the reduction in the work function is still not enough to explain the observed current densities in many arcs.

The need for a further effective reduction in the work function coupled with a reduction in the dependence of emission current on temperature made the field emission mechanism strongly favoured as the correct process to describe the electron extraction from the cathode, Ref (20). Although there are various refinements and supplements proposed for the construction of a satisfactory model based on the field emission mechanism. Essentially the Fowler-Nordheim equation is coupled with eq. (3.26). The Fowler-Nordheim equation for field emission is

$$j = 6 \times 10^{-6} \frac{(E_F/e\varphi)^{\frac{1}{2}}}{E_F + e\varphi} E^2 \exp.-\left(\frac{6.8 \times 10^7 \varphi^{3/2}}{E} \right)$$

$$j \cong 6 \times 10^{-6} E^2 \exp-\left(\frac{6.8 \times 10^7 \varphi^{3/2}}{E} \right) \qquad (4.13)$$

Where j, E_F, e, φ are the current density, Fermi-Level energy, electronic charge, and the work function respectively. With E approximately equal to 10^7 V/cm and $\varphi = 4.5$eV as for mercury, current densities of the order of $j = 10^3$ A/cm^2 are predicted. A further slight increase in E introduces a large increase in the current density however. For $E = 10^8$ V/cm , j becomes $= 10^7$ A/cm^2 which is of the right order of magnitude for the observed current densities, which can be as high as 10^8 A/cm^2.

It should also be pointed out that even at electric fields of the order of 10^6 V/cm, the calculated current densities from the field emission equation are higher than thermionic current densities even when corrected for the Schottky effect. Thus, from quantum statistics/mechanics

considerations, increasing the field up to 10^6 V/cmincreases the emission current because more electrons can escape from the cathode over the reduced barrier (Schottky effect). A new escape route opens up with further increase in E towards 10^9 V/cm , whereby electrons, instead of having to climb over the potential barrier set up by the work function, by virtue of their wave properties pass through the barrier, by the 'tunnelling' effect. The effect of the electric field is to reduce the thickness of the potential barrier as well as reducing the height. The barrier becomes totally transparent to the electrons with the right energy (and hence the right frequency) as opposed to being partially transparent as in the case of the Schottky effect.

The precise origin of these very strong electric fields still remains undecided. Proposed suggestions are vague and open to question, and this has led to a variety of different models. While it is true that existence of these fields does not necessarily require high discharge voltages, and that intense electric fields can be produced by space charges over very short distances, actual mechanisms for this are not clear. Classical considerations predict maximum field strengths which are two orders of magnitude too low at best.

For example, it is usually assumed that the thickness 'd_c' of the cathode region should be of the same order of magnitude as the electronic mean free path. From Child's law for space charges this order of magnitude necessitates current densities of the order of $= 10^5 - 10^6$ A/cm^2 and results in electric fields of the order of 10^5 V/cm . This value of the electric field, when applied to the Fowler-Nordheim equation yields 10^{-78} A/cm^2 for electron current densities. When coupled with eq. (3.26), maximum values of E_c necessitate $j_e = 0$ and still the quantitative agreement is far from being satisfactory.

4.3 The Effect of Protrusions and Oxide Layers

Models have been proposed to show that the local field strength due to microscopic protrusions are much higher than the average field strength. Also it has been pointed out that the presence of surface layers of gases or oxides can enhance the electric field to the right order of magnitude to produce field emission. Among the various models proposed, one giving good quantitative results in the case of surface layers will be discussed.

It was Druyvesteyn (1936) and H. Pateow (1937) Ref(23), who first suggested that positive ions from the discharge could produce high electric fields across the surface layers on the electrode. Later confirmed by Llewellyn Jones Ref. (24), the same effect was reported by Guntherschulze and Fricke and also by Malter in his work, Ref. (25), investigating the influence on the statistical time lags of the oxide layers on tungsten electrodes. Accordingly A.E. Guile and et. al, following the proposal Ref. (26), suggest that high current densities are associated with tunnel emission of electrons through the naturally occurring insulating oxides on metal cathode surfaces, across which very high electric fields are established by the accumulation of positive ions from the cathode fall. The mechanism they suggest is as follows; if these layers are semi-insulating, positive ions are trapped in them prior to their neutralization, and their concentration builds up to create a high local field at a cathode spot. Thus local failure of the surface layer results as a consequence of ion bombardment and ohmic heating. Micro-explosive disruption of the layer then causes the local field to diminish and the electron emission ceases. The process is then transferred to the next available site which is sufficiently charged by the trapped ions.

The working of this mechanism requires semi-insulating oxide layers of $\simeq$ 10A thickness, and $10^{16}/m^2$ positive ion density on the

surface to produce fields of the order of 10^9 V/m . This mechanism, although suggesting a possible explanation for the necessary high electric fields for the electron emission of the right order of magnitude, as well as for the motion of the cathode spot, does not offer any explanation for the cold-cathode discharges for which "naturally occurring oxide layers" cannot be postulated. It should also be said that, to charge the oxide layer as suggested the layer should have diode properties as well, that is, it should conduct one way only. The majority of the available measurements refer to a sequence of unipolar impulses with the same amplitude applied to the electrodes. Are the results the same if the polarity is changed from impulse to impulse? If not this may support the hypothesis of charge deposition on surface layers.

Models offering explanations for the high electric fields at the cathode mostly draw the bulk of their evidence from experimental investigations conducted under vacuum breakdown conditions with short electrode distances. Early evidence Ref(25) from experiments in which proper discharge surface conditioning for the electrodes was applied (to smooth the surface), showed that higher breakdown fields were required, which appears to show that surface irregularities are important. Further evidence in support of this conclusion comes from experimental investigations in which small particles of various insulating materials such as porcelain, silicon carbide, or alumina were placed on the electrode surfaces, Ref. (28). The experimental results obtained can be explained in terms of local electric field intensification in the presence of particles.

Thus the experimental evidence relating to the breakdown mechanism in vacuum, it is suggested, appears to be strongly related to the cathode asperities. It is also suggested that surface protrusions result in local field amplifications of an order or two higher in magnitude than the average electric field. To sum up the numerous reports and suggestions

in the literature of gas discharges, it could be said that the effects of micro-protrusions are considered under two plausable hypotheses:-

a) That the local electric field strengthening around the protrusions causes local microscopic regions in the volume of the gas to become ionized. The effect is pressure dependent

b) That electron emission from the electrode surface is caused by field emission from surface irregularities.

The first of these two hypotheses seems to have more support recently Ref(29). There are suggestions however to reconcile the two. The difficulty, it seems, is the ill-defined nature of the surface and the experimental difficulty in evaluating and differentiating between the quantitative effects both of these hypotheses cause, because both result in lowering of the breakdown voltage.

A.E. Vlastos reports of an attempt to differentiate between the two effects. In his investigation an attempt was made to suppress electron emission from the cathode by covering it with a thin insulating oxide layer. The oxide layer was 10 A thick. "The results presented support the argument that the lowering of the breakdown voltage may not be attributed only to the gas but it may also be due to the electron supply from the cathode surface produced by the high field strength prevailing at the top of the ridges", Ref. (30). In these investigations co-axial cylinder electrodes were used (30/70mm diameter) and voltages up to $\cong$ 500kV were applied. The working gas was SF_6

Under these experimental conditions, whether or not electron emission could be said to be supressed is open to question. Although it has been suggested that it is only in thin films less than about 5-10nm thickness that tunnel emission of electrons occurs and that the oxide layer in the experiment is thicker than this, it has been suggested by A.E. Guile Ref(31) and later supported by Ref (32), (33),(34)

that when the arc cathode oxide film is thicker than 10nm, then

multiple emitting sites occur at the ends of the filementary conducting channels formed through the oxide layer, as the electrical conductivity increases by several orders of magnitude. It should be pointed out that in the majority of the experimental reports the average roughness of the surface, and presumably the average thickness of the oxide layer is stated. It would be interesting to know, the maximum and minimum values of the distance between the trough and the crest lines, so that one could determine the relative importance of the surface layer and surface asperities, since in all cases, positive ions and/or asperities on the surface are suggested to be necessary for electron emission.

A variation in the models proposing field emission mechanism, is where an increase in local surface temperature, as a result of local field currents is suggested to be aiding in electron emission, i.e. producing a, combination of thermionic emission and field emission Ref. (35), (36). This does not bring any major improvement in qualitative and quantitative comparisons with the experimental evidence and does not change the basic conclusion that only a minority of cases are explainable in terms of classical mechanisms or combination of mechanisms. It seems that as long as cathode asperities and impurities can be used as arguments for and against the validity of the Fowler-Nordheim equation no strong case for or against such models can be made.

4.4. Metal Vapour Effects

Another approach to the problem is to inquire into the function and the role the dense vapour clouds, whose existence has been well documented in the literature Ref.(37),(38),(39) and (40) It is suggested that excited atoms exist in large concentrations in the dense vapour, Ref. (20). If the thickness of this region is small enough, they cannot lose energy by radiation (crossing life $<$ life time). Therefore they part with their energy on impact with the cathode surface, provided their energy

is greater than or equal to the work function of the cathode, where they release electrons with a high yield coefficient. The electrons can then acquire sufficient energy in the cathode fall to excite atoms, so that volume of the cathode fall potential need only be at about the excitation potential and below ionization potential of the gas. The small size of the spot can be due to the magnetic self restriction of the electron, which is opposed by radial diffision of charges.

Rothstein Ref. (40) has suggested that in this dense vapour region, produced and maintained by positive ions impinging on the cathode, and perhaps 10^{-5} cm thick, the interatomic fields would be high enough for the electron energy levels to become energy bands so that metallic conduction can take place, from cathode to the cloud.

Quantitatively one can set a variety of mechanisms in the dense vapour clouds incorporating diffusion of resonant photons, metastable atoms and/or molecules, and resulting in electron extraction from the cathode. Photo-ionization can also occur in steps although the process only becomes significant for high concentration of excited atoms Ionization of H_g is also possible by low energy quanta (λ>2537A) producing two excited atoms. The ionization process is most probably as follows Ref. (20).

$$H_g + h\nu \longrightarrow H_g\ (6^3 p_1) \qquad (4.14)$$

$$H_g\ (6^3p_1) + H_g\ (6^3p_o) \longrightarrow H_{g2}^{+} + e \qquad (4.15)$$

The available energy in the second step taking into account the heat of dissociation can provide sufficient energy for ionization. For photo electric emission from the cathode the condition that $h\nu > e\varphi$ must be satisfied Ref. (2) and the energy of the released electrons is

$$E = h\nu - e\varphi$$

Positive ions approaching a metallic cathode might be reflected as positive ions, atoms or excited atoms. Alternatively they can cause sputtering of the cathode surface or electron emission due either to the kinetic energy release on impact or the double process of metastable atom formation and radiationless transition. Finally the impact may result in the formation of negative ions.

Metastable atoms on impact with the cathode surface, may be reflected, may eject electrons (provided $E_m > e\varphi$) or may lose an electron to the metal cathode and so provide an ion, if $e\varphi \geq E_i - E_m$. For mercury this condition is just satisfied ($e\varphi$ = 4.5eV E_m = 5.9eV E_i = 10.4eV).

Finally a model which incorporates the charge exchange mechanism, but which may be further refined or complemented by the above mechanisms should be mentioned. It is suggested that a positive ion approaching sufficiently close to a clean metal surface can be neutralised. If it is a metal surface covered by a layer of physically adsorbed molecules of the same gas as the ion, the neutralisation can be preceded by a quasi-resonant charge exchange between the incident ion and the adsorbed molecule. The "adsorbed molecular ion" which results, is neutralised by the Auger process Ref. ([42]), which can then result in electron emission process. Since the neutralised ion distorts the isopotential surfaces outside the metal, the yield is higher than that calculated for secondary electron emission caused by incident positive ions. N.N. Khristov Ref. ([43]) suggests that the electric field established near the surface of a cold cathode glow is such that the velocities of the incident ions make charge exchange possible, and that this may be one of the factors governing the transition of the cathode fall from normal to abnormal form. The efficiency of this emission would be a strong function of the ion flux to the cathode.

Models based on or combining the physical mechanisms discussed cannot yet be subjected to rigorous and detailed quantitative analysis and compared with experimental physical data such as reaction cross-sections, mobilities, yield coefficients of various processes, and also because, more often than not, available basic data was only obtained under experimental conditions which are not comparable with the conditions in the cathode region of cold-cathode discharges.

Extrapolations of the various curves used as the basic data could lead to fortuitous results to cite one example usually the functions of $\alpha(E)$ where α is Townsend's coefficient, are measured at low pressures and then extrapolated to higher pressures according to the scaling law $Nf\ (E/N)$. This cannot be true for all values of the ratio E/N . Suppose that the appearance of an electron could be through a reaction, where an atom or molecule has been excited and then collides with an unexcited atom. Thus

$$A^* + B \longrightarrow (AB)^+ + e$$

where A^* is an excited atom or molecule and B is an atom or molecule in the ground state. But this process should be proportioned to N^2 rather than N, so that if it played an important role in α , the above scaling law would lead to erronous results.

4.5 Dynamic Field Emission

The various models that have been described in this chapter are characterised by the static treatment of stable emission processes. J. Mitterauer Ref (44) proposes a dynamic model " The Dynamic Field Emission" model. The model combines thermionic emission, thermionic field emission and electron yield due to positive ion bombardment as specific phases of a common phenomenon. The model is too complex

and detailed to discuss in detail. Briefly it represents a secondary phenomenon originating from any quasi-stationary emission mechanism, which appears only after passing a critical power density on an "initial centre". The geometric dimensions and structure of the cathode are the defining conditions for the existence of the centre. The "initial centres" are destroyed due to irreversible thermal effects of avalanche-like "micro-explosions" if a critical power density is reached. Emission centres are then transferred to other locations due to different effects of the "micro-explosions". The dynamic field emission model describes non-stationary processes due mainly to thermal instabilities. Onset of these istabilities is coupled with the critical power-density at the "initial centres". The further development of such instabilities depends on the "feed-back effects" of the thermal processes on the emission mechanism itself.

Although it is claimed that a new model is presented explaining in a plausable and con-contradictory manner the characteristics of cathode spots, it is again difficult to put a case for or against such a model. It seems that, a dynamic model of such complexity and with various feedback mechanisms, even if all basic data were available, would necessitate elaborate numerical analysis, methods of simulation, and more precise methods of diagnostics, for a quantitative check to be made.

4.6 Continuous Transition from Solid/Liquid to Plasma

From all these models proposed and from discussion in the literature it is quite clear that the cathode spot is a consequence of the discharge itself. It is also apparent that some kind of new mechanism is needed. By "new" is meant "different from the known classical mechanisms by which electrons at the Fermi-level can be raised over and/or tunnelled across the potential barrier between the solid/liquid metal

and a more disordered medium plasma/vacuum".

In the dynamic envelope comprising the cathode spot and its immediate vicinity, it is quite likely that the observable properties on the macroscopic level, such as the current density, spot size, cathode fall voltage, and free and forced motion, including 'the retrograde" motion, are the consequences not only of the state of matter within this dynamic envelope but also of the interactions taking place with the surrounding matter (both solid/liquid and plasma) at the boundaries of the envelope. It is also likely that these observable properties are the result of the complex positive as well as negative feedback mechanisms including transient, dynamic and probably regenerative behaviour as well.

Tackling the problem on a microscopic level, in terms of giving a complete description of the 'state of matter' within the dynamic envelope, because there is not yet a unifying model for all states of matter, would appear to involve dealing with problems as yet unsolved in other parts of physics. Even if a reasonably accurate description were possible, it would be probably beyond present computing capabilities and diagnostic methods to obtain adequate results to check the theory in a quantitative manner.

Lastly it might also be the case that some mechanism, which is not necessarily new would be overlooked because it was intrinsic, implicit or neglected in the assumptions. However, suggestions have been made to describe the state of matter within this dynamic envelope. A very dense plasma is considered in front of the cathode spot, and modifications are introduced in the Fowler-Nordheim equation as a result of the difference between the average field and the "stochastic" field resulting from the ions Ref. (9). An alternative approach is to consider a metallic vapour of very high density in front of the cathode spot such that its electrical conductivity is still of the metallic type

as opposed to the plasma type.

The difference between the two is represented in Fig. (3) and Fig. (4). Fig. (3) represents the plasma-type description, where an electron is either free or bound to an ion, together they represent a neutral particle (in the ground state or excited). Fig. (4) represents the metallic-type; in which some of the electrons are semi-free; that is they are free from the individual ions but bound to them as a whole and located in the Fermi-Sea. Since the distance between the neighbouring ions is very small they could also tunnel across the potential barriers. Thus there is no clear-cut difference between the bound atoms and semi-free electrons.

In such conditions it would be considerably easier to remove an electron from the undisturbed solid or liquid cathode through the envelope than through the normal surface, if the contact between the 'state of matter' in the envelope and the cathode beneath is not perfect so that the fermi-levels are not at the same level, a strong current density will flow between the two; thus if it is assumed that the surfaces of the two are not at the same potential and that an electric field exists between the two conservation of energy will not be violated if the work done in the field is equal to the difference in their work functions. Since the work functions enter the relevant equations through exponential equations a slight lowering of the work function yields significant increases in the current density (see page (46)).

However, it is more likely that a discrete 'state of matter' within the cathodic region is an oversimplification. More plausable is the picture in which a continuous sequence of states of matter diffused into each other exists between the normal cathode material and the plasma above it. In such conditions the classical meaning of the work function would need re-defining.

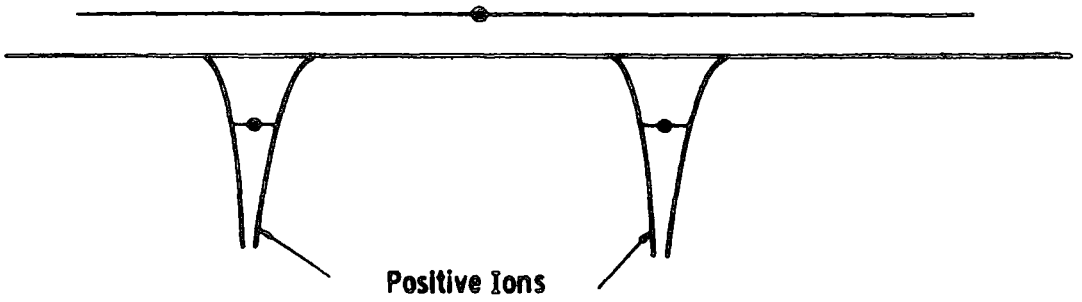

FIG. 3 PLASMA TYPE CONDUCTIVITY . THE ELECTRON IS EITHER FREE OR BOUND TO ANION

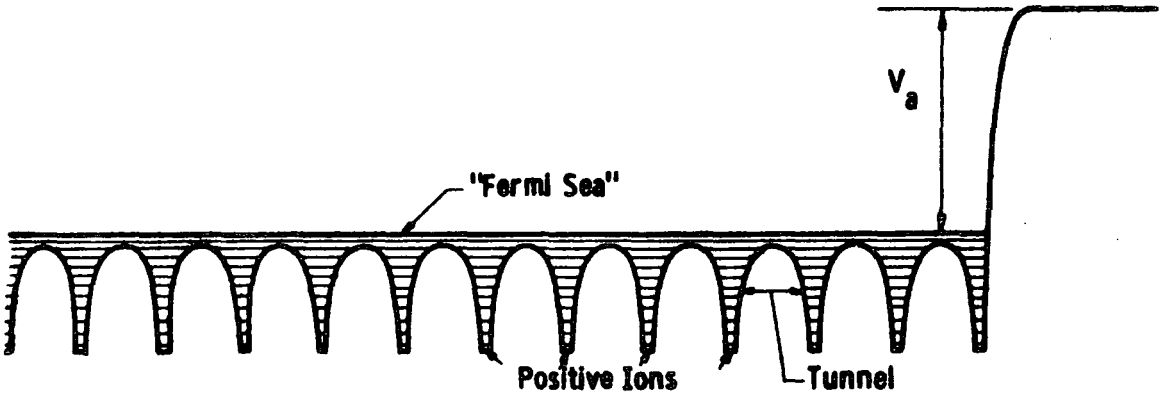

FIG. 4 METALLIC TYPE ; SEMI-FREE ELECTRONS IN THE FERMI-SEA AND TUNNELING EFFECTS FROM ONE ION TO ANOTHER

A.L. Longini Ref. (9) considers an intermediate layer made of cathodic material leaving the cathode as a result of the high current density. A possible mechanism for this could be that the number density of electrons leaving the cathode is so high that they leave behind them a positive space charge, which results in mutual repulsion of ions. The electrons would probably be emitted essentially by field emission with a strong feed-back from the mechanism described here. So at least in the region where metallic conductivity applies one could regard the material as being made of layers of positive ions but with the important property of increasing lattice pitch in the direction of motion, of the electrons. Some form of recombination process would have to be introduced in the model to account for the fact that the material is mainly composed of neutral atoms. Also the positive ions impinging on the cathode need to be explicitly introduced into the model.

An approximate solution of the Schrödinger equation known as the WKB (Wentzel - Kramers - Brillouin) approximation (in one dimension) is

$$\frac{d^2\psi}{dx^2} + \frac{2m}{\hbar^2}\,[E - V(x)]\,\psi = 0 \qquad (4.16)$$

where ψ = wave function; V = potential energy

E = energy (eigen value); $\hbar = \frac{h}{2\pi}$.

Bloch's theorem Ref(47) states that electrons in a periodic potential can be treated in terms of a wave function of the form

$$\psi = u_k(x)\ \exp ikx \qquad (4.17)$$

where $U_k(x)$ is the periodic function with the periodicity of the lattice; $k = 2\pi/\lambda$; where λ is the Broglie wave-length.

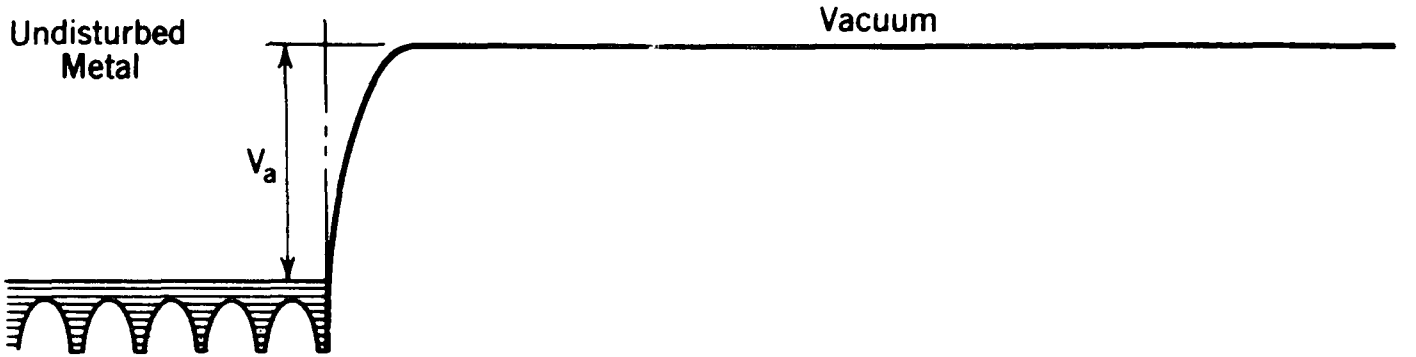

FIG. 5 METAL VACUUM BOUNDARY

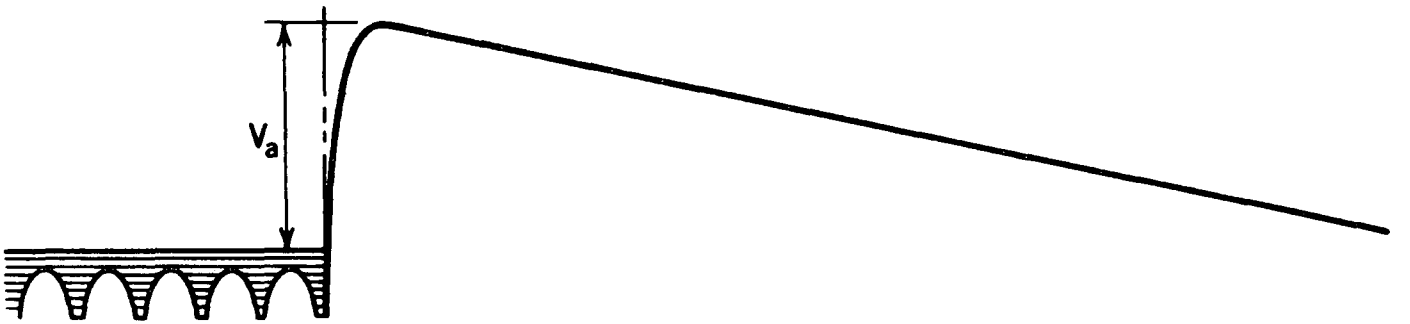

FIG. 6 EFFECT OF THE ELECTRIC FIELD

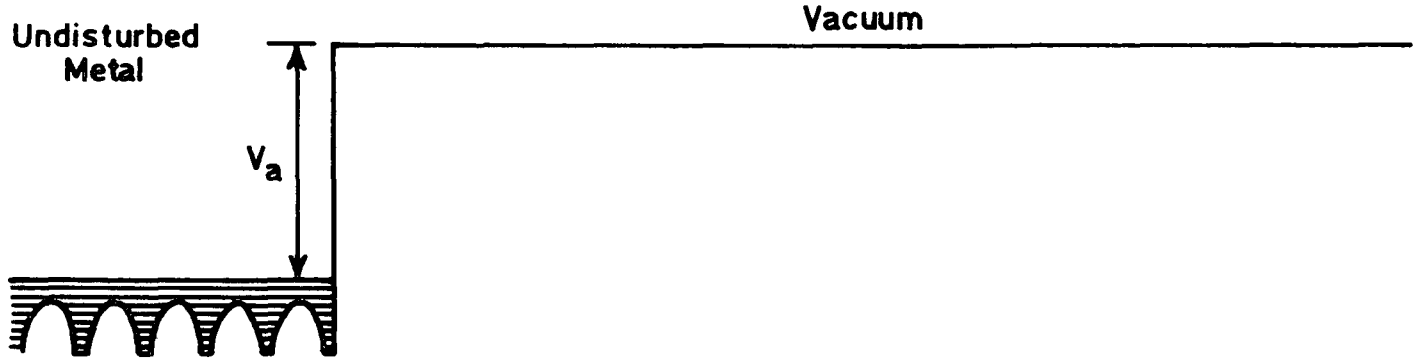

FIG. 6a METAL VACUUM BOUNDARY (WITHOUT CHARGE CORRECTION)

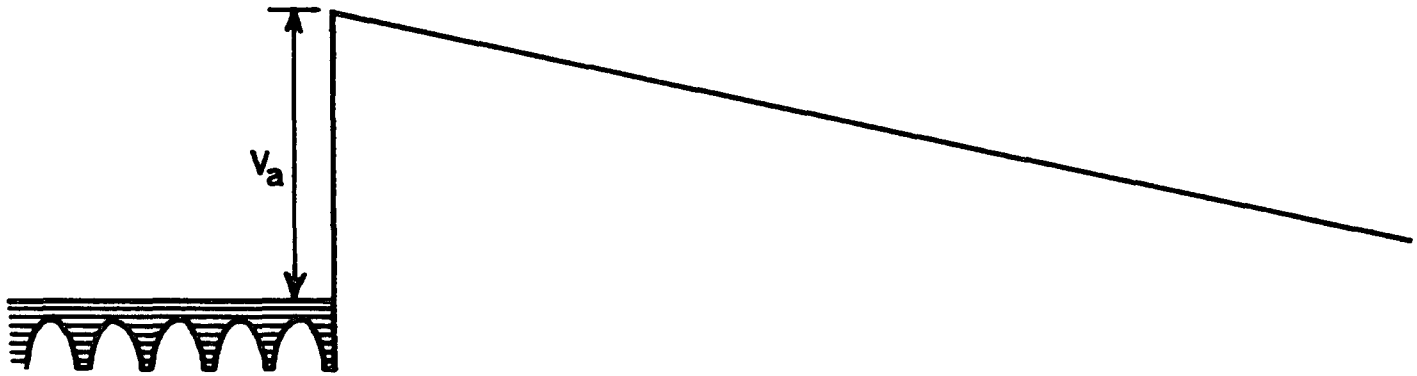

FIG. 6b APPLIED ELECTRIC FIELD

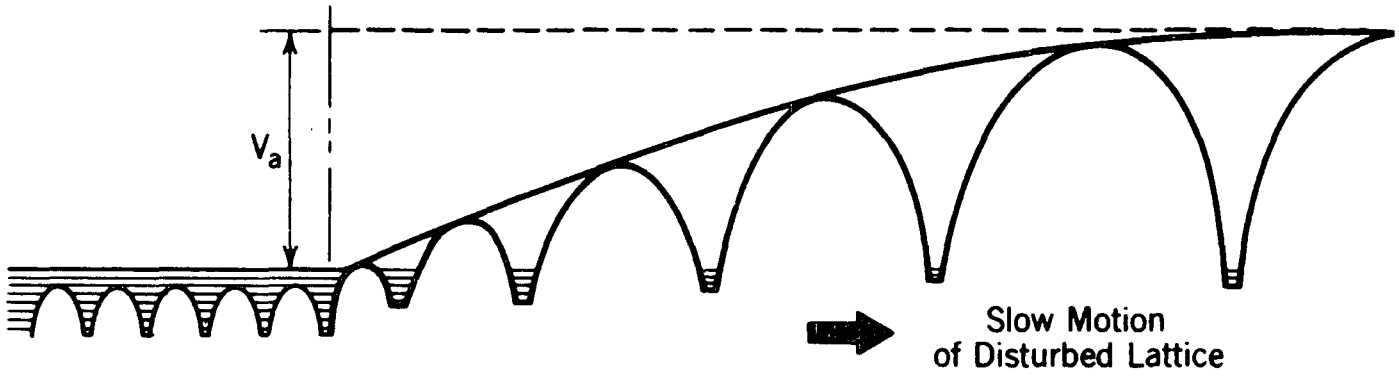

FIG. 7 LONGINI'S MODEL

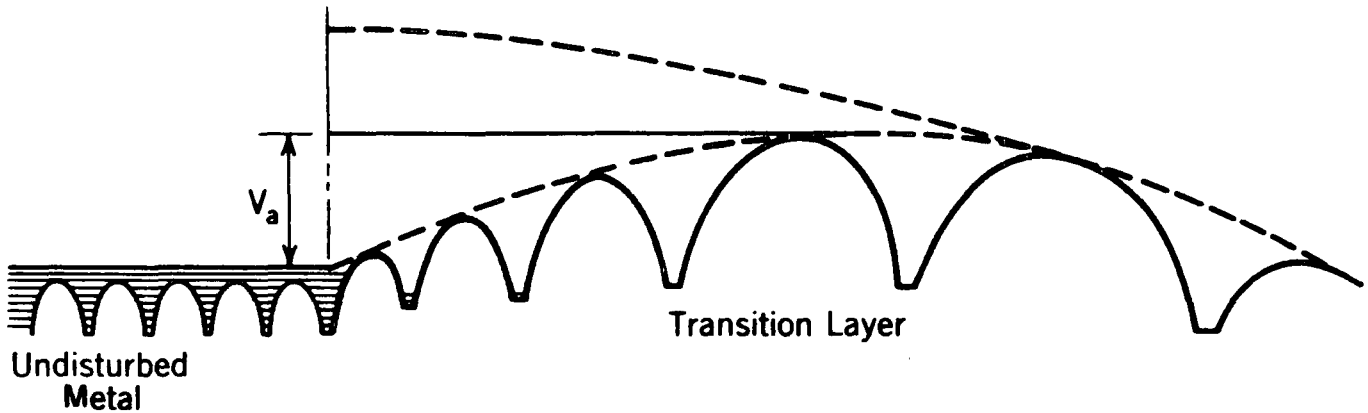

FIG. 8 LONGINI'S MODEL WITH ELECTRIC FIELD

For this wave-function eq (4.16) becomes

$$\frac{d^2U}{dx^2} + 2k\frac{dU}{dx} + \left(\frac{2m}{\hbar^2}\right)(E-E_k-V)U = 0 \qquad (4.18)$$

where;

$$E_k = \frac{\hbar^2 k^2}{2m}$$

The second term in the equation is the imaginary damping term in the equation. It changes the phase of the solution, as a function of the slowly increasing lattice separation. As for E_k although it will vary in the periodic potential for our purposes, may be taken as constant. Then the variation in the amplitude of ψ can be predicted from the evaluation of the third term. The amplitude U and therefore of ψ will be proportional to the inverse square root of the wavelength in U which is simply the lattice pitch. A classical approach can be used to visualise the model with the aid of following figures:-

Fig. (5) is a classical picture of the metal-vacuum interface. Fig. (6) shows the image-charge correction. Fig. (6a) is the potential curve due to the applied electric field. Fig. (6b) shows the summation of the curves, representing the Schottky, or if the applied field is sufficiently high, the Fowler-Nordheim effects. Fig. (7) represents the potential barrier of the interface due to increasing lattice pitch. Fig. (8) shows how it is thought that summation of Fig. (7) and Fig. (6a) could reduce the work function.

A slowly increasing lattice pitch results in slowly increasing potential curve as opposed to the steeply increasing potential barrier at the vacuum-metal interface. Thus a bigger reduction in the potential barrier is possible with electric fields of the same order of magnitude when increasing lattice pitch is introduced. Therefore if we consider the potential at a distance x from the surface, it will be due to the sum of two effects,

a) the average potential depression between two ions, which is proportional to the inverse of the lattice pitch.

This is a coulomb potential well. Longini suggests it could be expressed as

$$V_1 = Ajx^{-1} \tag{4.19}$$

the coefficient of proportionality being higher as the current density is increased.

b) The cathodic sheath electric field. Longini regards the penetration of this field as an effect of resistivity, due to increasing lattice imperfection, and again assumes a linear law with the coefficient of proportionality proportional to the current density. The resistivity ρ is then

$$\rho = Bjx \quad \text{with} \quad E = \rho jx \tag{4.20}$$

and $dE/dx = V_2 = 1/2\ Bj^2x^2$

Adding up the two effects we get

$$V = V_1 + V_2 = 1/2\ Bj^2x^2 + Ajx^{-1} \tag{4.21}$$

and differentiating to find the minimum,

$$dV/dx = Bj^2x - Ajx^{-2} \tag{4.22}$$

which is zero for

$$x = x_{critical} = A\ 1/3\ j^{-1/3} \tag{4.23}$$

The decrement in the work function

$$V(x_{cr}) = \frac{3}{2} A^{2/3} B^{1/3} j^{4/3} \qquad (4.24)$$

With this sort of relation, there must be an upper limit to the current density. Certainly the relation would become physically meaningless if $V(x_{cr})$ is greater than the work function itself. In this case it may be that the solid state random current density is the maximum limit.

Without any further knowledge of the constants involved in the above equation, conclusive comments are not possible except to say that if a plausable mechanism could be found for the formation of positive ion layers with an increasing lattice pitch and with very slow motion of these positive ion layers so that the individual electrons see an almost static picture, the wave analysis could be applied with more confidence and we would be a step nearer to the solution of this puzzling phenomenon.

CHAPTER FIVE

5. EXPERIMENTAL APPROACH

5.1 Object of the Present Investigation

5.2 Criteria for the Experimental Design

5. EXPERIMENTAL APPROACH

Unfortunately, the very small dimensions of the arc cathode spot, 10^{-2} - 10^{-3}cm Ref.(48) and the very fast and apparently random motion of the spot 10-10^{3}cm/sec Ref. (48), together with the emission of large amounts of vapour makes direct observations of the spot difficult. The uncertainty in measuring the temperatures of cathode spots, together with the relatively scarce and sometimes inconsistent information about constants and coefficients used in the equations of the proposed models and theories do not render it possible to verify these theories experimentally in a detailed quantitative way or even to distinguish between them experimentally.

However, there seems at least to be common agreement in the literature that the presence of the metal vapour is essential for the burning of the arc. Also a strong correlation between emission of vapour and clustering of spots has been reported by Zykova Ref. (48). His results confirm that highly mobile spots have high local vapour densities and dissipation of energy in these spots is extremely local in nature, so that the metal is rapidly and locally heated to a temperature at which intense evaporation gives high vapour densities in the cathode spot. The rise of cathode spot temperature is limited by large energy loss on metal evaporation.

Thus, as one might have expected, the very fast motion of the spots cannot be interpreted as a proof that there is neither time nor sufficient energy to evaporate the cathode material. Also the fact that in arc discharges the cathode fall voltage lies between the ionization potential of the gas and the cathode material strongly suggests that presence of vapour is essential. Von Engel Ref. (20) suggests that with the heat released through low speed ion bombardment of the cathode, direct evaporation of a thin surface layer could occur rather than actual melting. Spectroscopic work seems to confirm this,

Ref. (20). Rothstein Ref. (40) also suggested that a region of perhaps 10^{-5}cm thickness of very dense metallic vapour is formed near the cathode and that a vapour cloud is maintained by ion bombardment of the cathode.

Plesse Ref. (25) also concluded from his experiments that if metal vapour was formed at the cathode in sufficient quantities a glow would change into an arc. He also records the occurrence of high frequency oscillations in the glow-to-arc transition, in the range 10^{5} to 2×10^{6} Hz depending on circuit parameters.

There is also much evidence of existence of metal vapour in the cathode region from spark studies conducted by various workers. These studies establish that copious evaporation of metal from the cathode occurs often in the form of luminous clouds of excited vapour. There has been a number of investigations of these "vapour jets", Ref. (50) Since the measured and calculated speeds are too high, it is difficult to account for them as jets of positive ions.

Furthermore, there have been reports of discontinuous metal vapour emission by Craggs and Hopwood, Ref. (51) and several other investigators Ref. (52). There have also been reports of droplet ejection from the cathode of a liquid mercury discharge. D.J. Airey et. al. Ref. (53) record that "at the cathode of the mercury discharge the intense localised heating of the mercury surface causes ejection of cathode material in the form of both vapour and droplets". In their work, which was an investigation into the abnormal glow discharge in mercury and xenon, A.J.T. Holmes and J.R. Cozens, Ref. (54) also suggests that the gas density increases towards the cathode.

5.1 Object of the Present Investigation

There is in fact wide agreement that as a result of intensive local heating, liquid metal is observed on the surface of solid metallic

cathodes with a vapour cushion next to it, while in the case of liquid cathodes a dense vapour cushion is present at the cathode spot. It is also agreed that the cathode spot has unusual properties. There exists some kind of 'patch' where matter is in a transition state which is between solid and plasma or liquid and plasma. It is possible that a continuous transition from undisturbed cathode material to 'normal' plasma, takes place. It seems reasonable to assume that in the volume of the discharge, starting from a very dense saturated vapour next to the cathode spot a slow continuous transition to the plasma state in the positive column of the discharge takes place.

Low temperatures observed in the cathode region of metal vapour arcs have been estimated to be less than 1000K and the pressures of the dense metal vapour cushion next to the cathode are thought to be near the corresponding vapour pressures. One of the assumptions made in 'cold-cathode' arc theories and models is that this dense metal vapour cushion must be an insulator. When theoretical electrical conductivities, using classical discharge theory and Saha's equation based on thermodynamical equilibrium considerations, are worked out, they indeed yield very low values of electrical conductivity for the temperatures and pressures of interest.

Although there is experimental evidence, to justify using Saha's equation to calculate electrical conductivities of vapours at elevated temperatures, there seems to be no experimental evidence recorded in the literature to support or contradict such theoretical calculations at low temperatures apart from the work of Endean and Christopoulos Ref. (55).

It would seem that it is vitally important to establish at least the electrical behaviour of the metal vapour in the temperature and pressure regime thought to be applicable to the dense vapour cushion next to the cathode spot. This should be investigated and fully

understood as a first step towards an acceptable cold-cathode arc model or theory.

5.2 Criteria for the Experimental Design

As has been mentioned in the previous section, an experimental investigation was carried out on caesium vapour by Endean and Christopoulos, at medium pressures and low temperatures, ($P \cong 0.3 - 2.10^3$ Pa and $T_1 \cong 600 - 1100$K.). Caesium vapour was chosen because of its low boiling point and low ionization potential, to facilitate a wide range of easily attainable temperatures and pressures and sufficient ionization at low temperatures for measurable electrical conductivities to be produced. Since the results seemed to indicate that the ionization potential was not a dominant factor at all, the next logical step was to investigate a metal vapour with a much higher ionization potential but still with a low boiling point.

These considerations led to the choice of mercury with an ionization potential of 10.4eV Ref. (56), much higher than the ionization potential of caesium 3.9eV Ref. (57), and a low boiling point 356.58°C, (≅ 629K). Von-Engel Ref. (20) reported that the surface temperature of the mercury cathode spot is 360°C and the dense vapour cushion next to it ≅ 600°C. The criteria for the design of the test apparatus was that the apparatus could be used over the temperature range 300K - 900K, and also that the mercury vapour pressure could be accurately controlled and measured. To justify the use of Saha's equation for theoretical calculations, design of the apparatus and experimental conditions has to be such that local thermodynamic equilibrium was attained. A plasma in a state of local thermodynamic equilibrium is a plasma in a state of complete thermodynamic equilibrium within each small volume element chosen large in comparison with the mean free path. Thus, for several theoretical and practical reasons, a large interelectrode gap and a low electric field were considered appropriate.

CHAPTER SIX

6. APPARATUS AND EXPERIMENTAL METHOD

6.1 Experimental Assembly

6.2 Electrical Connections

6.3 Experimental Method

6. APPARATUS AND EXPERIMENTAL METHOD

6.1 Experimental Assembly

Fig. (9) shows a pyrex vacuum chamber. The chamber contains the experimental assembly, which consists of the test tube, thin stainless steel radiation shields, the cylindrical heating unit and two chromel-alumel thermocouples. In order to conduct the investigations in the temperature range desired, high temperature glass had to be used. Due to difficulties in achieving metal to glass vacuum seals in pyrex, the part of the tube which had to be sealed with the tungsten metal pin electrode (which was needed for electrical contact with the mercury pool), had to be constructed from soda glass.

The lower end of the tube was used as a mercury reservoir and the desired pressure range could be attained within the working temperature range ($\lesssim 300^{o}C$) of the soda glass. The upper part of the test tube was placed inside a cylindrical heating unit, which was constructed by winding a length of resistance wire on a grooved re-crystallised alumina tube (see Fig. 9). The radiation shields were arranged so as to obtain a sharp temperature gradient just above the mercury reservoir, thus keeping the mercury reservoir temperature lower than the rest of the tube.

The top of the tube was covered by a steel cap which had "O" ring grooves and was clamped to the tube by using a "C" clamp to make it vapour tight. A hollow stainless steel tube passed through the middle of the cap and had a flat circular electrode fitted to its lower end. Mercury vapour could escape slowly through a small hole in the electrode (see. Fig. 9), passing through the hollow stainless steel tube and condensing in the tubular attachment. This arrangement allowed the tube to be evacuated at room temperatures while at the same time ensuring that significant quantities of mercury could not escape from the vacuum chamber.

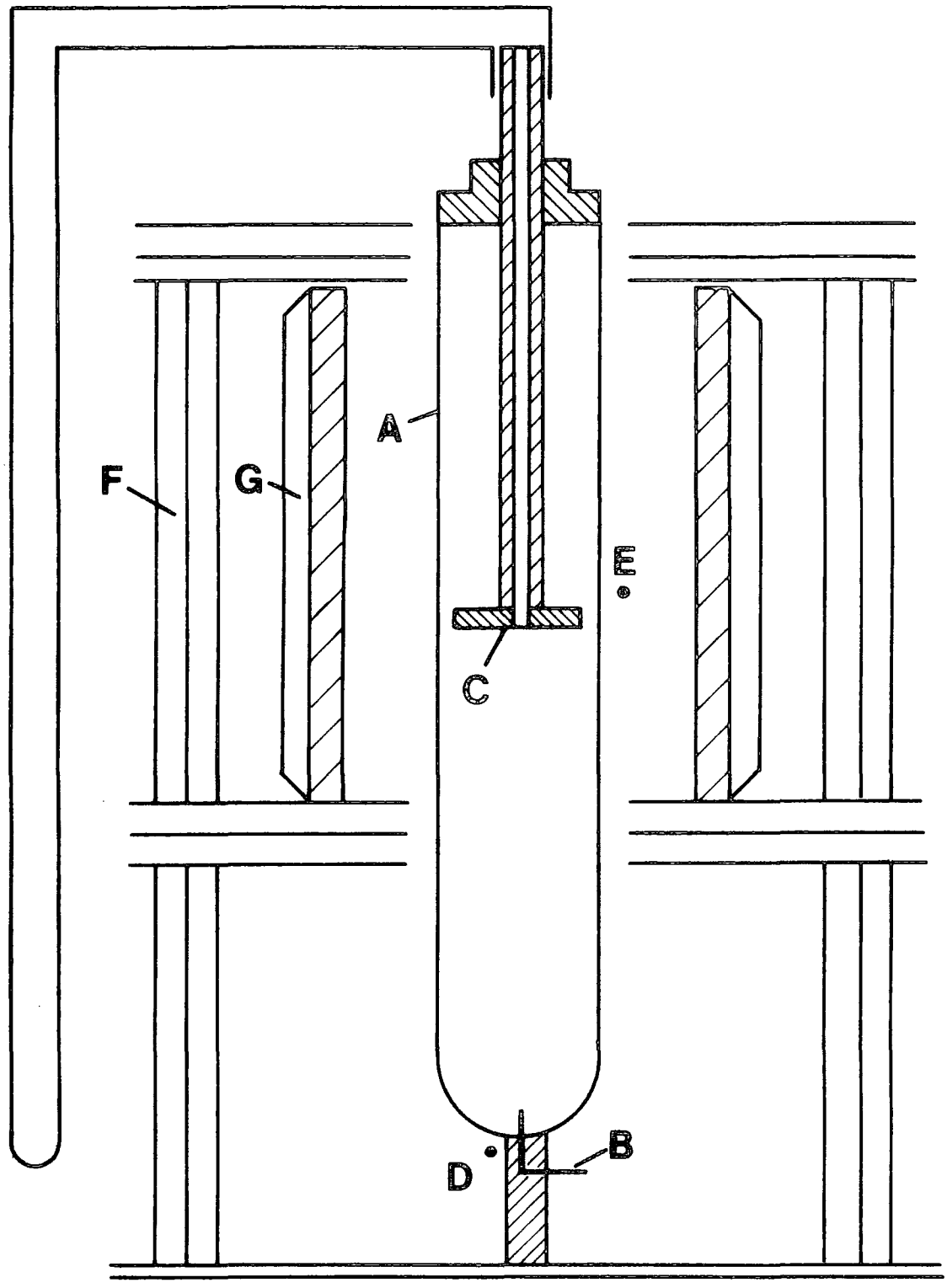

FIG.9 EXPERIMENTAL ASSEMBLY.

A - Discharge tube ; B - Tungsten pin electrode ;
C - Upper electrode ; D, E - Thermocouples ;
F - Radiation shields ; G - Heater unit .

The experimental assembly was seated on a metal platform with a locating hole to house the glass stalk attached to the lower end of the test tube. This arrangement was used to hold the tube upright and to centre it in the heating unit and the assembly. The metal platform was suspended using three metal rods, from the circular aluminium-cap covering the top end of the pyrex-vacuum chamber.

The aluminium cap had an "O" ring groove cut on the inside surface, and holes for the electrical feedthrough fittings had been bored through it. The electrical feedthrough fittings all had high vacuum seals.

No arrangements were made to clamp the cap to the rims of the pyrex-vacuum chamber. The weight of the aluminium cap, the smooth and clean contact of the "O" ring and the low temperature of the joint were sufficient to establish a high vacuum seal between the metal cap and the rim of the pyrex-chamber. Standard high vacuum methods were used throughout the experimental investigations.

The top thermocouple was used to monitor the gas temperature 'Tg' and the lower one was used to monitor the mercury reservoir temperature. Considerable care was taken in the latter case to establish a firm contact between the reservoir part of the test tube and the thermocouple. Placing the experimental assembly into a vacuum chamber and evacuating at room temperature also eliminated the problems of oxidation and heat convection currents from one part of the experimental assembly to the other.

6.2 Electrical Connections

Fig. (10), shows the electrical circuit used to measure the conductivity of the mercury vapour. The upper and lower electrodes of the discharge tube were brought out to the external electrical circuit via the electrical feedthrough fittings together with the connections for the heating unit and the connections for the thermocouples. A

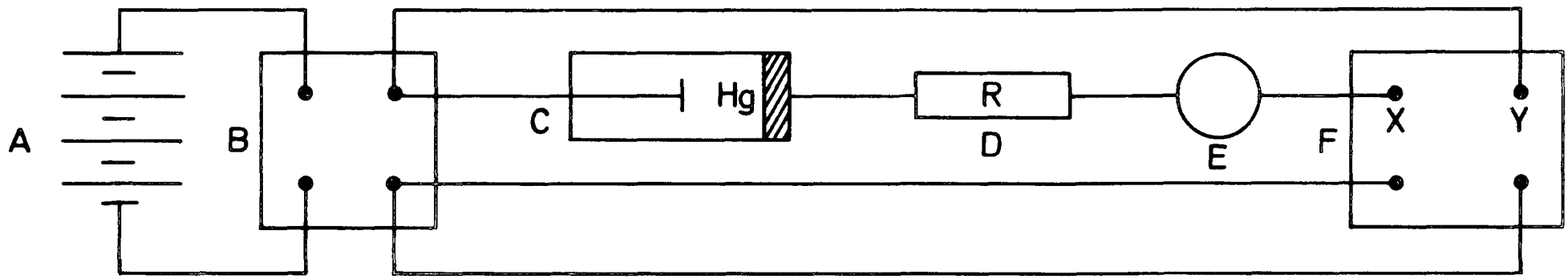

A - D.C. Voltage source ; B - Polarity switch box ;
C - Test tube containing Hg. ; D - Series resistance ;
E - Ammeter ; F - X-Y Plotter.

FIG. 10 ELECTRICAL CONNECTION DIAGRAM OF THE EXPERIMENT

stabilised d.c. supply was used to apply d.c. voltages across the electrodes. The supply was capable of delivering 200mA and 350V d.c. A digital multi-meter was connected in series with the discharge tube to monitor the discharge current. Basic accuracy ± 0.2% of reading, ± 0.1% of range, current range 10pA - 2 A, shunt resistance 10MΩ at 10nA and 1 Ω at 10mA. A one kilo-ohm resistance with one watt power capacity was also inserted into the circuit, in series, for meter protection, in case the discharge went into an arc. The analogue output of the meter was fed into one channel of an X-Y pen recorder, while the voltage across the electrodes was fed to the other. Simultaneous measurements, of voltage and current were thus possible. Two digital voltmeters were used to monitor the e.m.f. outputs of the two chromel-alumel thermo-couples, recording vapour temperature 'T_g' and liquid reservoir temperature 'T_l' respectively to an accuracy of ±0.75%. The accuracy of the multimeters used to monitor the e.m.f. outputs of the thermocouples was 0.04% for the ranges used in the measurements.

6.3 Experimental Method.

The experimental assembly was evacuated by the rotary pump to a pressure lower than 10^{-1} Pa - ultimate vacuum without gas ballast $> 10^{-2}$ Torr with gas ballast 5×10^{-2} Torr - at room temperature, to prevent oxidation problems and also to eliminate heat convection currents between different parts of the experimental assembly. Then the heater was switched on. The arrangement of the radiation shields kept the mercury reservoir temperature 'T_l' at a lower temperature than the mercury vapour temperature 'T_g'. The equilibrium temperature of the glass wall around the liquid mercury reservoir was recorded and the vapour pressure read from the tables (see table 1). When the desired vapour pressure and temperature had been reached, a d.c. voltage was applied up to 300-350V d.c. (For the large electrode gap used, the minimum breakdown

VAPOR PRESSURE OF MERCURY

Vapor pressure of mercury in mm. of Hg for temperatures from −38 to 400°C. Note that the values for the first four lines only, are to be multiplied by 10^{-6}

Temp. °C	0	2	4	6	8
	10^{-6}	10^{-6}	10^{-6}	10^{-6}	10^{-6}
−30	4.78	3.59	2.66	1.97	1.45
−20	18.1	14.0	10.8	8.28	6.30
−10	60.6	48.1	38.0	29.8	23.2
− 0	185.	149.	119.	95.4	76.2
+ 0	.000185	.000228	.000276	.000335	.000406
+10	.000490	.000588	.000706	.000846	.001009
20	.001201	.001426	.001691	.002000	.002359
30	.002777	.003261	.003823	.004471	.005219
40	.006079	.007067	.008200	.009497	.01098
50	.01267	.01459	.01677	.01925	.02206
60	.02524	.02883	.03287	.03740	.04251
70	.04825	.05469	.06189	.06993	.07889
80	.08880	.1000	.1124	.1261	.1413
90	.1582	.1769	.1976	.2202	.2453
100	.2729	.3032	.3366	.3731	.4132
110	.4572	.5052	.5576	.6150	.6776
120	.7457	.8198	.9004	.9882	1.084
130	1.186	1.298	1.419	1.551	1.692
140	1.845	2.010	2.188	2.379	2.585
150	2.807	3.046	3.303	3.578	3.873
160	4.189	4.528	4.890	5.277	5.689
170	6.128	6.596	7.095	7.626	8.193
180	8.796	9.436	10.116	10.839	11.607
190	12.423	13.287	14.203	15.173	16.200

Temp. °C	0	2	4	6	8
200	17.287	18.437	19.652	20.936	22.292
210	23.723	25.233	26.826	28.504	30.271
220	32.133	34.092	36.153	38.318	40.595
230	42.989	45.503	48.141	50.909	53.812
240	56.855	60.044	63.384	66.882	70.543
250	74.375	78.381	82.568	86.944	91.518
260	96.296	101.28	106.48	111.91	117.57
270	123.47	129.62	136.02	142.69	149.64
280	156.87	164.39	172.21	180.34	188.79
290	197.57	206.70	216.17	226.00	236.21
300	246.80	257.78	269.17	280.98	293.21
310	305.89	319.02	332.62	346.70	361.26
320	376.33	391.92	408.04	424.71	441.94
330	459.74	478.13	497.12	516.74	537.00
340	557.90	579.45	601.69	624.64	648.30
350	672.69	697.83	723.73	750.43	777.92
360	806.23	835.38	865.36	896.23	928.02
370	960.66	994.34	1028.9	1064.4	1100.9
380	1138.4	1177.0	1216.6	1257.3	1299.1
390	1341.9	1386.1	1431.3	1477.7	1525.2
400	1574.1	.....	.....	.....	.....

TABLE 1

potentials reported in the literature were 360-385 V d.c.) It was possible to make simultaneous measurements of the voltage and current using an X-Y pen recorder to record the VI characteristics of the discharge.

CHAPTER SEVEN

7. RESULTS

7.1 Description of the Measurements

7.2 Analysis of the Results

7.3 Accuracy and Reliability

7. RESULTS

7.1 Description of the Measurements

The pre-breakdown electrical conductivities of a nearly saturated mercury vapour were calculated from the experimentally plotted voltage/current characteristics, over a range of vapour temperatures and pressures. The vapour temperature was varied between 600 and 900K, while the vapour pressure was varied between 0.1 Pa and 10^4 Pa, corresponding to reservoir temperatures between 300K and 600K.

During the measurements, a d.c. voltage source was used to take the discharge up to the breakdown region, while the current flowing through the discharge tube was monitored and recorded. The experimental set-up facilitated recording the voltage-current characteristics with an X-Y plotter, with simultaneous monitoring of the vapour pressure and temperature. The slopes of the voltage/current characteristics in the pre-breakdown region of the discharge were then multiplied by the cross-sectional area of the mercury column (taken as approximately equal to the cross-sectional area of the discharge tube), and divided by the inter-electrode separation, to yield values for the pre-breakdown electrical conductivities of the mercury vapour at different vapour pressures and temperatures.

For small currents through the discharge tube, there was no experimental evidence of a substantial sheath potential, and therefore the effect on the calculated values was not considered. Fig (11) is a typical voltage current characteristic. Voltages of up to 350V d.c. were applied, to take the discharge up to the breakdown region, (the minimum breakdown potential for mercury is quoted to be 330-380V d.c. in the literature Ref. (58), (59) (60)). During the measurements, currents varying from tens of nA up to several mA were measured depending on the experimental conditions (electrode separation, pressure, temperature).

For small applied voltages, the discharge behaved as a constant

resistance, there was a slight change of slope at points C and P, Fig (11), respectively as the applied voltage was increased. The resistance was generally approximately the same whether the upper electrode (hot) or the lower electrode (cold/reservoir) was treated as the cathode, and when different did not show any significant correlation to the other experimentally measured quantities.

The voltage step was not significant when the polarity was reversed in increasing the applied voltage, when the upper (hot) electrode was treated as the cathode, a point 'A' was reached, where the slope of the characteristics would suddenly undergo a significant increase. Further increase in the applied voltage resulted in a new straight line, up to point 'B', after which the current through the discharge started increasing more rapidly. Beyond this point the discharge would sometimes start to glow. The glow could be visually observed surrounding the upper (hot) electrode. The experimental set-up did not permit visual observation of the rest of the discharge tube. The corresponding voltage/current characteristic when the glow was visually observed was not that of a "normal" glow, Fig. (12) and Fig. (13) are also representative of the voltage/current characteristic when a glow around the top electrode was visually observed. The discharge was prevented from going into the arc mode for instrument protection by using a series resistance in the measuring circuit, thus ensuring that the discharge did not short the measuring instruments. Sometimes, as in Fig. (14) the discharge would go through a non-conducting region, until point "P" was reached. Then the current would increase suddenly and at point "C" it would settle into a straight line until point "A" where the characteristic would again undergo a change in the slope and follow another straight line. This continued until point "B" was reached, after which the discharge would always experience a transition to a glow which could also be observed visually. This type of characteristic was obtained at high vapour pressures and temperatures.

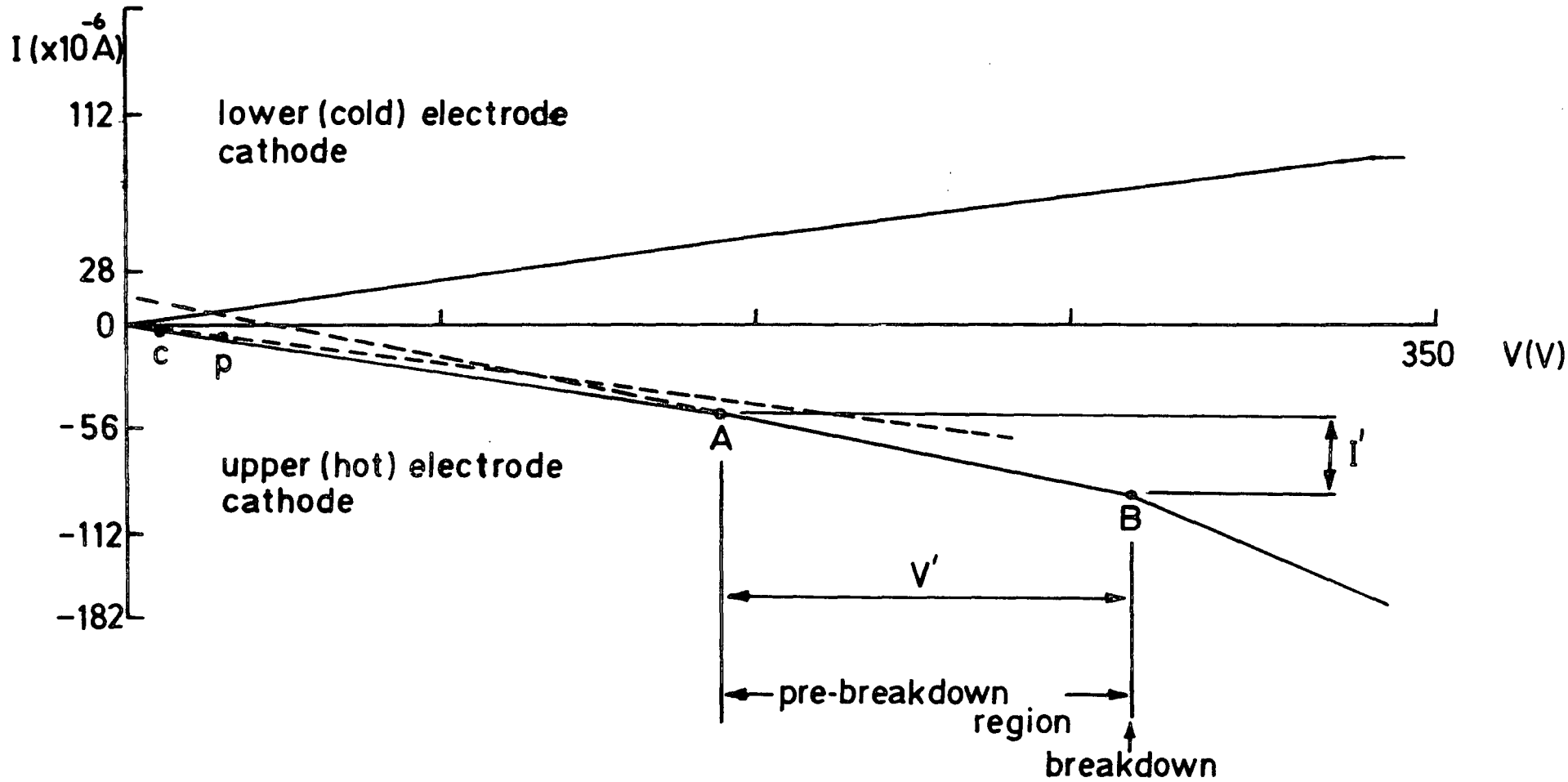

FIG. 11 DISCHARGE VOLTAGE – CURRENT CHARACTERISTICS

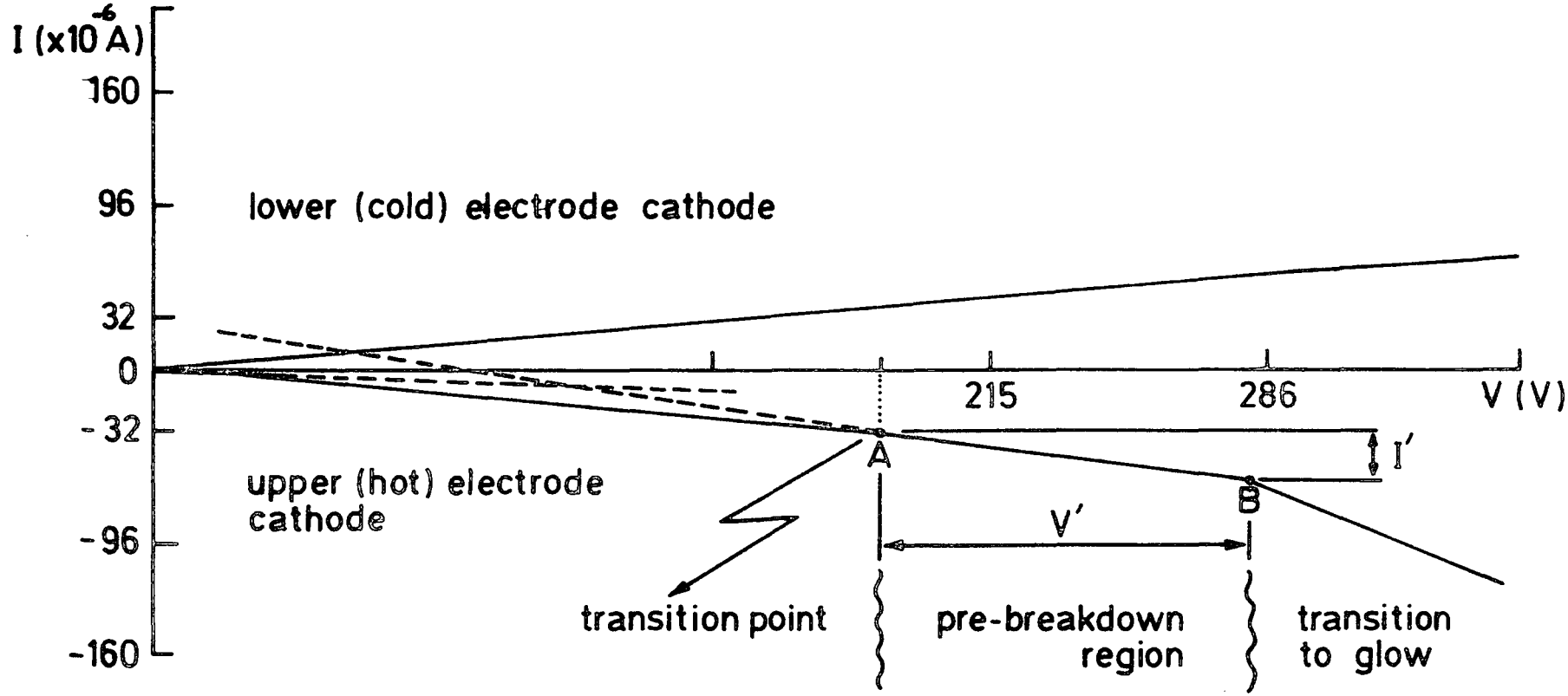

FIG. 12 DISCHARGE VOLTAGE - CURRENT CHARACTERISTIC

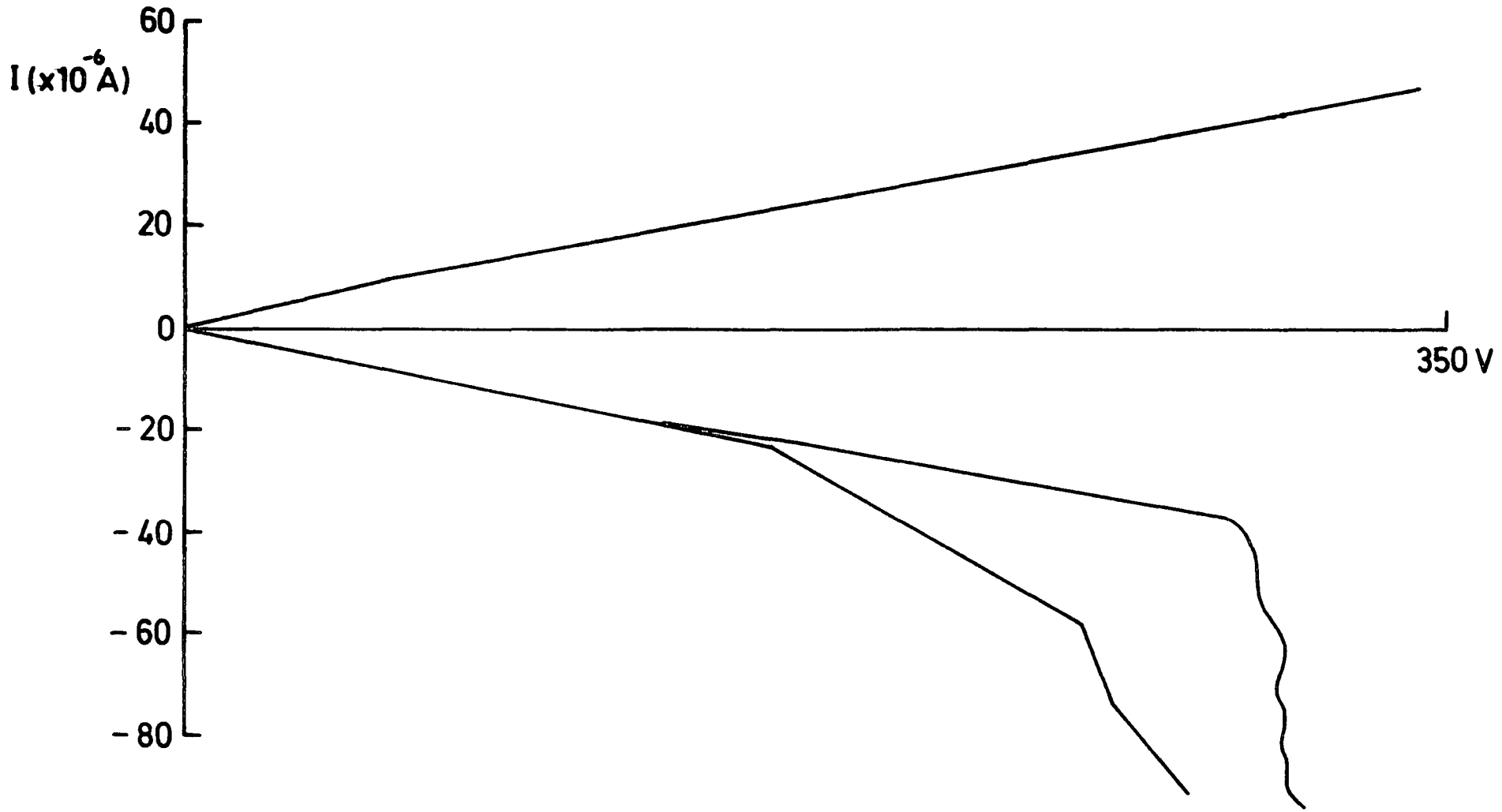

FIG. 13 DISCHARGE VOLTAGE - CURRENT CHARACTERISTIC

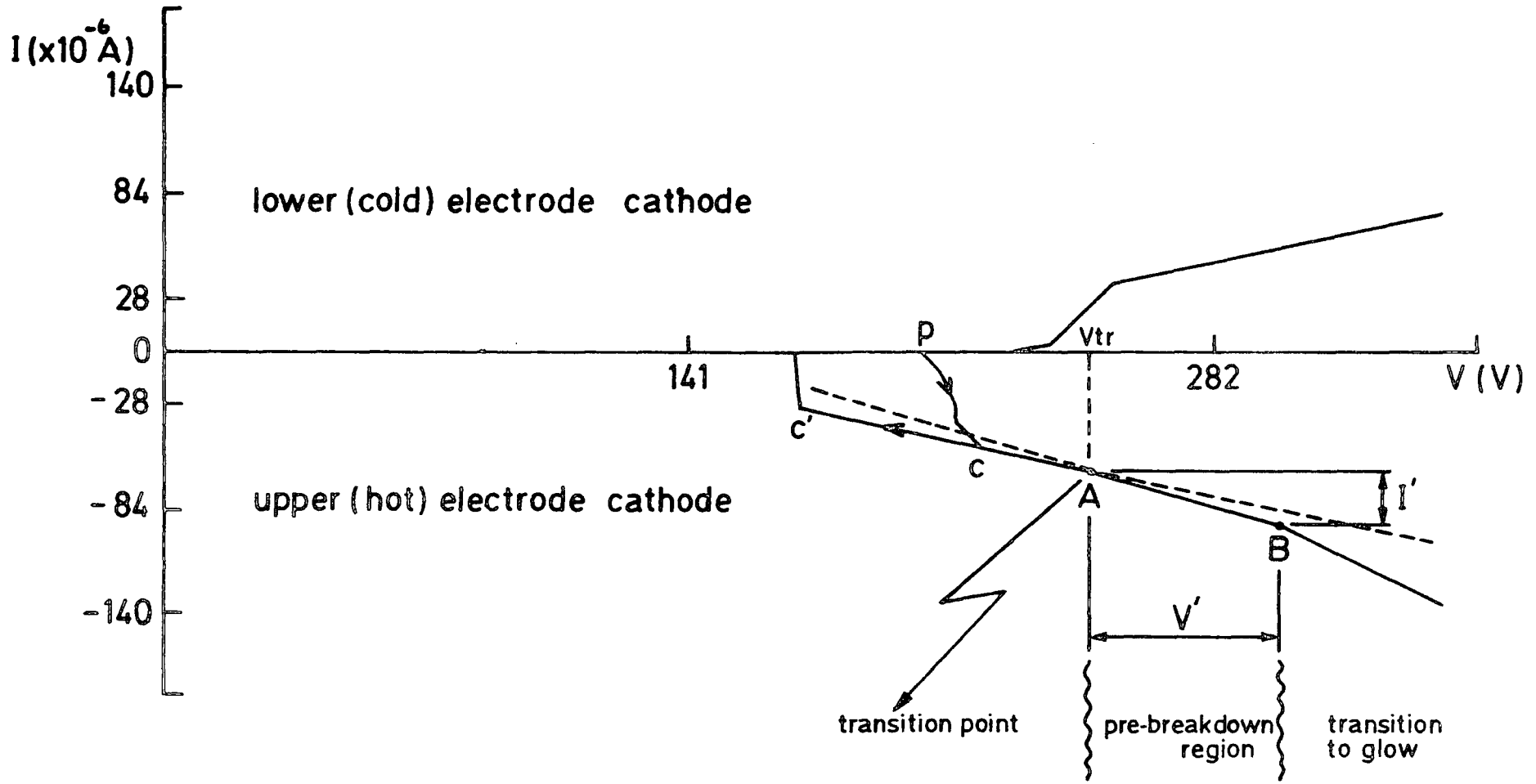

FIG. 14 DISCHARE VOLTAGE - CURRENT CHARACTERISTIC

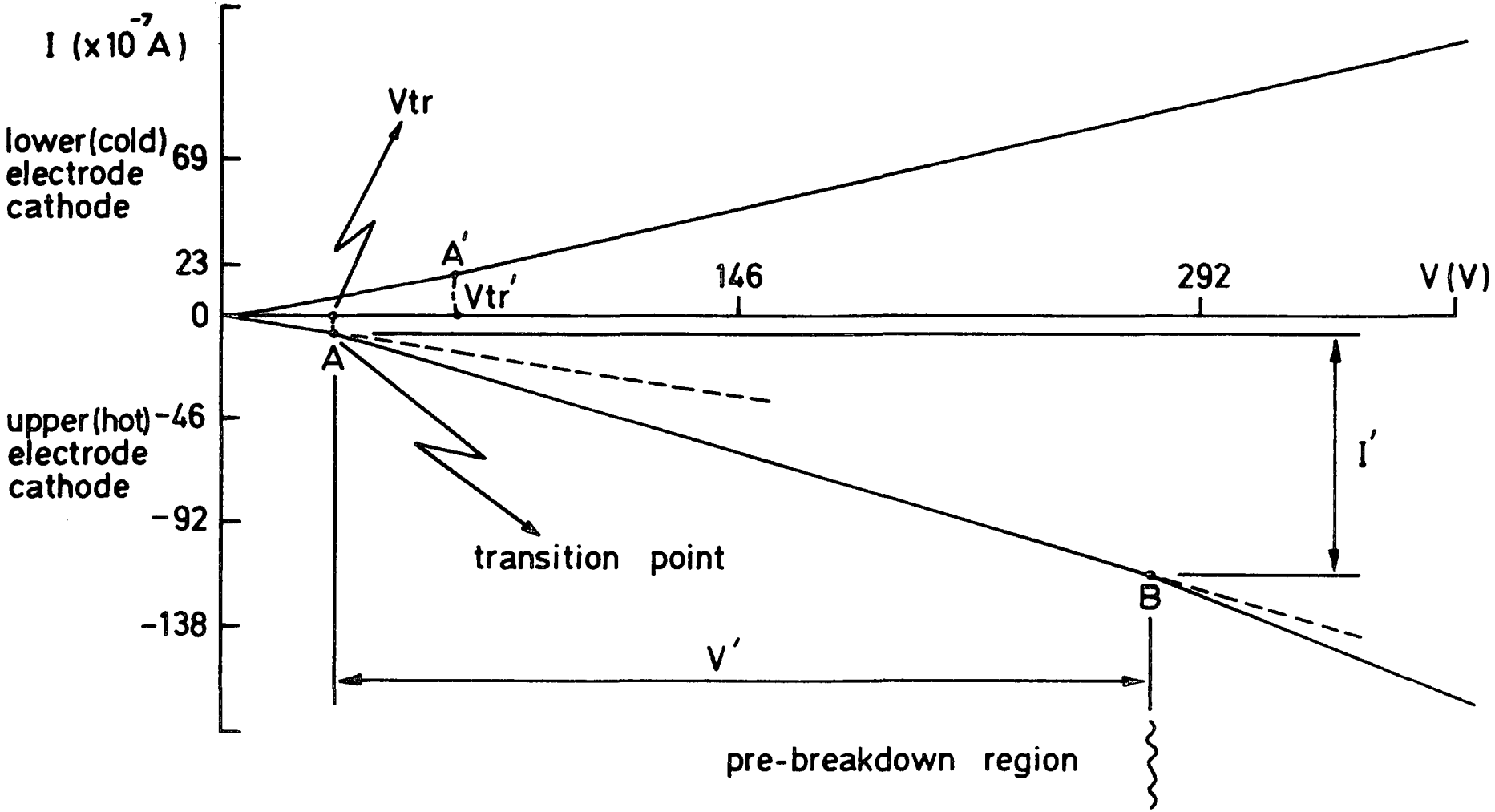

FIG. 15 DISCHARGE VOLTAGE - CURRENT CHARACTERISTIC

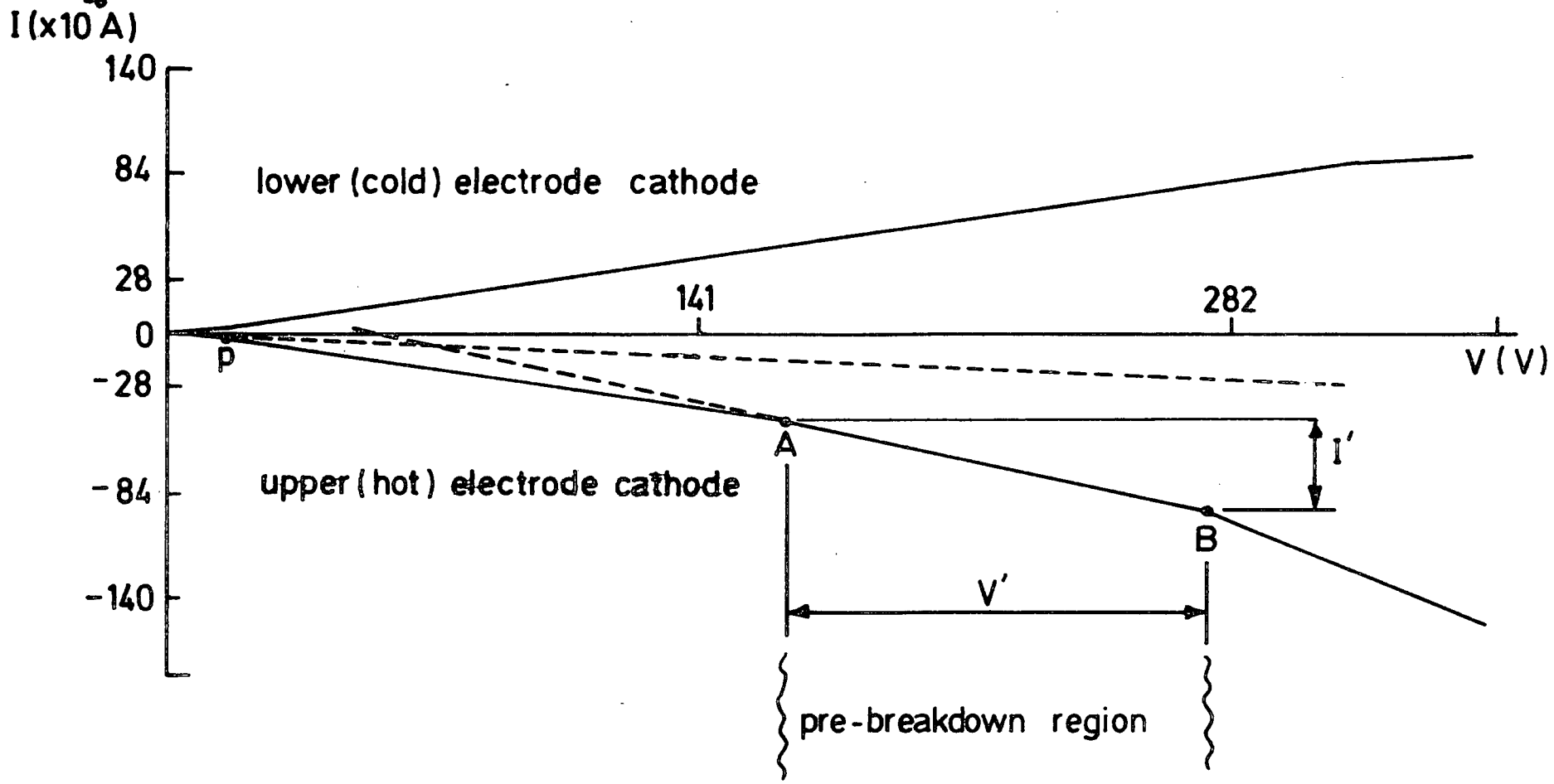

FIG. 16 DISCHARGE VOLTAGE - CURRENT CHARACTERISTIC

With the lower (cold/reservoir) electrode as the cathode, the discharge, after the initial constant resistance up to the transition point A, would rarely depart from the initial straight line, Fig. (15), except at high values of T_l (vapour pressure). Then the behaviour of the characteristic would be similar to that with the upper electrode as the cathode, Fig. (14). The slope of the straight line after A' would be approximately the same, but usually accompanied by a higher transition voltage (Fig. (14), Fig. (15)).

In calculating the electrical conductivities, when changes of slope could be detected as in points C and P Fig. (11), the initial straight line DC was interpreted as being due to the wall leakage currents in parallel with the normally expected current due to charge collection at low applied voltages. The straight line CP was then taken as being due to the saturation current in parallel with the wall leakage current. Further increase in the slope after point P up to point A was then attributed to the initiation of charge multiplication (primary ionization coefficient "α").* Finally the section AB of the characteristic was taken as the region where the primary charge multiplication was being supplemented by some secondary processes, i.e., the pre-breakdown region. Therefore the section AB was considered, as the slope that should be used for calculating the pre-breakdown electrical conductivity. The slope of the line AB V'/I' was taken to be the resistance of the discharge itself in parallel with the wall leakage resistance. When the leakage currents were thought to be considerable they were subtracted from the measurements, (see Fig. (16)). The main criterion was to use the last change in the slope as the applied voltage was increased (before the glow when it was visually observed). It was further assumed that the effect of the sheath resistance on the slope AB was negligible since the error introduced by this assumption would fall within the error limits

---

* i.e. avalanche effect - Townsend's first coefficient "α".

of the calculated values for the present investigation. The value of the transition voltage V_{tr} showed no significant correlation with the other experimentally measured values.

It should also be mentioned that the voltage/current characteristics of the discharge tube differ from the "normal" voltage/current characteristics of gas discharges as described in standard text-books, in that they do not exhibit a constant current region (saturation region) independent of the applied voltage. Neither, strictly speaking do they exhibit a clearly defined Townsend region in the sense that they do not show a sudden increase in current independent of the applied voltage, only to be limited by the internal resistance of the d.c. voltage source (with the possible exception of the cases where the discharge suddenly started conducting without going through the usual constant resistance region, see fig. (14)). Another clearly defined feature was that when it was possible for the glow to be observed, the corresponding voltage-current characteristics were similar to those of an abnormal glow.

The measureable range of conductivities was limited at the lower extreme at $= 3 \times 10^{-7} \Omega^{-1}\text{-m}^{-1}$ by the fact that the wall leakage currents appeared to be dominant since it was not possible to detect reliably the change of slope at point A; and at $10^{-3} \Omega^{-1}\text{-m}^{-1}$ at the higher extreme by the discharge going into the glow region.

In the calculations that followed the measurements the mercury vapour pressure was determined by the recorded liquid reservoir temperature and the published mercury vapour pressure data see table (1). Vacuum instrumentation was available down to 10^{-3} mm Hg with a pirani-type gauge mounted on the pumping system. The normal pressure of the mercury vapour (at room temperature) is 10^{-3}mm Hg, and according to the published vapour pressure data, rises to atmospheric pressure at about 630K. The number density of the vapour was determined from the following relation

$$P = 1.035 \times 10^{-9} \text{ nT}$$

vapour densities n_1 and n_2 (in cm^{-3}), corresponding to vapour temperatures T_1 and T_2 (in K) respectively were related to each other by

$$\frac{n_1}{n_2} = \frac{T_2}{T_1} \times \frac{P_1}{P_2}$$

Before a series of measurements the vacuum chamber was pumped down to pressures less than 10^{-1} mm Hg, heated to temperatures up to 900K for prolonged periods and then cooled down to desired temperatures for the measurements. Due to the expected vapour leakage from the discharge tube, the system was continually pumped, during the measurements. Regular visual checks ensured that the mercury reservoir was kept at approximately the same level and never significantly depleted due to this leakage. At the same time the discharge tube was also checked for deposits on the wall and kept thoroughly clean.

As a first order approximation, a uniform homogeneously distributed positive column was assumed to fill the volume of the discharge tube up to the reservoir section with the arrangement of the radiation heat shields ensuring a sharp temperature gradient at the boundary.

Normally during the measurements at constant gas temperature the liquid temperature was increased until $(T_g - T_L) \cong 100^{\circ}C$. The difference in the temperatures was never allowed to be less than 100°C, in order to ensure that there would be no liquid mercury deposited on the walls of the discharge tube and thus increasing the degree of confidence in the results.

Calculated $\ln\sigma$ values from the conductivity measurements were then

plotted against the reciprocal of vapour temperatures (T_g) and liquid reservoir temperatures (T_L). Significant variations in the pre-breakdown electrical conductivities were frequently observed with slight changes in (T_g) and (T_L), with no apparent pattern in the distribution of the plotted points and with no significant correlation with (T_l) and (T_g). Repeat measurements were carried out to ensure that the results were real and not due to experimental errors of a random nature or to leakage currents. The discharge tube was then rapidly cooled down and conductivity measurements immediately attempted on the cold discharge tube with negative results, the circuit behaving as an open circuit. It was thought that if the measured conductivities had been due to liquid mercury being deposited on the walls of the discharge tube, surface tension would have kept the liquid deposited on the walls after the tube was cooled down so that it would still have been detectable. Dummy runs with an empty discharge tube was also carried to test the volume conductivity of the discharge tube, again with negative results. The measured currents were not significant.

7.2 Analysis of the Results

From standard theories for the electrical conductivity of a weakly ionised gas (see App. II) for derivation) it was expected that, even if the results were not in full agreement with the quantitative predictions, a good approximation for their behaviour would be governed by an exponential factor, such as

$$\sigma \propto \exp\left(-\frac{eV_i}{2kT_g}\right)$$

similarly, assuming that the momentum transfer cross-section did not depend on the vapour pressure

$$\sigma \alpha \exp\left(-\frac{eV_{evap.}}{2kT_L}\right)$$

where V_i and $V_{evap.}$ are the ionization and evaporation potentials for mercury.

This was not the case. The calculated values did not produce a set of straight lines parallel to each other, and parallel to the $^1/T_L$ axis when plotted as $\ln\sigma + eV/2kT_g$ against $^1/T_L$, with $V_i = 10.4$ eV. However there was one outstanding feature. This was that the experimental values were many orders of magnitude higher than the values that could be predicted by standard theoretical predictions based on Saha's equilibrium analysis for the experimental vapour pressure and temperature ranges.

With the same experimental set-up further measurements were carried out, this time the current through the discharge tube was plotted against T_g and T_L alternatively Fig. (17),(18),(19),(20). As a result the following facts were established. The conductivity depended both on T_L (vapour pressure) and T_g (vapour temperature) by varying degrees in different temperature and pressure ranges. Their relative magnitudes were an important determining factor in influencing this dependency and the magnitude of the conductivity. There were minimum thresholds for this dependency. Conclusions drawn from Fig. (17) to Fig. (20) are summed up in table (2).

Considering both sets of data, and at this point having apparently established that the degree of saturation $(^1/T_L - ^1/T_g)$, is also an important parameter in determining the conductivities, in mercury vapour, as was suggested by Endean and Christopoulos for caesium vapour, it was then decided that $(^1/T_L - ^1/T_g)$ should be treated as one of the variables instead of $^1/T_L$ or $^1/T_g$.

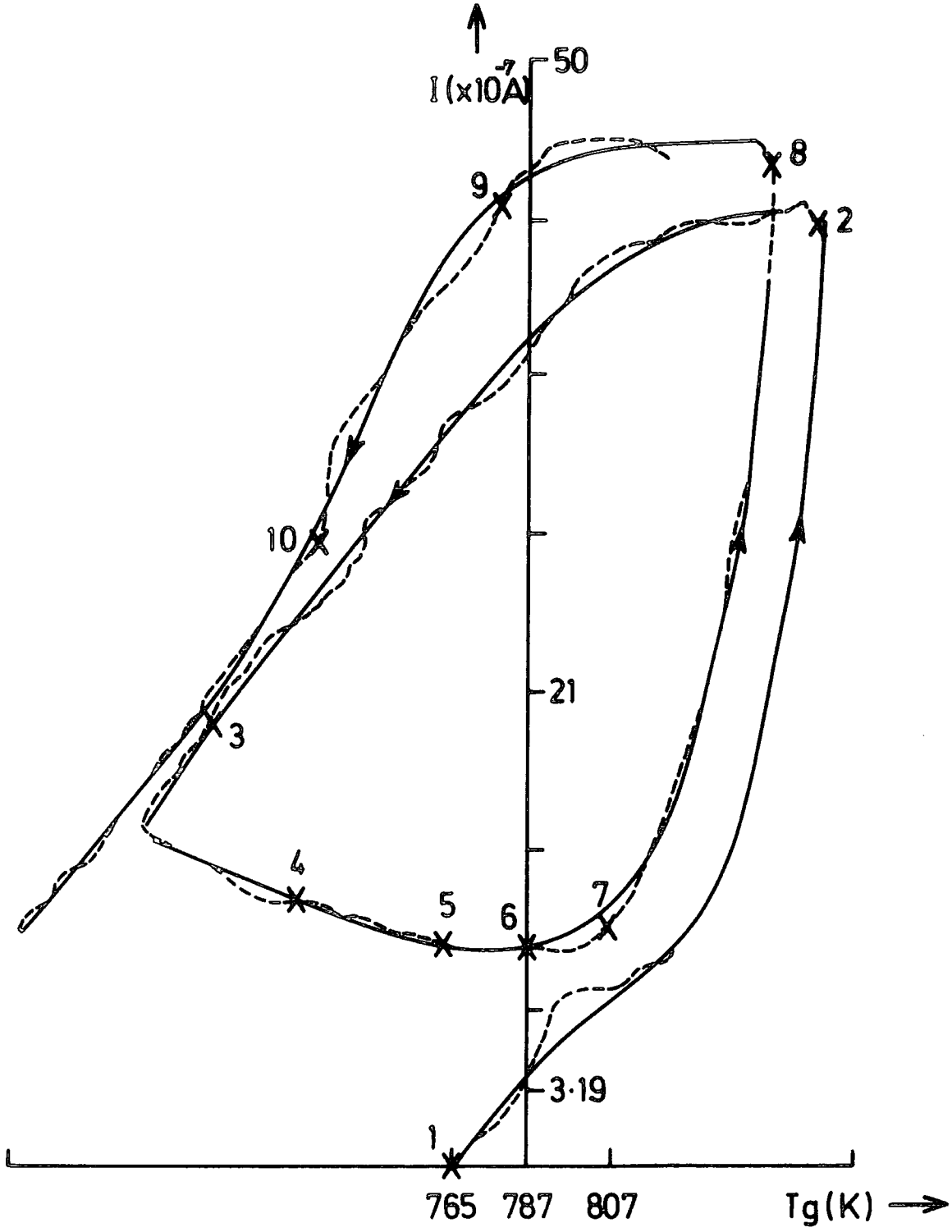

FIG. 17

	T_L(K)	T_g(K)		T_L(K)	T_g(K)
1 –	416	743	6 –	444	785
2 –	485	852	7 –	445	829
3 –	460	692	8 –	470	840
4 –	450	725	9 –	468	777
5 –	446	744	10 –	464	727

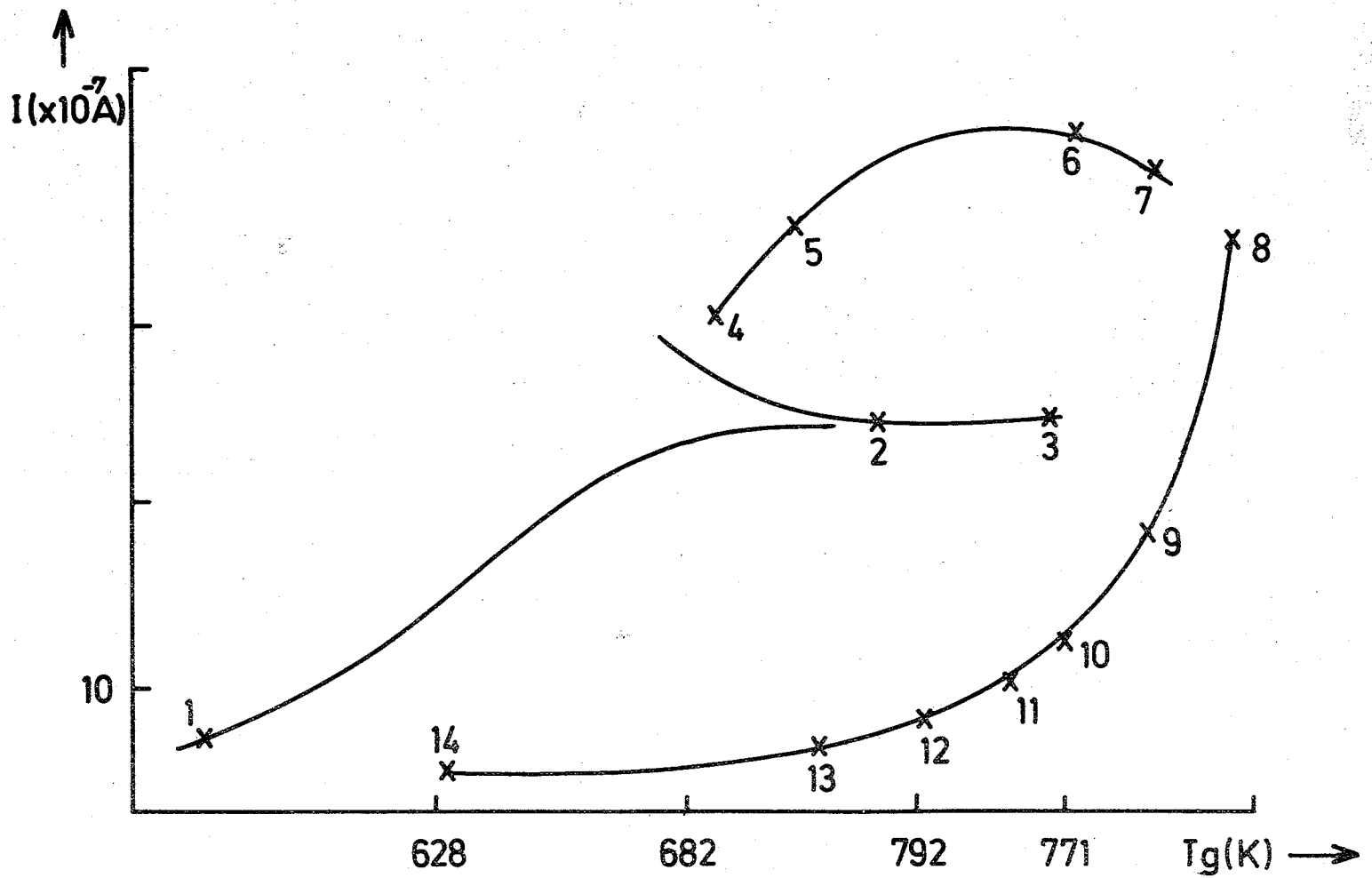

FIG. 18

T_L (K) ; $10^3(\frac{1}{T_L}-\frac{1}{T_g})$	T_L (K) ; $10^3(\frac{1}{T_L}-\frac{1}{T_g})$	T_L (K) ; $10^3(\frac{1}{T_L}-\frac{1}{T_g})$
1 – 5·11 ; 0·77	6 – 6·52 ; 1·01	11 – 5·15 ; 1·19
2 – 6·14 ; 0·97	7 – 6·53 ; 1·02	12 – 5·12 ; 1·17
3 – 6·07 ; 1·07	8 – 6·33 ; 1·08	13 – 4·92 ; 1·15
4 – 6·34 ; 0·90	9 – 8·66 ; 1·14	14 – 4·97 ; 0·94
5 – 6·42 ; 0·90	10 – 8·27 ; 1·19	

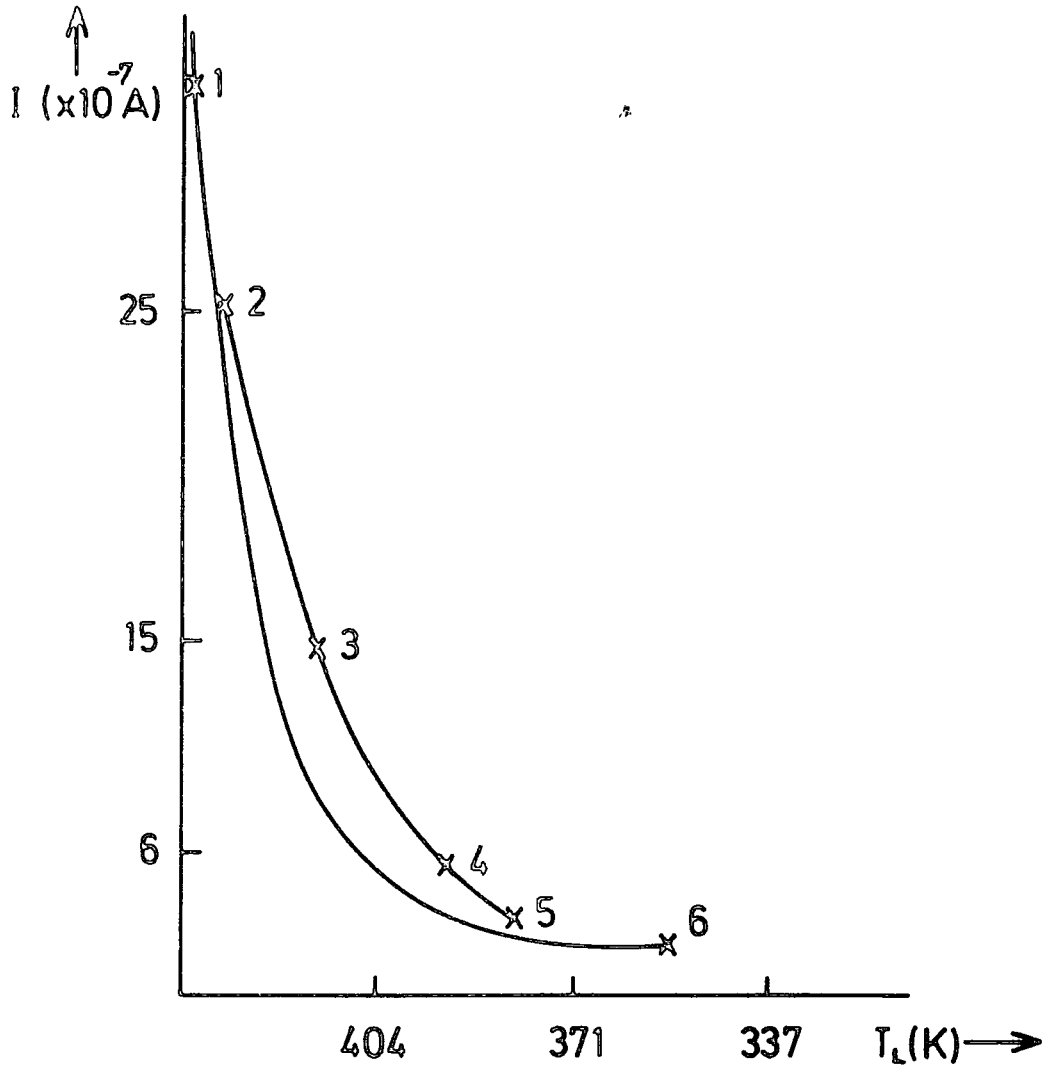

FIG. 19

	T_g(K)
1 —	832
2 —	844
3 —	845
4 —	816
5 —	800
6 —	451

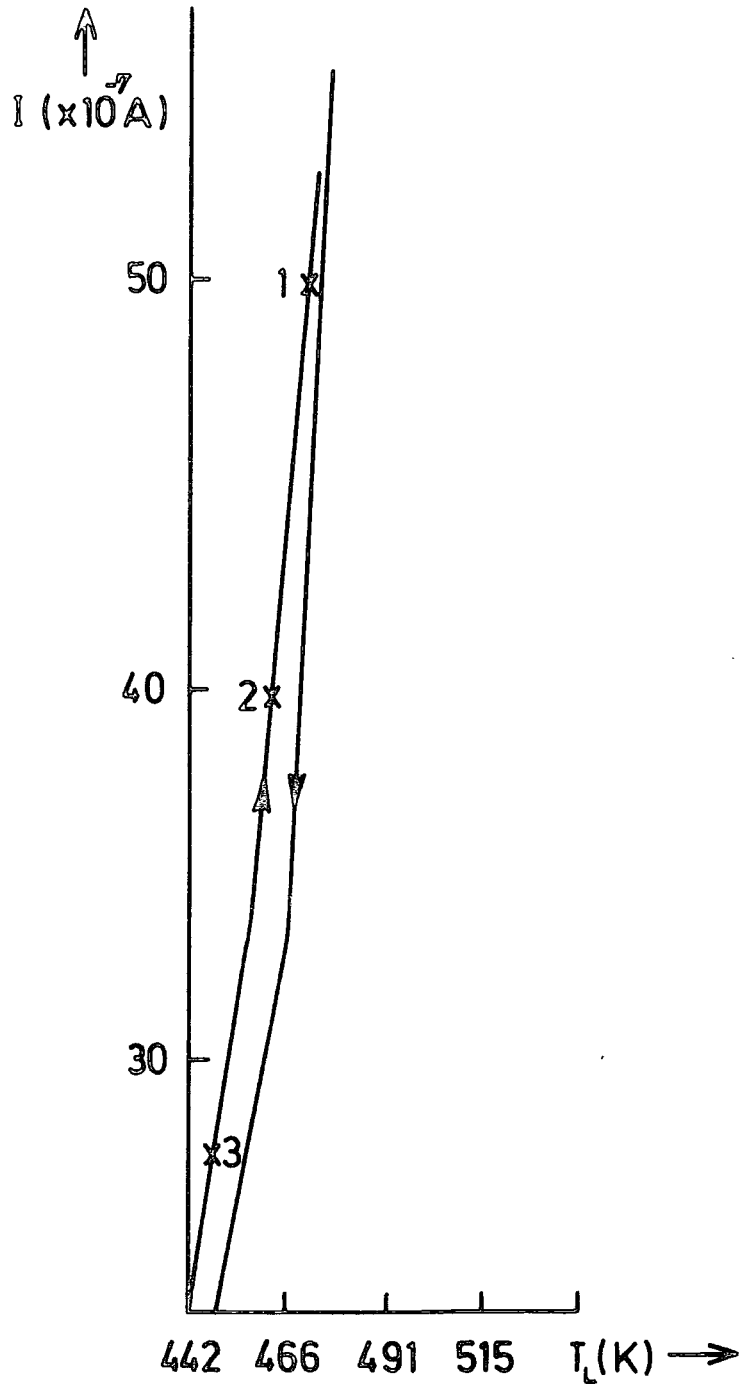

FIG. 20

T_g

1 – 872
2 – 863
3 – 805

				Assuming Constant Crossection
$T_g \searrow$	$T_l \nearrow$	Saturation $\nearrow$	I $\nearrow$	$\sigma \nearrow$
$T_g \nearrow$	$T_L \nearrow\nearrow$	Saturation $\nearrow$	I $\nearrow$	$\sigma \nearrow$
$T_g \nearrow\nearrow$	$T_L \nearrow$	Saturation $\searrow$	I $\nearrow$	$\sigma \nearrow$
$T_g \nearrow$	$T_L \searrow$	Saturation $\searrow$	I $\searrow$	$\sigma \searrow$
$T_g \searrow$	$T_L \searrow\searrow$	Saturation $\searrow$	I $\searrow$	$\sigma \searrow$
$T_g \searrow\searrow$	$T_L \searrow$	Saturation $\nearrow$	I $\searrow$	$\sigma \searrow$

TABLE 2a

After this exercise the data appeared to collapse more readily onto a single curve. In order to obtain an empirical correlation between the measured quantities (T_g and T_L) and calculated values ($\ln\sigma$), it was decided that ($\ln\sigma + e\bar{V}/2kT_g$) and ($\ln\sigma + e\bar{V}/2kT_L$) were suitable choices of variable to be plotted against the similarity variable ($^1/T_L - ^1/T_g$). During this exercise it became clear that with a suitable choice for $\bar{V}$ the data would tend to collapse onto a single curve. There started to emerge a significant correlation between the variables plotted, and a recognisable pattern of the distribution of the plotted points. At first the data obtained at constant vapour pressure was plotted. The set of resulting curves were then superimposed on each other except for slight phase shifts, which were not regular nor periodic the superimposed curves collapsed onto a single curve. Different values for $\bar{V}$ were tried within the range of 1-2eV with the one criterion that all given data 'should' collapse into a single curve. The resulting value of $\bar{V} = 1.55$eV was obtained after a lengthy trial and iteration period. The results are shown in Fig. (21) and Fig. (22). The mean values of ($\ln\sigma + e\bar{V}/2kT_g$) and ($\ln\sigma + e\bar{V}/2kT_L$) were obtained by successive averaging of data points over intervals of 0.05 on 10^3 ($^1/T_L - ^1/T_g$) axis with a 0.025 overlap. Which corresponds to a maximum of $\pm$ 20K error in determining the gas temperature and a maximum of $\pm$10K error in determining the reservoir temperatures or a maximum 900K and 600K vapour and reservoir temperatures, respectively, and the error bars represent the rms error of the data points in these intervals.

Example:- To obtain one point with error bars, say between 1.95 and 1.90. All readings taken between 1.95 and 1.90 were assembled. The average values of ($10^3/T_L - 10^3/T_g$) was calculated. This value was the horizontal coordinate. Then the average value of ($\ln\sigma + e\bar{V}/kT_g$) and ($\ln T + e\bar{V}/2kT_L$) for these readings were calculated. This was taken as the vertical coordinate. To calculate the vertical error bars. The average values

of $(\ln\sigma + \frac{e\bar{V}}{2k\bar{T}_g})$ and $(\ln\sigma + \frac{e\bar{V}}{2k\bar{T}_L})$ were subtracted from the respective individual readings from which the averages were calculated, and the root mean square of the remainder evaluated. This gave the size of the error bar. The same process was repeated for all readings between 1.925 and 1.975 and so on, until all available data was exhausted.

The two straight lines drawn through fitted to the plotted points in Fig. (22) obey the following empirical equations; with a change over point at $10^3 (\frac{1}{\bar{T}_L} - \frac{1}{\bar{T}_g}) = 1.05$

$$\ln\sigma + \frac{e\bar{V}}{2k\bar{T}_g} = -\frac{eV1}{2k}(\frac{1}{T_L} - \frac{1}{T_g}) + C_1 \qquad (7.1)$$

for $10^3 (\frac{1}{T_L} - \frac{1}{T_g}) < 1.05$ and

$$\ln\sigma + \frac{e\bar{V}}{2k\bar{T}_g} = \frac{eV2}{2k}(\frac{1}{T_L} - \frac{1}{T_g}) + C_2 \qquad (7.2)$$

for $\bar{V} = 1.55V$ $V_1 = 1.3V$ $V_2 = 0.35V$

The two straight lines drawn through the data in Fig. (21) obey exactly the same equations, with the same change over point, thus providing a valuable cross-check on the reliability of the data and the fit of the straight lines passed through it.

From Fig. (21) and (22), it can also be seen that, there is a possible oscillatory behaviour along the best fit straight lines, but the relative magnitude of the error bars and the oscillation did not make it possible to draw firm conclusions, just from this set of data. However when the results were compared, with that of Endean and Christopoulos, it was seen that the double-exponentially-growing curve that their measurements have yielded, grew in magnitude towards saturation, and

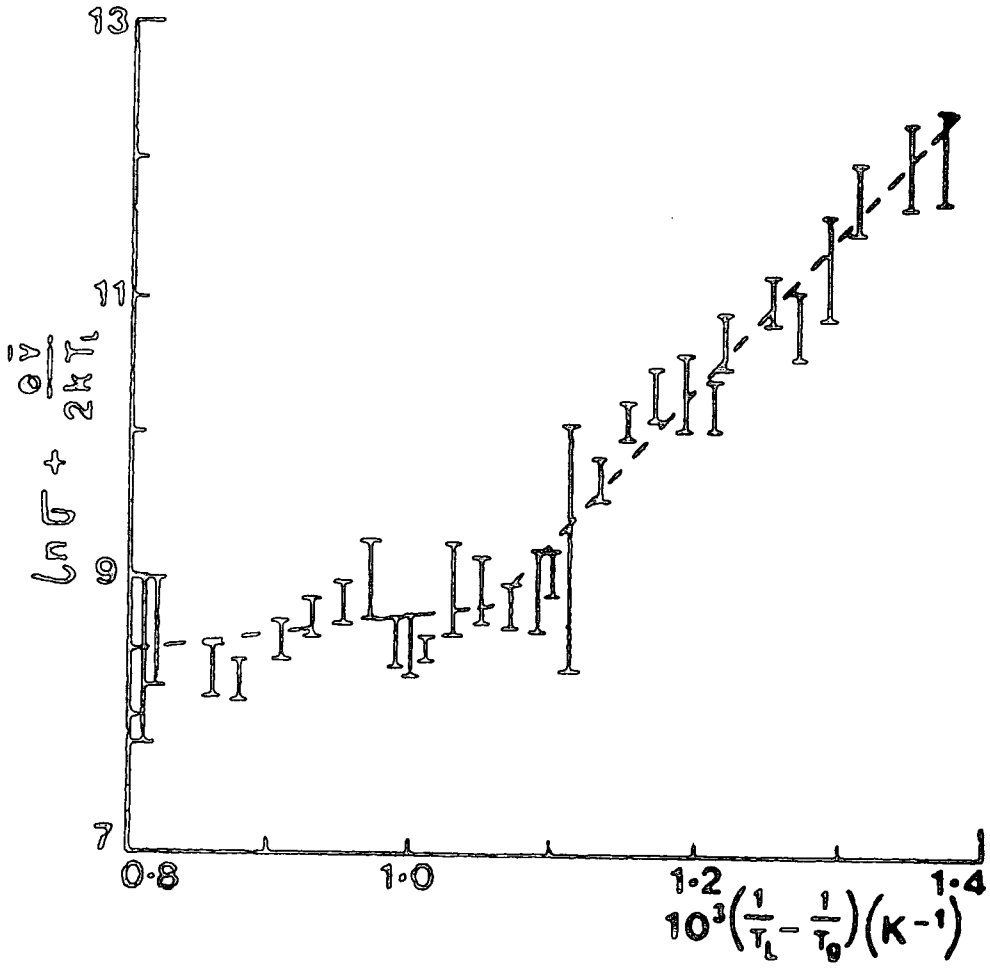

Fig.21 Functional dependence of electrical conductivity and reservoir temperature on degree of saturation.

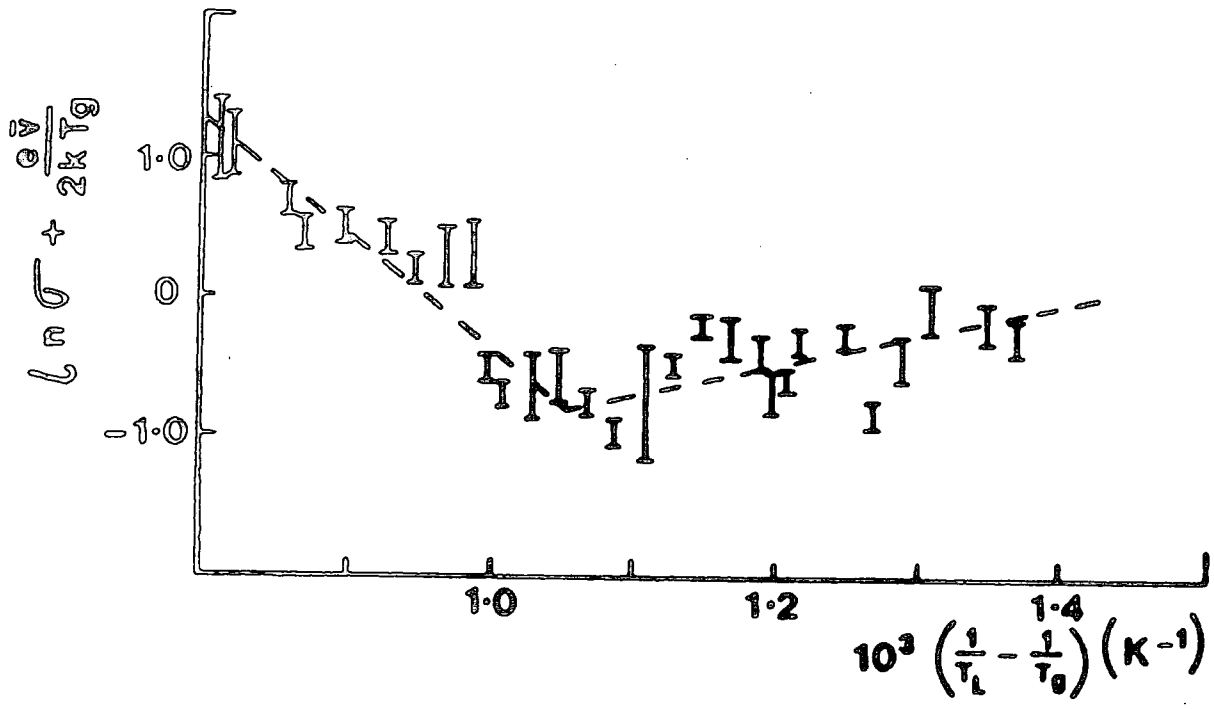

Fig.22 Functional dependence of electrical conductivity and gas temperature on degree of saturation.

settles down to smaller magnitudes as the degree of saturation decreases. This indicated the need to extend the measurements towards full saturation for a better comparison, since with the present measurements the magnitude of the error bars also tended to get smaller after the change over point at $(10^3/T_l - 10^3/T_g) = 1.05$, as the plotted point started exhibiting Saha-type of behaviour (dependent on the vapour temperature), as the degree of saturation was decreased.

Therefore a new set of measurements were carried out where the discharge was driven still closer to saturation. (For these measurements, although a different discharge tube was used, it had the same cross-section area (d=1.2cm) and inter-electrode separation (L=16cm) as the discharge tube used in the previous measurements). Results were plotted in Fig. (23) and Fig. (24). After this set of measurements, further measurements were also carried out, with a larger inter-electrode separation (l=20cm), in an attempt to correlate the measured conductivity to the inter-electrode gap. Data obtained, was treated and plotted similarly and the results are shown in Fig. (25) and Fig. (26).

It was possible to fit the two straight lines in Fig. (22) corresponding to the empirical equations eq. (7.1) and eq. (7.2), to both sets of data, in Fig. (23) and Fig. (25), represented by the solid lines. However, straight lines corresponding to eq. (7.1) and (7.2) were not necessarily the best fit straight lines that could be passed from the plotted data points. There is a possible shift of -1 and +1.5 in Fig. (23) and (25) respectively. Considering the fact that different discharge tubes were used, and also taking into account the magnitude of the error bars, to conclude that the conductivity remains constant independent of the inter-electrode separation would be consistent and non-contradictory, given the present experimental results and their error margin. Nevertheless it should also be said the degree of confidence

that could be attached to this conclusion again because of the error margin cannot be very high. There could be other interpretations put on the shift of the straight lines. Since the interelectrode distance for both sets of data in Fig. (22) and (23) was equal, the mean of the shift could be taken as due to the experimental error, and therefore the real shift in Fig. (25) is $\simeq 1$. This shift would correspond to a change by a factor of 2.7, in the conductivity. In terms of the inter-electrode separation the conductivity would change as

$$\sigma \propto d^{n} \quad \text{where} \quad n = 0.36$$

It could be that some support for this analysis and conclusion, could be found in I.M. Bortniks suggestion Ref (59), where it is suggested that the pre-breakdown currents at constant fields and pressures, depend on the electrode separation, as

$$I = d^{n}$$

where n is quoted to be $0 < n \leq 0.5$. However we should be safe in our assumption that even if the conductivity changes with the electrode distance it is not strongly dependent on it.

For the three sets of measurements, the results are in reasonable agreement with the empirical expressions of (7.1) and (7.2) with plots of $\ln\sigma + \frac{e\bar{V}}{2kT_L}$ against $10^3 \left(\frac{1}{T_L} - \frac{1}{T_g}\right)$ in Fig. (21), (24) and Fig. (26) supporting the reliability of the data.

7.3 Accuracy and Reliability

No difficulties were experienced with the measurements of the voltage and current in the pre-breakdown region, all conductivities were calculated

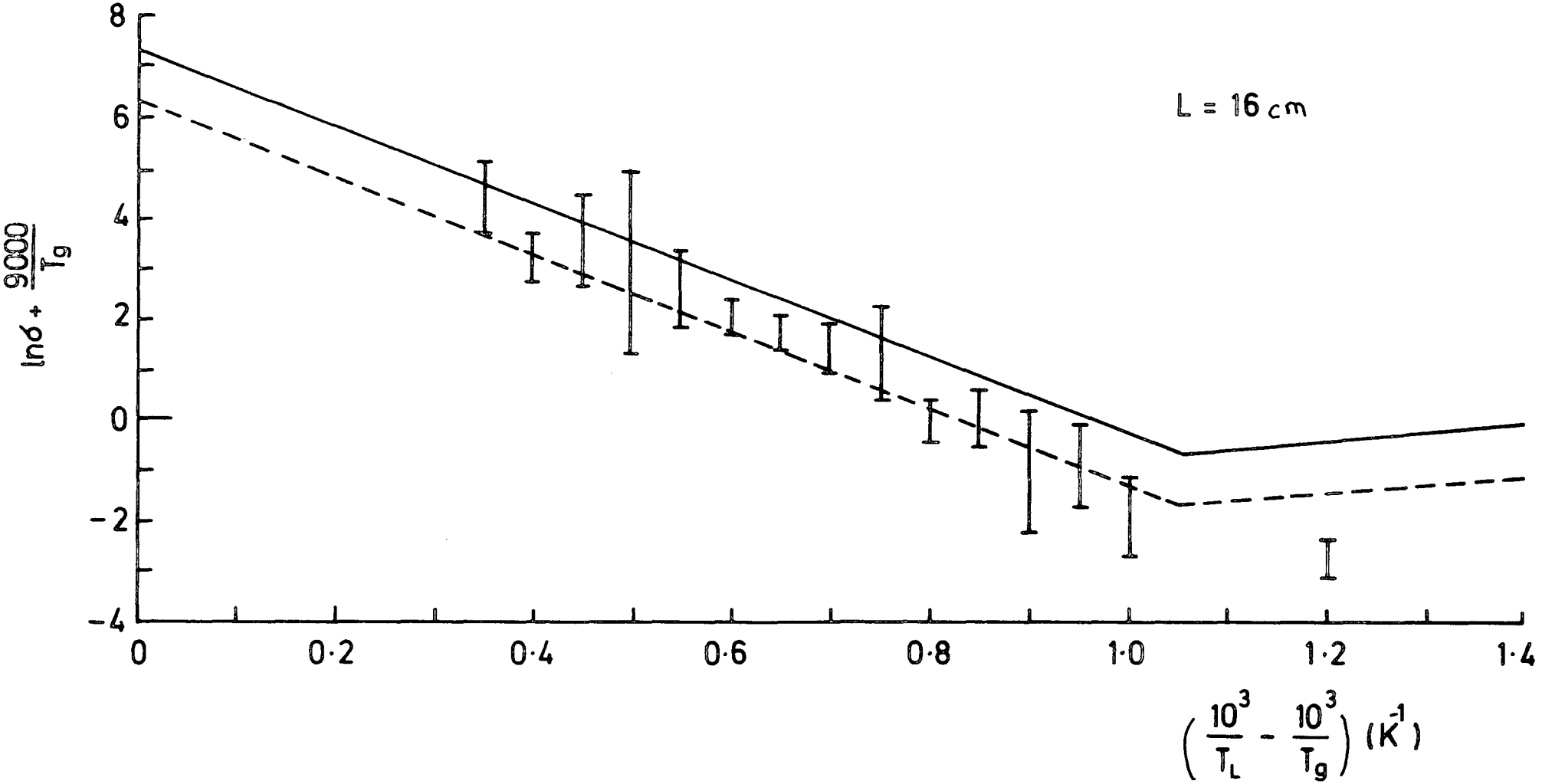

FIG. 23 FUNCTIONAL DEPENDENCE OF ELECTRICAL CONDUCTIVITY AND GAS TEMPERATURE ON DEGREE OF SATURATION

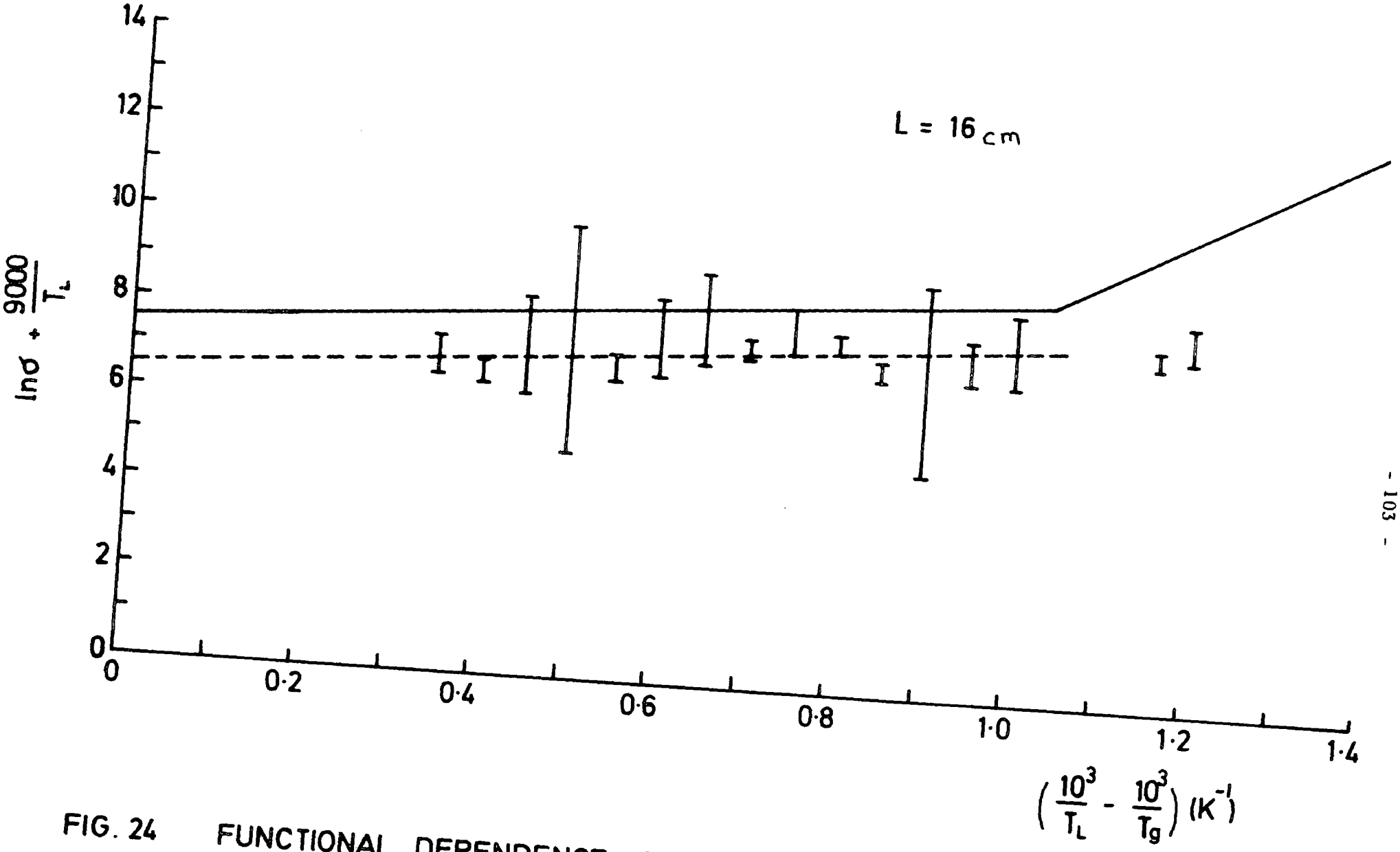

FIG. 24 FUNCTIONAL DEPENDENCE OF ELECTRICAL CONDUCTIVITY AND RESERVOIR TEMPERATURE ON DEGREE OF SATURATION

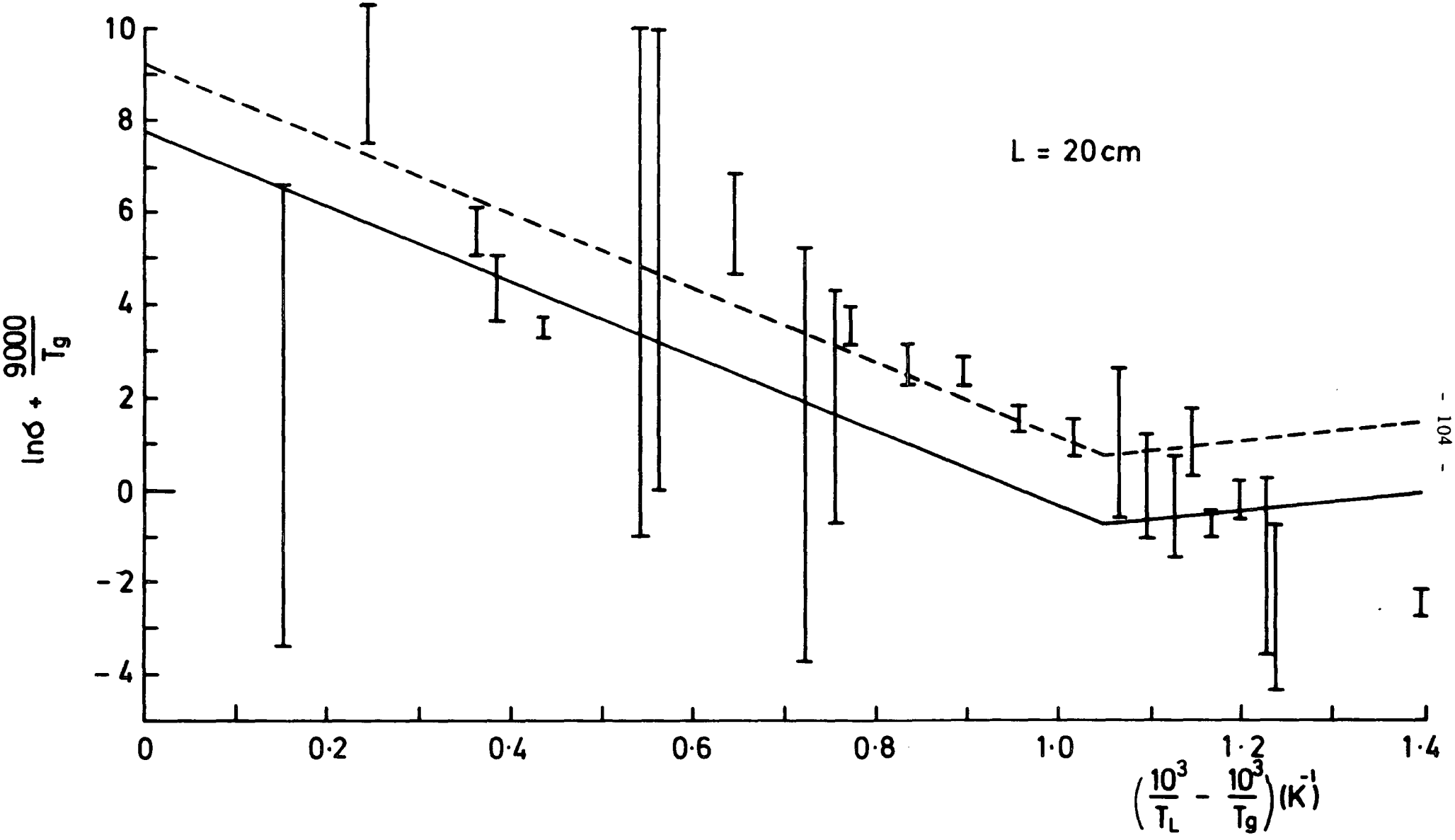

FIG. 25 FUNCTIONAL DEPENDENCE OF ELECTRICAL CONDUCTIVITY AND GAS TEMPERATURE ON DEGREE OF SATURATION

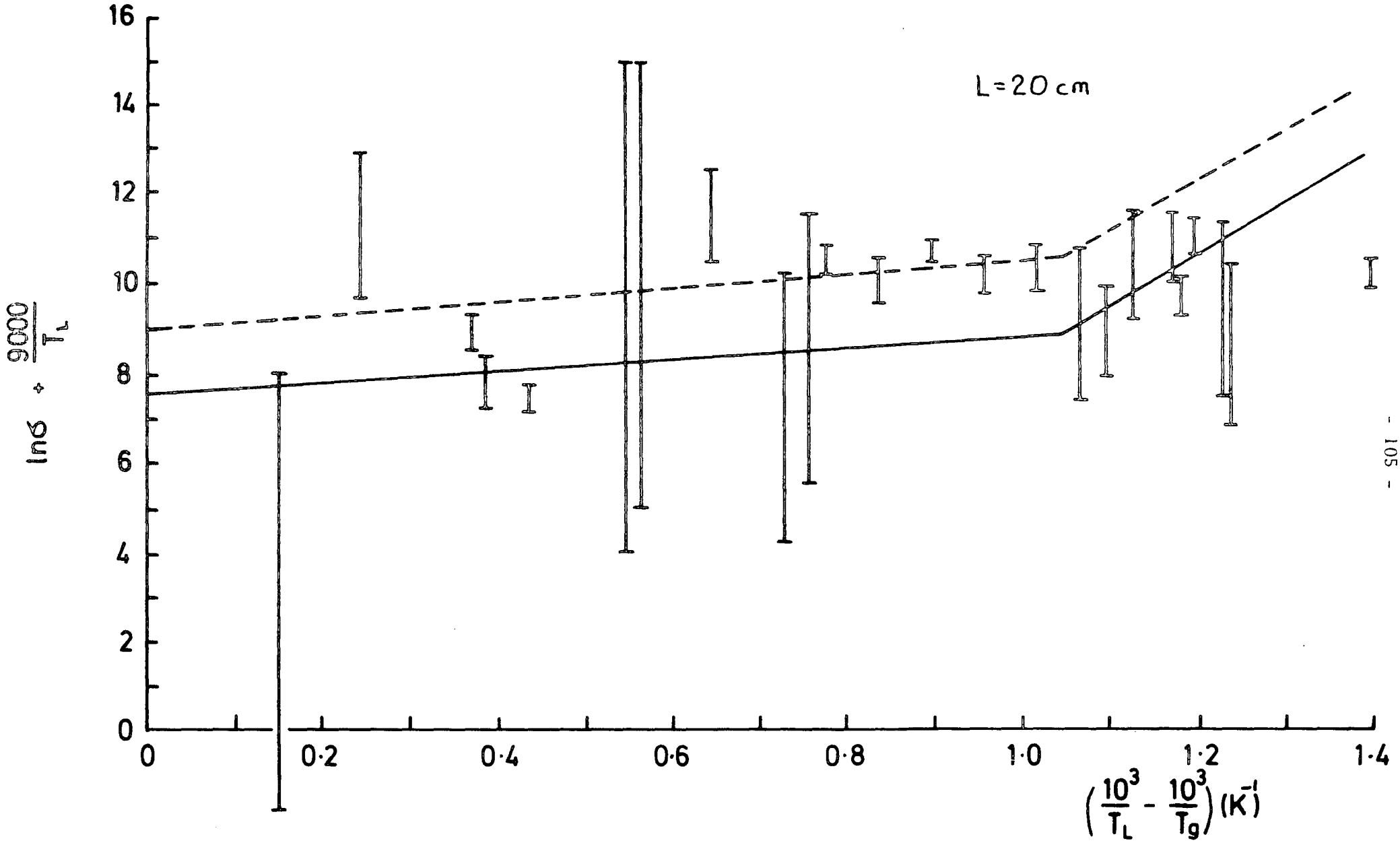

FIG. 26 FUNCTIONAL DEPENDENCE OF ELECTRICAL CONDUCTIVITY AND RESERVOIR TEMPERATURE ON DEGREE OF SATURATION

from voltage/current characteristics where the change of slope could be reliably detected, and therefore $\ln\sigma$ values we considered to be precise and reliable. The possibility that conduction through the walls constituted a major source of error was considered to be unlikely, since the walls of the discharge tube were kept at considerably higher temperatures ($> 100^{o}C$ higher) than the liquid reservoir and the tests conducted by rapidly cooling the discharge down to room temperatures yielded negative results. There remains the possibility of a thin film of mercury on the discharge walls. This can also be ruled out on the grounds that it is difficult to see how a wall conduction mechanism through a thin layer of mercury film would give rise to the transition voltage V_{tr} and conduct in one direction only. It should also be mentioned that the measured conductivities at the higher extreme are of the order of $10^{-3}\Omega^{-1}\text{-m}^{-1}$ with an inter-electrode distance of L=16cm correspond to conductances of the order of $10^{-7}\Omega^{-1}$ with a mercury film of 10^{-5}cm thickness on the walls the discharge would have conductances of the order of $\simeq 10^{-4}\Omega^{-1}$.

Even though possible oscillatory behaviour can also be seen to persist in Fig. (23) - (26) the evidence is not conclusive. If this effect is not real, the scatter of data was probably caused by thermal-time lags associated with the temperature reading, and by possible systematic errors due to the temperature gradient existing between the thermocouples, the vapour/liquid reservoir due to the positioning of the thermocouples and also due to the transient behaviour of the discharge itself.

CHAPTER EIGHT

8. DISCUSSION

8.1 Comparison of Theoretical Predictions and Experimental Results

8.1.2 Theoretical electrical conductivities

8.1.3 Comparison of theoretical and experimental electrical conductivities

8.1.4 Apparent ionization and evaporation potentials

8.1.5 Pressure dependence on full saturation

8.1.6 Relevence of the results to existing cold-cathode theories

8.1.6.1 Vapour cloud effects

8.1.6.2 Saturation effects

8.2 Interpretation in Terms of Droplets

8.2.1 The need for further explanation

8.2.2 The Kelvin equation

8.2.3 The droplet hypothesis

8.2.4 Calculation of the droplet radius and average random velocity

8.2.5 Droplet collision cross-sections and mean free paths

8.2.6 Droplet formation

8.2.7 Charged droplets

8.2.8 Possible conduction mechanisms based on the droplet concept

8.2.9 Longini's model and droplet hypothesis

8. DISCUSSION

8.1 Comparison of Theoretical Predictions and Experimental Results

In this chapter, a comparison is made between the electrical conductivity values calculated from standard theories (based on thermodynamic equilibrium considerations and Saha's equation) and the values calculated from the empirical equations derived from the results of the present investigation. The discrepancy between the theoretical predictions and the experimental results is then discussed. Next some possible interpretations of the results are presentedwith reference to the present theories about cold cathode arcs. Finally, proposed outlines of a possible alternative model are discussed.

The expression used for theoretical predictions of the electrical conductivities, has been derived and discussed in Appendix (I). The discussion that follows is conducted within the framework of that derivation.

8.1.1 Calculated values from empirical expressions

The results of the experiments yield from Fig. (22), (23) and Fig. (25), (Chapter 7).

$$\ln\sigma + \frac{e\bar{V}}{2kT_g} = \frac{eV_1}{2k}\left(\frac{1}{T_L} - \frac{1}{T_g}\right) + C_1 \qquad (8.1)$$

for values of $10^3\,(1/T_L - 1/T_g) > 1.05$ and

$$\ln\sigma + \frac{e\bar{V}}{2kT_g} = \frac{eV_2}{2k}\left(\frac{1}{T_L} - \frac{1}{T_g}\right) + C_2 \qquad (8.2)$$

for values of

$$10^3\,(1/T_L - 1/T_g) < 1.05$$

where

$$\bar{V} = 1.55V;\ V_1 = 0.35V;\ V_2 = 1.29V$$

$$C_1 = -2.7;\ C_2 = 7.25$$

Tables (2)(3)(4)(5) were compiled using the empirical relations of eq (8.1) and eq (8.2) for the experimental vapour pressure and temperature ranges. Extrapolation towards full saturation is also shown. Table (6) is an extrapolation to atmospheric pressure ($\sim 10^5$ Pa).

8.1.2 Theoretical electrical conductivities

The following expression for the electrical conductivity of a weakly ionised gas (vapour) may be derived from the standard theories.

$$\sigma = \frac{(n_a n_F)^{\frac{1}{2}} e^2 \exp\left(-\frac{eV_i}{2kT}\right)}{n_a m_e Q(V_{th}) V_{th}} \qquad (8.3)$$

where n_a, n_F, e, k, T, m_e, $Q(V_{th})$ and V_{th} are, the neutral number density, fermi number density, electron charge, Boltzman's constant, Temperature, electron mass momentum cross-section, and thermal velocity of electrons respectively and V_i is the ionization potential of the gas (vapour). The above expression has been derived in appendix and the underlying assumptions are discussed there.

Accordingly, the thermal velocity of the electrons can be estimated by the expression (from the kinetic-theory of gases)

$$\frac{1}{2} m_e V_{th}^2 = \frac{3}{2} kT \qquad (8.4)$$

therefore,

$$V_{th} = 6.7 \times 10^3 T^{\frac{1}{2}} \text{ m - sec}^{-1}$$

The momentum transfer cross-section $Q(V_{th})$ can be estimated (see App I) by the expression

$$Q = \pi r^2$$

where, r is the effective radius of the mercury ion. Which in turn can be calculated as follows:

Molar volume V_o of mercury, by definition is,

$$V_o = \frac{\text{(atomic mass of mercury)}}{\text{(density of mercury)}}$$

therefore $V_o = 14.7 cm^3$. The molar volume divided by Avogadro's number gives the volume of a mercury ion,

$$V_o(H_g) = \frac{V_o}{N_A}$$

$$V_o(H_g) = 2.5 \times 10^{-23} \ cm^3$$

Then, from the hard sphere model

$$V_o(H_g) = \frac{4}{3} \pi r^3$$

$$r = 1.8 \times 10^{-10} m$$

therefore $Q(V_{th}) = 1 \times 10^{-19} m^2$. However this value is likely to be an overestimation. Alternatively Y. Nakamura and J. Lucas, have quoted a theoretical value of $3 \times 10^{-20} m^2$, for $Q(V_{th})$ in mercury vapour, which they have suggested produces a good agreement between the calculated and experimental values of the drift velocities, see Fig. (27) Ref(60). Accoringly this value of $Q(V_{th})$ was used in

$T_g(K)$	$10^3\left(\frac{1}{T_L} - \frac{1}{T_g}\right)$	σ
630	0	$8{\cdot}8 \times 10^{-4}$
700	0·23	$6{\cdot}5 \times 10^{-4}$
800	0·41	$8{\cdot}3 \times 10^{-4}$
900	0·55	$1{\cdot}0 \times 10^{-3}$
1000	0·66	$1{\cdot}2 \times 10^{-3}$

$T_L = 600\,K$

TABLE 2

$T_g(K)$	$10^3\left(\frac{1}{T_L} - \frac{1}{T_g}\right)$	σ
300	0	$1{\cdot}3 \times 10^{-10}$
400	0·83	$4{\cdot}7 \times 10^{-10}$
Changeover Point →		
500	1·33	$1{\cdot}0 \times 10^{-8}$
600	1·66	$6{\cdot}0 \times 10^{-7}$
700	1·90	$7{\cdot}8 \times 10^{-6}$
800	2·08	$5{\cdot}6 \times 10^{-5}$
900	2·22	$2{\cdot}6 \times 10^{-4}$
1000	2·33	$8{\cdot}8 \times 10^{-4}$

$T_L = 300\,K$

TABLE 3

T_g(K)	$10^3\left(\frac{1}{T_L}-\frac{1}{T_g}\right)$	σ
400	0	$2\cdot0 \times 10^{-7}$
500	0·50	$5\cdot0 \times 10^{-7}$
600	0·83	$8\cdot0 \times 10^{-7}$
700	1·07	$1\cdot22 \times 10^{-6}$
Changeover Point		
800	1·25	$1\cdot1 \times 10^{-5}$
900	1·39	$4\cdot9 \times 10^{-5}$
1000	1·50	$1\cdot66 \times 10^{-4}$

$T_L = 400K$

TABLE 4

T_g(K)	$10^3\left(\frac{1}{T_L}-\frac{1}{T_g}\right)$	σ
500	0	$2\cdot14 \times 10^{-5}$
600	0·33	$3\cdot6 \times 10^{-5}$
700	0·57	$5\cdot1 \times 10^{-5}$
800	0·75	$6\cdot6 \times 10^{-5}$
900	0·89	$8\cdot0 \times 10^{-5}$
1000	1·00	$9\cdot61 \times 10^{-5}$

$T_L = 500K$

TABLE 5

T_g(K)	$10^3\left(\frac{1}{T_L}-\frac{1}{T_g}\right)$	σ
630	0	$8\cdot7 \times 10^{-4}$
700	0·16	$1\cdot1 \times 10^{-3}$
800	0·34	$1\cdot4 \times 10^{-3}$
900	0·48	$1\cdot75 \times 10^{-3}$
1000	0·58	$2\cdot24 \times 10^{-3}$

$T_L = 630K$

$P \sim 1Atm\ (10^5 Pa)$

TABLE 6

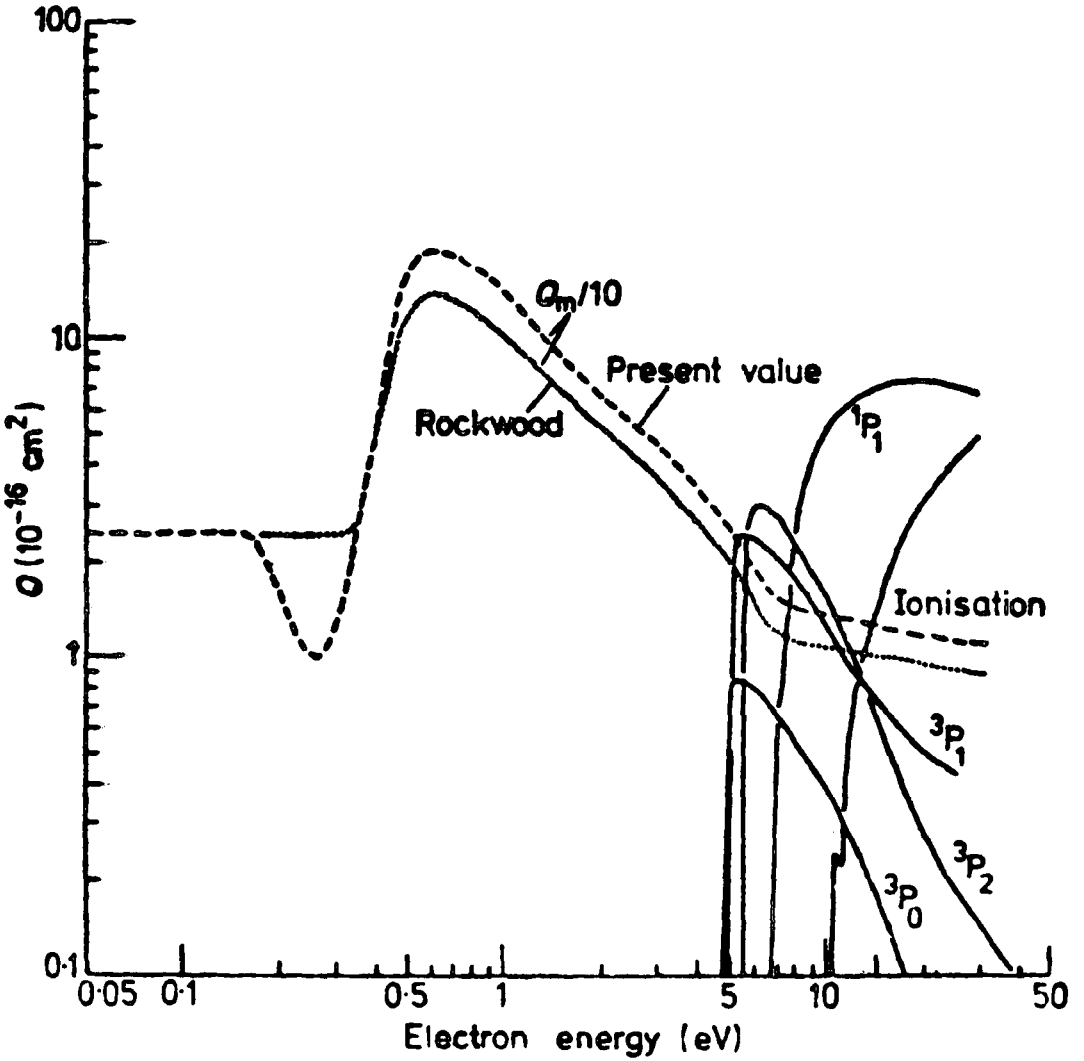

FIG. 27 **Elastic- and inelastic-scattering cross-sections for electrons with mercury atoms as a function of electron energy: · · · Q_m from Rockwood (1973); – – – Q_m present value.***

* Ref. (60)

the calculations.

The neutral number density n_a in eq. (3) was replaced by the following equation, (from ideal gas laws)

$$n_a = \frac{P}{kT} \qquad (8.4)$$

which resulted in

$$\sigma = 3.6 \times 10^7 \, T_g^{\frac{3}{4}} \, p^{-\frac{1}{2}} \exp\left(-\frac{eVi}{2kT_g}\right) \qquad (8.5)$$

The following tables (7)(8)(9) show the calculated theoretical electrical conductivities of the mercury vapour at 10^5Pa ($\simeq$ 1Atm), at the highest experimental pressure 5.57×10^4 P_a, and finally at the lowest experimental pressure 3.16×10^{-3} Pa , respectively for various vapour temperatures (T_g) .

$T_g(K)$	$T_g^{3/4}$	$\exp\left(-\frac{eV_1}{2kT_g}\right)$	$\sigma\ (\Omega^{-1}m^{-1})$
600	121	$2{\cdot}18 \times 10^{-44}$	$3{\cdot}0 \times 10^{-27}$
700	136	$3{\cdot}77 \times 10^{-38}$	$5{\cdot}8 \times 10^{-31}$
800	150	$1{\cdot}80 \times 10^{-33}$	$3{\cdot}0 \times 10^{-26}$
900	164	$7{\cdot}81 \times 10^{-30}$	$1{\cdot}46 \times 10^{-22}$
1000	177	$6{\cdot}36 \times 10^{-27}$	$1{\cdot}28 \times 10^{-19}$

$$\sigma = 3{\cdot}6 \times 10^{-7}\ T_g^{3/4}\ p^{-1/2} \exp\left(-\frac{eV_L}{2kT_g}\right)$$

$T_L = 630K$; $p \simeq 1\,Atm \simeq 10\,Pa$; $p^{-1/2} = 3{\cdot}16 \times 10^{-3}$

TABLE 7

$T_g(K)$	$T_g^{3/4}$	$\exp\left(-\frac{eV_1}{2kT_g}\right)$	$\sigma\ (\Omega^{-1}m^{-1})$
600	121	$2{\cdot}18 \times 10^{-44}$	$3{\cdot}99 \times 10^{-27}$
700	136	$3{\cdot}77 \times 10^{-38}$	$7{\cdot}75 \times 10^{-31}$
800	150	$1{\cdot}80 \times 10^{-33}$	$4{\cdot}08 \times 10^{-26}$
900	164	$7{\cdot}81 \times 10^{-30}$	$1{\cdot}94 \times 10^{-22}$
1000	177	$6{\cdot}36 \times 10^{-27}$	$1{\cdot}70 \times 10^{-19}$
1300	216	$7{\cdot}10 \times 10^{-21}$	$2{\cdot}32 \times 10^{-13}$
1800	276	$7{\cdot}80 \times 10^{-15}$	$3{\cdot}26 \times 10^{-9}$
2400	343	$1{\cdot}22 \times 10^{-11}$	$6{\cdot}33 \times 10^{-4}$
5000	595	$5{\cdot}76 \times 10^{-6}$	$5{\cdot}18 \times 10^{2}$
10000	1000	$2{\cdot}40 \times 10^{-3}$	$3{\cdot}63 \times 10^{5}$

$T_L = 600K$; $p = 5{\cdot}57 \times 10^{\hat{}}Pa$; $p^{-1/2} = 4{\cdot}2 \times 10^{-3}$

TABLE 8

T_g(K)	$T_g^{3/4}$	$\exp\left(-\frac{eV_i}{2kT_g}\right)$	σ (Ω^{-1} m^{-1})
600	121	$2{\cdot}18 \times 10^{-44}$	$1{\cdot}61 \times 10^{-34}$
700	136	$3{\cdot}77 \times 10^{-38}$	$3{\cdot}14 \times 10^{-28}$
800	150	$1{\cdot}80 \times 10^{-33}$	$1{\cdot}65 \times 10^{-23}$
900	164	$7{\cdot}81 \times 10^{-30}$	$7{\cdot}84 \times 10^{-20}$
1000	177	$6{\cdot}36 \times 10^{-27}$	$6{\cdot}89 \times 10^{-17}$
1300	216	$7{\cdot}10 \times 10^{-21}$	$1{\cdot}20 \times 10^{-10}$
1800	276	$7{\cdot}80 \times 10^{-15}$	$1{\cdot}32 \times 10^{-4}$
2400	343	$1{\cdot}22 \times 10^{-11}$	$2{\cdot}56 \times 10^{-1}$
5000	595	$5{\cdot}76 \times 10^{-6}$	$2{\cdot}10 \times 10^{6}$
10000	1000	$2{\cdot}40 \times 10^{-3}$	$1{\cdot}47 \times 10^{8}$

$T_L = 300\,K$; $p = 3{\cdot}6 \times 10^{-1}\,Pa$; $p^{-1/2} = 1{\cdot}7$.

TABLE 9

8.1.3 Comparison of theoretical and experimental electrical conductivities

As can be seen from the compiled tables of the previous sections, the discrepancy between the theoretically calculated Saha conductivities and empirical conductivities derived from the experimental measurements, is many orders of magnitude.

This outcome, although striking, is by no means experimentally unique. Endean Ref (61) was the first who reported measured conductivities in caesium vapour higher than that which could be predicted from Saha's equation, the work was followed by C. Christopoulos who confirmed the results. Since then Christopoulos and Endean have published a joint work, with more detailed results. The work was conducted within pressure and temperature ranges similar to those of the present investigations. Only recently I.T. Yakubov in 1979 has reported that "the measured values of the electrical conductivity on the saturation line exceed the results of the usual estimates (The Saha equation and the Lorentz formula) by five orders of magnitude". Ref. (62).

The smallest discrepancy obtained in the present work within the experimentally attainable vapour pressure and temperature ranges occurs when the liquid reservoir temperature is near room temperature, and at the highest vapour temperatures ($\sim$ 900K). But even then the discrepancy is 16 orders of magnitude.

Although strict quantitative agreement with the theory was not to be expected, this order of magnitude in discrepancy clearly cannot be attributed to the crudeness of the model used, to the simplifying assumptions made, or to the derivation of the theoretical expressions.

However, it must also be emphasised that the theoretically calculated values, are clearly not acceptable for most of the experimental range, for the following reason. If a cylindrical unit volume of mercury

is taken with a $1cm^2$ cross-section, and a potential of one volt is applied across it, then from the expression for the current density,

$$j = \sigma E$$

therefore,

$$I/A = \sigma \frac{V}{d}, \quad \text{with} \quad \sigma = 10^{-37} \Omega^{-1}\text{-m}^{-1}$$

the lowest conductivity given by the theory, the current is $I = 10^{-39}$ A(C/sec) which corresponds to 10^{-20} electrons/sec, or alternatively one electron in 10^{11} centuries!

The highest electrical conductivity that can be calculated from the theoretical expression eq. (8.3) (within the experimental range) is of the order of $10^{-20}\Omega^{-1}\text{-m}^{-1}$, which corresponds to 10^{-3} electrons/sec. This would be the right order of magnitude for solid insulating materials. (e.g. $Al_2 O_3$ with $\sigma = 10^{-19}\Omega^{-1}\text{-m}^{-1}$).

Finally one probability to be considered is that an effect similar to that of the Ramsauer-Townsend effect which operates at low electron drift velocities; is a strong function of $\frac{eV}{2K}\left(\frac{1}{T_L} - \frac{1}{T_g}\right)$. Except that the Ramsauer-Townsend effect is dependent on the energy of the incident electron, and a sharp dip in the momentum-transfer cross-section of many orders of magnitude at least for mercury vapour remains to be experimentally proven. At the moment, theoretical predictions do not make such a conclusion possible.

8.1.4 Apparent ionization and evaporation potentials

For values of $10^3(1/T_1 - \frac{1}{T_g}) > 1.05$, the experimental results settle into a Saha type of behaviour, in that the dependence of the electrical conductivity switches over from predominantly a function of vapour pressure

to predominantly a function of vapour temperature. As a further comparison between theory and experiment the apparent ionization and evaporation potentials were calculated as follows.

For mercury over the entire range from its melting point to its critical point (1760 ± 15K; 1510 ± 30 bar), the logarithm of the saturation pressure is a linear function of the reciprocal of temperature Fig. (28) which is normal for most substances and has been experimentally confirmed for mercury in Ref. (63).

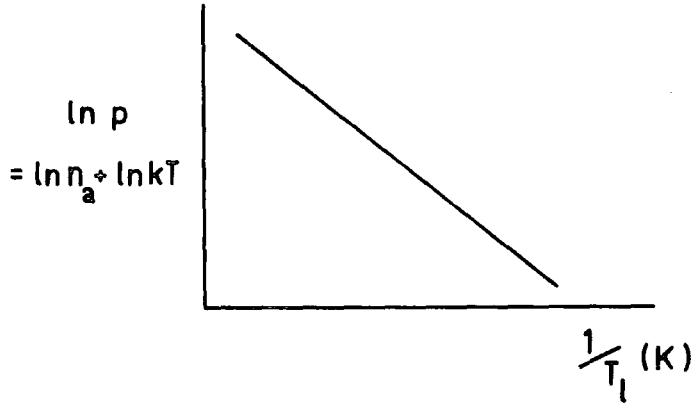

Fig. (28)

therefore at constant gas (vapour) temperature

$$p \alpha n_a \alpha -^{1}/_{T_L}$$

From Boltzmann's relation the number density of the mercury atoms n_a is

$$n_a = n_{ao} \exp\left(-\frac{e\ Vevap}{kT_L}\right) \qquad (8.6)$$

Substituting (8.6) into eq. (8.3) results in

$$\sigma \simeq \text{Constant}\ (T_g)^{3/4} \exp\left(\frac{eVevap}{2kT_L}\right) \exp\left(-\frac{eVi}{2kT_g}\right) \qquad (8.7)$$

Accordingly the empirical relation in eq. (8.1) could be re-arranged to yield; for $10^3\ (1/T_1 - 1/T_g) > 1.05$

$$\sigma = \exp\left(\frac{eVi}{2kT_1}\right) \exp\left(\frac{e(\bar{V} + V_1)}{2kT_g}\right) e^{-2.7} \qquad (8.8)$$

The apparent ionization potential $V_{i(ap)}$ would therefore be $\bar{V} + V_1 = 1.9V$. Similarly the apparent evaporation potential is $V_1 \simeq 0.35V$. The actual values for the ionization and evaporation potentials for mercury are 10.4V and 0.54V respectively.

The apparent lowering of the ionization potential is again not a unique experimental result. One of the reasons for starting the present investigations on mercury with a high ionization potential was also to check the conclusions arrived at by Endean and Christopoulos; that the ionization potential is not a too important parameter, for the observed behaviour of the electrical conductivities for vapours at low temperatures and medium pressures.

Yakubov, Ref (62) has also suggested lowering of the the ionization potential by an amount nearly equal to the work function of the vapour. With the present investigations however the ionization potential seems to have been lowered by twice the work function of mercury.

8.1.5 Pressure dependence on full saturation

From the empirical formula of eq. (8.2)

$$\ln \sigma + \frac{e\bar{V}}{2kT_1} = \text{constant} \qquad (8.9)$$

where $\bar{V} = 1.55V$; $V_{evap} = 0.35V$. Therefore $V_{evap} = \frac{\bar{V}}{4.3}$

An expression for the pressure could be written as

$$p = p_o \exp\left(-\frac{eVevap}{kT_1}\right) \qquad (8.10)$$

Taking the logarithm of both sides yields

$$\ln p = \ln_{po} - \left(\frac{eV_{ap}}{kT_l}\right), \quad \text{or}$$

$$\ln p - \ln_{po} = -\left(\frac{e\bar{V}}{kT_l}\right) \left(\frac{1}{4.3}\right)$$

substituting the above expression into eq. (8.9)

$$\ln\sigma - (\ln p - \ln_{po})\ \frac{4.3}{2} \simeq \text{constant} \qquad (8.11)$$

therefore

$$\sigma \alpha p^{2.15} \qquad (8.12)$$

For a comparison of this proportionality with other reported experimental data, the conductivity of critical mercury was calculated, as follows.

Experimentally calculated value of the conductivity at atmospheric pressure is $8.8\text{x}10^{-4}\Omega^{-1}\text{-m}^{-1}$ (from table(6)), and the critical pressure of mercury is reported to be $\simeq$ 1500Atm. ,therefore the conductivity of critical mercury could be approximated as

$$\sigma_{cr} \simeq \frac{\sigma atm\ p_{cr}^{2.15}}{p\ atm^{2.15}} \qquad (8.13)$$

$$\sigma_{cr} \simeq 5.9 \times 10^{3}\ \Omega^{-1}\text{-m}^{-1}$$

where σ_{cr}, σ_{atm}, p_{cr} and p_{atm} are conductivity of critical mercury, conductivity of mercury at atmospheric pressure, critical pressure of mercury and atmospheric pressure respectively.

This value of conductivity is in reasonable agreement with the experimentally

measured value of $\simeq 9 \times 10^{3} \Omega^{-1}\text{-m}^{-1}$ reported by F. Hensel and E.W. Franck Ref. (63)(64).

It should also be pointed out that within the experimental accuracy of the present investigations the conductivity could be taken as being proportional to the square of the pressure. Before passing on to discuss possible interpretations that could be placed on the lowering of the ionization potential and the derived pressure dependence, one final comparison will be made between Saha, reported experimental measurements of Hensel and Franck and the results of the present investigations.

Thermal ionization of the mercury gas at 1973k and at 1 atmosphere ($\simeq$ 1 bar) using Saha's equation (eq.(8.3)) could be calculated to give $\simeq 10^{-9} \Omega^{-1} cm^{-1}$. The conductivity determined experimentally by Hensel and Franck is $2 \times 10^{-2} \Omega^{-1} cm^{-1}$, , that is seven orders of magnitude higher. Using eq. (8.13) derived from the results of the present investigation seven orders of magnitude change could also be predicted. The empirically derived proportionality seems to be in agreement with the experimentally measured values of super-critical conductivities of mercury.

8.1.6 Relevance of the results to existing cold-cathode theories

8.1.6.1 Vapour cloud effects

Ruling out thermionic emission, and a number of alternative suggestions involving extraneous effects i.e. loose particles or various impurities on the cathode which perhaps should not be taken as fundamental mechanisms for low boiling melting point and high vapour pressure cathodes, then, as the review of the literature in Chapter Four showed, at the present time, the explanation of the emission processes from such cathodes, i.e., Cu, Hg etc., seems to favour the field emission mechanism. In the field emission theory, in order to obtain sufficient density of emission

current, electric fields of the order of 10^7-10^8 V/cm are needed. This in turn requires high ion current densities to form the space charge in front of the cathode. In order to obtain such high electric field intensities, the ion current density should be of the order of $10^6 A/cm^2$. This value of ion current density corresponds to $\simeq 10^{19}$ ions/cm^3, which leaves the origin of these ions open to question. If they were created by thermal ionization in the positive column (see Chapter Two and Four), then, for the mercury vapour values of 10.4V for the ionization potential and $\simeq$ 5000K for the temperature of the positive column used in conjunction with the Saha's equation, the calculated values for the ion number density fall five orders of magnitude short. There is little doubt about the approximate temperature of the positive column used in the calculations. On the other hand if the apparent ionization potential 1.9V calculated from the results of the present investigations is used to calculate the ion number density instead of 10.4V, it yields values of the order of 10^{18} ions/cm^3, which is in suprisingly good agreement, with the values necessary for field emission. Of course this itself could be a fortuitous result without a plausible explanation for the lowering of the ionization potential and also for the electrical conductivities measured in the present investigations. Such an explanation is now attempted.

V.I.Rakhovskii Ref. (65) from similar considerations, i.e., taking the ion current density as $\simeq 10^6 A/cm^2$ and using the assumption made in the field emission theories that the ions loose their energy directly to the metal/liquid cathode, has suggested that each lattice ion collides with 10^9 ions/sec whose energy significantly exceeds the binding energy with the lattice, which should be $\simeq$ 1eV as suggested by Rothstain Ref. (40). From this Rakhovskii concludes that with these energy densities the cathode surface is in continuous thermal explosion leading to high neutral

particle densities above the liquid metal and that it should not be feasible to use the cathode characteristics whichapply only in the case of solid or liquid metal. The existence of high vapour densities, or high vapour density regions do not contradict the experimental data (Chapter 5), nor the earlier theoretical predictions. The idea of vapour cathode was first proposed by Slepian Ref(67) in 1926, and was later used by Rothstein who supplemented it by a new concept, that of the possibility of metallic conduction in the metal vapour cloud, due to high concentration of neutral particles.

A.W. Hull in Ref. (68), who proposed a field emission model for mercury arc spots, favours the idea that the ionization takes place within a distance of $25\lambda_e$ (where λ_e is the electron mean free path) from the cathode region and is due to the step-wise ionization with primary electrons accelerated in the cathode region with energies (10.4-4.5) $\simeq$ 5.5eV ,which excite the metastable level $V_m \simeq$ 5.44eV. . The calculations of A.W. Hull yield $\simeq 10^{21}$-10^{22} ions/ cm^2 striking the cathode. As Rothstein suggests, many of them may penetrate to a depth of one or more atomic diameters before releasing their energy. Again if one considers that the binding energies of the lattice atoms are of the order of $\simeq$ 1eV one comes to the conclusion that the conditions within this volume should resemble that of a highly compressed gas in the super-critical region.

Although Rothstein holds the view that this dense vapour cloud emits electrons thermionically, alternatively, it could also be proposed that this dense vapour cloud with metallic behaviour could be used to explain the possible lowering of the ionization potential, as follows.

A.W. Hull has estimated the cathode spot temperatures of the mercury spot as $\simeq$ 573K ,which is in good agreement with the value $\simeq$ 600K Von Engel reports Ref. (68)(20). It is also suggested that the vapour

cloud temperature above the cathode spot could be assumed to be 1.5 - 2 times higher Ref. (65) that is $\tilde{<}$1000K . As can be seen, these values are within the experimental range of the present investigations. With these pressure and temperatures, the number density of neutrals could be estimated as 10^{18} particles/cm^3 and the degree of saturation to be $\lesssim$ 1. Therefore we could use the experimentally derived values of $\tilde{>}$ 1.9V for the apparent ionization potential.

Although theoretical estimates by Mott Ref. (69) using the relation $n^{1/3} a_o \geq 0.25$, suggest that 10^{22} particles/cm^3 are needed for transition to the metallic state, a result which seems to have been confirmed by the experimental work of Birch, Franck and Hansel Ref. (63)(64)(70), it is possible that in the vapour cushion, that is, in this case for mercury vapour with 10^{18} particles/cm^3 there are localised microscopic volumes in which the particle density reaches the necessary order of magnitude therefore obtaining metallic character. Density fluctuation of the order of $\pm\sqrt{n}$ Ref. (22) could be one possible explanation (see Appendix for density fluctuations).

Assuming that this is so, it could therefore be possible to apply the Thomas-Fermi Model of the electron gas to these regions and calculate the fermi-level energies of the semi-free electrons, which work out to be of the order of $\tilde{=}$4.5eV for liquid mercury. Furthermore it is quite possible that these energies are higher because of the higher temperature of the vapour ($\tilde{=}$ 4.82 eV for $\tilde{=}$ 1000K).

This level of energy would provide sufficient energy to the fermi-electrons to excite a mercury atom/molecule considering that lowest excitation potential of the mercury is 4.86eV and the lowest metastable state is 4.6eV. Von Engel reports that if irradiated with an intercombination line 2537 (the $6^1s_0 - 6^3p_1$ resonance line) an H_g atom can become ionised although the transition is associated with only 4.86eV as

compared with the ionization potential of mercury 10.4eV Ref. ([20]). Support for excitation being responsible could also be probably drawn from the spark studies conducted by various workers, (see Chapter Five) in which luminous clouds of excited vapour were observed.

The assumption that density oscillations are responsible for attaining metallic character also helps to overcome the problem of the emission mechanism. Since the metallic regions are not of a static and stable character, when they are dense enough, electrons will be pumped up to higher levels of energy and, again due to oscillations, when the density drops to a level below that necessary for metallic behaviour, there will be localised volumes with excited and/or metastable particles.

As a result of the interaction of excited and/or metastable atoms/molecules, the available energies would be approximately 9.72eV (4.86+4.86) and 9.46eV (4.86+4.6) or 9.2eV (4.6+4.6), which would be considerably lower than the energies needed for ionization before reaching the positive column. However, the probability of ionization is quite reasonable ($V_i \div 9.72; 9.46; 9.2$) having crossed into the positive column. For thermal ionization energy levels of the order of 1.5eV are needed. This could be taken as being in reasonable agreement with the calculated apparent ionization potential ($\simeq$ 25% discrepancy). This would also explain cathode fall values of 10 eV.

It must be emphasised that the comparison and the analysis is too crude and approximate to yield strict quantitative agreement, and is only offered as one of the possible explanations of the results and several other experimental observations.

To sum up the arguments, localised dense vapour regions of vapour could acquire metallic character and due to the high temperatures (with respect to the solid/liquid cathode) of the vapour, would have higher fermi-energy levels. Contact with the cathode might then lead to an

uninhibited flow of electrons from the cathode into the dense vapour. The electrons thus transferred would be pumped up to higher energy levels, which in turn would produce excited atoms/molecules whose interaction could lead to ionization.

8.1.6.2 Saturation effects

If ionization was mainly due to the interaction of excited atoms, then one would expect the electrical conductivity to be proportional to the square of the pressure. This is also in suprisingly good agreement with proportionality derived from the results of the present investigations (eq.(8.13) Von Engel Ref.(20) has reported that ionization produced by the action of excited states is proportional to p^2 at low pressures rising to p^3 at higher pressures.

It should be pointed out however that this conclusion only applies for the experimental values of $(10^3/T_l - 10^3/T_g) \geq 1.05$ where the behaviour is clearly Saha type behaviour. It is not possible to explain the experimental results for values of $(10^3/T_l - 10^3/T_g) \leq 1.05$ (that is the dependence on the degree of saturation and the switching from pre-dominantly pressure dependence to temperature dependence of the electrical conductivity) on this basis. However, as far as cathode spots in mercury arcs are concerned, the average degree of saturation is more likely to be $\simeq 1$.

While there does not seem to be any theory in existence which would help to explain, the dependence on the similarity variable $(1/T_l - 1/T_g)$. (degree of saturation) there could be other possible interpretations of the results if linked with some of the well-known observed phenomena taking place in cold-cathode arcs, for example, instability of the cathode spot, if the large variations and possible oscillatory behaviour, mentioned in Chapter Seven, particularly closer to the full saturation value, were real and not random measurement errrors represented by error bars.

That would mean that very slight changes in the pressures and temperatures could produce significant variations in the electrical conductivity. In the previous chapter, it was shown that the averaging corresponded to a maximum of $\pm$ 20K in vapour temperature and $\pm$ 10K in the liquid temperature. A.W. Hull Ref. (68) estimates $\pm$ 2.5K variation in the spot temperature and accordingly there is probably a $\pm$5.6K variation in the vapour temperature above the spot. A detailed analysis might show that this is an underestimation and in any case, it is constricted to the spot region, not to the cathode surface and the cathode full volume. Larger temperature and pressure variations within the volume are to be expected. Further more there is quite likely to be a density gradient from the cathode to the positive column. Therefore, it could be concluded that the degree of saturation of the vapour would not be uniform throughout the volume of the vapour. At the mercury arc spot, temperatures are $\simeq$ 600K and at full saturation the experimental results predict $\simeq 10^{-7}\Omega^{-1}\text{-m}^{-1}$. If the slopes of the error bars for $(10^3/T_L - 10^3/T_g) \leq 1.05$ are extrapolated to full saturation, this corresponds to $\pm 10^3 - 10^4\Omega^{-1}\text{-m}^{-1}$ change in the conductivity. That is the conductivity of the vapour next to the cathode at full saturation could assume values between $\simeq 10^{10}\text{-}10^{11}\Omega^{-1}\text{-m}^{-1}$ and $10^4\text{-}10^3\Omega^{-1}\text{-m}^{-1}$.

If rapid transition between a highly insulating state to a conducting state becomes possible with slight variations of pressure and temperature, the instability and apparently random motion of the cathode spot becomes readily explainable. Conduction occurs at the appropriate degree of saturation; slight variations in the degree of saturation will cause the spot to transfer itself to the nearest appropriate site.

In Chapter four, in the review of the cold cathode theories, models which utilise tunnelling of electrons through semi-insulating

(oxide layers) were also discussed. This did not seem possible for liquid cathodes. Guile suggests that a semi-insulating layer of perhaps 10A is needed where ions could be trapped locally prior to their neutralization. Since very low levels of localised conductivities can be predicted from the present results and since $T_g \rightarrow T_l$ towards the cathode, there might exist a thin layer of vapour adjacent to the cathode satisfying this condition. The necessary semi-insulating layer would then be present and a detailed analysis might show that the layer takes on a thickness of 10A.

8.2 Interpretation in terms of droplets

8.2.1 The need for further explanation

It must be stressed that all the standard theories predict that mercury vapour at the low temperatures investigated is definitely an insulator, contrary to the results of the present experiments.

Mercury vapour does conduct at these temperatures and pressures under the right conditions, and apparently with a very sensitive dependence on the degree of saturation.

In the following sections, outlines of a possible new model will be developed. It is new in the sense that the concept has not been mentioned in existing theories of cold-cathode arcs. The original concept can be traced back to Lord Kelvin (1871).

8.2.2 The Kelvin equation

The Kelvin equation was derived by Lord Kelvin in 1871, and it relates the vapour pressure adjacent to a curved liquid surface to the vapour pressure in the bulk of the gas.

The original Kelvin equation is

$$P_d = P_o (1 - 2M\lambda_s/RT_L\rho r_d)$$

where P_d is the vapour pressure just outside a droplet of radius r_d and in equilibrium with the droplet surface, P_o is the saturation vapour pressure over a plane liquid surface ($r_d \rightarrow \infty$), λ_s is the surface tension, M is the molecular weight of the liquid, ρ is the density of the liquid, T_L is the liquid temperature. The Kelvin equation is usually derived by thermodynamical reasoning where the surface free energy of a droplet is calculated as it receives a small increment from the surrounding vapour and the exact form of the equation is as follows

$$\ln \left(\frac{P_d}{P_o}\right) = \frac{2M\lambda_s}{RT\rho r_d} \qquad (8.14)$$

This form of the equation has been shown to be a better fit for the experimental results Ref. (72). In the following sections, following a slightly different reasoning, a similar relation will be derived, and results relevant to the present investigation will be shown.

8.2.3 The droplet hypothesis

From ideal gas laws

$$p = nkT \qquad (8.15)$$

where p is the pressure, n is the number density of molecules, k is the Boltzman's constant, T is the temperature. At constant temperature pressure is directly proportional to the number density. If the vapour

is in equilibrium with its liquid with a flat surface, which also means that the liquid is just boiling or the vapour is just condensing, the rate of arrival of molecules at the liquid surface must be equal to the rate of escape. Making use of Boltzmann's law in equilibrium we can write

$$p = (\text{constant}) \quad \exp \quad \left(- \frac{eVevap}{kT_L}\right) \qquad (8.16)$$

where e is the electronic charge, k is the Boltzmann's constant p is the equilibrium pressure, T_L and $Vevap$ are the liquid temperature and evaporation potential respectively. The left hand side of the equation (8.16)is proportional to the number of molecules arriving at the surface. The right hand side of the equation (8.16)is proportional to the number of molecules escaping from the surface.

If one hypothesises the existence of droplets, one can follow the reasoning that in a droplet of radius r_d , the molecules of the droplet have greater energy when compared with the same number of molecules in the interior of a large mass of liquid; because surface tension gives the droplet a surface energy. A pressure of $2\lambda_s/r_d$ is exerted on the molecules in the droplet (where r_d is the radius and λ_s is the surface tension). Pressure being an energy density the extra energy can be expressed as $\frac{2\lambda_s V_d}{rd}$ where V_d is the volume of the droplet. Thus the activation energy for vaporization is reduced. As a result the vapour pressure of the droplet is increased; instead of the term $\exp(-eVevap/kT_L)$ we have $\exp\ (- eVevap/kT_L + 2\lambda_s v/r_d kT_L)$ where v is the volume of one molecule. Pressure increases because a molecule on the surface of the droplet has less bonds to break than a molecule in the bulk of the liquid, since it is surrounded by a smaller number of molecules. It can thus be justified by the above reasoning

that the pressure in the bulk of the liquid is higher than the pressure in the bulk of the vapour.

8.2.4 Calculation of the droplet radius and average random velocity.

In a droplet in equilibrium with the surrounding vapour, the rate of evaporation, compared with the plane surface, has increased by a factor $\exp(2\lambda_s v/r_d kT_l)$ (rate of escape of molecules from the droplet surface). The increase in the rate of arrival of the molecules should be equal to the vapour density increase P_d/P_o. Therefore

$$\frac{P_d}{P_o} = \exp(2\lambda_s v/r_d kT_l) \quad \text{or}$$

$$\ln\left(\frac{P_d}{P_o}\right) = \left(2\lambda_s v/r_d kT_l\right) \tag{8.17}$$

which is Kelvin's equation.

The practical significance of this equation is that, to maintain the convex interface of a droplet in equilibrium with its vapour, the vapour pressure P_d just outside a droplet of radius r_d and in equilibrium with the droplet surface must be higher than, the pressure P_o in the bulk of the gas. Such vapour would be called super-saturated.

The Kelvin equation is not suitable for calculating the limiting radius of the liquid droplets on the saturation line, because no priori assumptions were made on how the nuclei of the droplets were formed, nor about their nature (which will be discussed in the coming sections). It should nevertheless give a fair physical picture, on which further refinements could be made.

To calculate the radius of the droplet from eq.(8.17) e.g. at T_l = 573K, we have to know the molecular volume which can be calculated as

$$V_o = \frac{\text{(Mass of molecule)}}{\text{(Density of molecule)}}$$

where V_o is the molar volume

$$v = V_o/N_A$$

where v is the volume of one molecule while N_A is the Avogadro's number. Therefore for mercury

$$V_o = 15.5 cm^3$$

$$v = 2.5 \times 10^{-23} cm^3$$

Taking the degree of saturation to be $P/P_o \simeq 1.05$ and $\lambda_s = 480$ dyne/cm

The radius of the droplet can be estimated to be

$$r_d = \left(\frac{2\lambda_s v}{\ln(P_d/P_o) k T_l}\right) \simeq 300A$$

Assuming perfect spherical shape, the volume of the droplet would be

$$V_d = 4/3\ \pi r_d^3 \simeq 1 \times 10^{-16} cm^3$$

from

$$(V_d)\ (n_a) = 6.8 \times 10^7 \text{ particles/droplet}$$

The maximum number of droplets per unit volume should be equal to

$$n_d = \frac{\text{(number density of the vapour at 573k)}}{\text{(number of particles/droplet)}}$$

$$n_d \simeq 6.12 \times 10^{10}/cm^3$$

We could also calculate the average distance between the centres of the

droplets. It should be

$$\bar{d} = \frac{1}{(nd)^{1/3}} = 2.54 \times 10^{-4} \text{cm}$$

The random speed of droplets could also be calculated as follows

(volume of molecule)(density) = mass of molecule (m)

$$m = 3.4 \times 10^{-22} \text{gm}$$

m_d (mass of droplet)=(mass of molecule)x(number of particles in droplet)

$$m_d = 2.31 \times 10^{-14} \text{ gm}$$

and assuming

$$\tfrac{1}{2} m_d v^2 = \tfrac{3}{2} kT$$

$$V = 3.2 \text{ cm/sec}$$

The physical significance our calculations have yielded at this point from the Kelvin's relation is one of large droplets with very low speeds, and quite a distance (when compared with the atomic dimensions) apart from each other in the volume of the vapour. It was thought that it would be of interest to know their collisional cross-sections and mean free paths. If they had been found to have a very short mean free path a collision type conduction mechanism could have been suggested, which could have explained the high experimental conductivities.

8.2.5 Droplet collision cross-sections and mean free paths

Assuming the system is in equilibrium, and the droplets are uniformly distributed, in space, with their velocities distributed according to the Maxwell-Boltzmann's law, then the fluctuations in the frequency of collisions about a mean value would be very small. Therefore the probability of a collision of a particle with velocity v could be written as

$$dp = nQ(V)dx$$

where n , Q(V) and dx are the number of particles per unit volume, a constant of proportionality, (effective cross-section of the collision) and distance travelled per unit time. From hard sphere model, and standard calculations, for the droplets in question

$$Q = 1.1 \times 10^{-10} \text{ cm}^2$$

The collisional frequency, or the probability of collision per unit time is

$$Q_T = nv\,Q(v) \simeq 21 \text{ collisions/second}$$

Therefore in between successive collisions the distance travelled is,

$$\lambda = 1.4 \times 10^{-1} \text{cm}$$

Since the results of the previous section yield 2.54×10^{-4} cm for the average distance between the centres of the droplets, and the mean free path comes out to be 1.3×10^{-2} cm, this rules out a collision-

based conduction mechanism, in which the droplets could have been thought as current carrying elements. It is necessary to look for other mechanisms in which the droplets, instead of carrying the current, bring about conditions necessary to liberate high charged particle densities in the surrounding vapour.

Before continuing the main discussion about droplets, one interesting fact should be pointed out. If it was possible to think that the droplet size could be reduced to molecular dimensions at the liquid cathode, then the number density of the droplets adjacent to the cathode could be taken as the liquid number density. Also a transition layer from the liquid cathode to the bulk of the vapour could be proposed in which the number density of the droplets in the vapour could be obtained from a Boltzmann's relation.

$$n = n_o \exp\left(\frac{eV}{kT}\right) \qquad (8.17a)$$

where the concentration gradient of droplets is assumed to be maintained in equilibrium by a potential field V, the nature of which would have to be identified. For the proposed number density of droplets, the potential would be $V = 1.48V$, which compares well with $\bar{V} = 1.55V$ in the empirical equations (7.1) and (7.2). Moreover, decreasing of the particle number density from liquid number densities of $\simeq 10^{23}$ to particle number densities of $\simeq 10^{2}$ per droplet, again from Boltzmann's relation, could be related with a potential of $\simeq 1.8V$ ($V_{i\,(apparent)} \simeq 1.9V$)

8.2.6 Droplet formation

A review of the literature about the phase transition from vapour to liquid state shows that two basic processes govern the transition, depending on the system in question, namely, "Homogeneous

nucleation" and "Heterogeneous nucleation". [(Ref. 71, 27, 41)]

The second process of vapour to liquid transition mentioned above occurs when the system contains vapour absorbent solids surrounded by the vapour. The absorbed vapour layer, around the solid increases in thickness as the vapour pressure approaches the saturation pressure and acts as a nucleus for liquid droplet formation. [Ref. 71].

The first process; the "Homogeneous nucleation" involves systems containing vapour alone where vapour is pressurised or cooled until the liquid phase forms. In this process liquid droplets form around a nucleus in the vapour, and thus the transition to the liquid state begins.

The only way in which the nucleus of the second phase may come about in such a system seems to be by the simultaneous meeting of sufficient molecules to form a stable phase. This kind of nucleation would be possible due to molecular density fluctuations. The fluctuation phenomenon is a well established phenomenon and is derived in Appendix (II). According to the results it can be shown that if n is the average number density of molecules per unit volume, the number density will change as: $n \pm \sqrt{n}$. If for example n was taken as 10^{18} molecules/cm^3, which is fairly representative of a gas state, then n would vary between $10^{18} \pm 10^{9}$ molecules/cm^3 which seems negligible, but over smaller volumes the probability of sufficient molecules meeting together to form a 'droplet nucleus' becomes higher, the minimum number of molecules necessary to form a stable nucleus depending on the gas 'PVT' characteristics. Some of the small drops thus formed by statistical fluctuations can then collide to form larger ones.

If we consider the interplay of energies in the system, the energy transfer is from the free energy of the bulk of the vapour to the surface free energy of the droplet. The decrease in the free energy of

the vapour should be proportional to the mass of the vapour condensed. It could also be considered as the work done or required to form a droplet

(number of particles in the droplet) x (energy of a particle)

Which is from Kelvin's equation

$$(g)\left[\quad \left(\frac{2\lambda_s w}{r_d kT_l}\right)\right] \qquad \text{or}$$

$$(g)\left[\ln \left(\frac{p_d}{p_o}\right)\right] \qquad \text{where}$$

$$(g) = \frac{4}{3}\pi n_l r_d^3 \qquad ; \; n_l \text{ is liquid number density}$$

g is the number of particles in the droplet. The increase in surface energy of the droplet is proportional to the surface area of the droplet which is

$$4\pi\lambda_s r_d^2$$

Thus from the above equations, the increase in surface energy due to surface tension is proportional to the droplet radius squared, while the decrease associated with the work done in forming the droplet is proportional to the droplet radius cubed. Initially with the small radii involved the squared term is greater than the cubed term. As the radius increases from zero, the droplet acquires more energy than could be supplied by the system and hence the origin of the energy barrier that stops direct transition from the vapour to the liquid state.

8.2.7 Charged droplets

The simultaneous meeting of sufficient numbers of molecules, due to fluctuation pheonomena could overcome this barrier through the binding energies of the molecules. Up to this point in the discussion the vapour has been assumed to contain no ions.

Solidification of liquid helium is well known (Atkins crystallites) Ref. (45), and it is also known that in gaseous helium droplets may form Ref. (46). Although temperatures in dense metal vapours are far higher, so is the attraction of an atom towards an ion many times higher than in helium. In dense metal vapours the binding energy of the ions could overcome the energy barrier and helped by density fluctuations, the ions could become the nuclei for liquid droplet formation, with the difference that now the liquid droplets would be charged.

The change in the energy of the system with the introduction of ions should be

$$\Delta E = -g \ln \left(\frac{P_d}{P_o}\right) kT + 4\pi\lambda_s r_d^2 + A^+ \qquad (8.18)$$

where A^+ is the binding energy of the positive ions.

$$\Delta E = -\frac{4}{3}\pi_l \sigma r_d^3 \ln \left(\frac{P_d}{P_o}\right) kT + 4\pi\lambda_s r_d^2 + A^+ \qquad (8.19)$$

Differentiating with respect to r_d should give the most probable radius for the droplets.

From

$$\frac{d\Delta E}{dr_d} = 0$$

$$\ln \left(\frac{P_d}{P_o}\right) = \frac{2\lambda_s}{r_d} \left(\frac{1}{n_l}\right) \left(\frac{1}{kT}\right) \qquad (8.20)$$

which is similar to Kelvin's original equation.

As can be seen from the above discussion the nucleation of the droplets around a positive ion does not alter the relation derived for droplet dimensions. On the other hand, the charged droplet concept makes it possible to think of a positive sheath in front of the cathode, where charged particles have gathered due to the effect of the applied electric field. As the droplets drift towards the cathode, they will form a layer where they will just be touching the neighbouring droplets before they are all joined, and transformed into the complete liquid state. In the limit next to the cathode, the distances between the centres will be $\simeq 2r_d$. Hence their number density could be calculated through the relation,

$$\text{average distance between the centres} = \frac{1}{(n_d)1/3}$$

therefore, the number density of the droplets $n_d = 4.6 \times 10^{15}/cm^3$.

From,

$$n_d = n_{do} \exp \left(\frac{eV}{kT} \right)$$

The potential associated with this layer is $V = 0.56V$ and it can be compared with the evaporation potential of mercury. Furthermore if beyond this region the number density of the droplets somehow approaches the number density of the vapour, which would mean the droplet dimensions being reduced to the molecular dimensions, again from eq. (5.17a) $V = 0.35$ volts, which also compares well with the results of the present investigation which give an apparent evaporation potential of 0.37V. Presumably increasing temperature towards the positive column would act to destroy the droplets.

The thickness of the sheath could be calculated from

$$\lambda_D = \left(\frac{kT\epsilon_o}{2n_d e^2} \right)^{1/2},$$

$$\lambda_D = 4.7 \times 10^{-6} m \quad r_d = 300A$$

The electric fields set up across a positively charged droplet layer of this thickness would be of the right order of magnitude for appreciable field emission ($\sim 10^9$ V/cm).

I.T. Yakubov recently Ref. (62) has also suggested the existence of charged droplets, in dense caesium vapour, and derives similar equations with corrections to the binding energy of positive ions due to the finite radius of the droplet. His equations take the following form

$$\Delta\phi = -Tg \ln\left(\frac{Ps}{p}\right) - 4\pi\lambda_s R^2 + A^+ - \frac{e^2}{2R\epsilon} \qquad (8.21)$$

where R, λ_s, A^+, e, P_s, ϵ are the radius of droplet, surface tension, binding energy of the ion, electron charge, saturation pressure and the dielectric constant.

$$T\eta_l \ln\left(\frac{p}{p_s}\right) = \frac{2\lambda_s}{R} - \frac{e^2}{8\pi R^4 \epsilon} \qquad (8.22)$$

at the saturation line $p = p_s$

$$R = \left(\frac{e^2}{16 \pi E_o \gamma} \right)^{1/3} \qquad (8.23)$$

$$R = 4.9A$$

The volume of the droplet then would be $4/3\ \pi R^3 = 4.9 \times 10^{-22} cm^3$ and the number of particles per droplet 2.9×10^2. Assuming that the droplets are just touching, then from

$$\left(\frac{1}{2R}\right)^3 = \text{number of droplets } 'n_d'$$

then $n_d = 1.06 \times 10^{21}$ droplets/cm^3. It looks as though the suggestion that was made before that the droplet size could gradually reduce to molecular dimensions seems to be justified, through a correction as shown by Yakubov, to the binding energy of the positive ions due to the finite radius of the droplets.

8.2.8 Possible conduction mechanisms based on the droplet concept.

The possible existence of liquid droplets suspended in the vapour is a new phenomena, and could also lead to other mechanisms to explain the high experimental conductivities, such as an increase in the efficiency of the thermal ionization. Compared with ionizing the atoms of the vapour it should be much easier to ionize liquid droplets. In a neutral plasma the positively charged droplets must be surrounded by electrons and these could be in the form of electron clouds around the droplets. Although the results of the calculations seems to indicate that droplets are collisionless and therefore not the current carrying

elements, the loosely bound electron clouds could be the answer. The electrons could hop from cloud to cloud, producing a conduction mechanism similar to the conduction mechanism in semi-conductors. Or the electron clouds could be overlapping each other. In this case it is possible for the electrons to swim through the fermi-level of the liquid cathode into the electron clouds of the droplet layers next to the cathode, and it may be that at a point where the electron clouds do not overlap due to decreasing number density of the charged droplets towards the anode (hence increasing the distance between the droplets), the electrons could shoot straight through to the anode without any further encounters.

It was thought that it would have been of interest if the thickness of the electron cloud was known. Therefore the following attempt was made.

From Gauss' law

$$4\pi r^2 E = 4\pi \left[Ze + \int_0^r -e\rho(r') \, 4\pi r'^2 dr' \right] \qquad (8.24)$$

The left hand side of the equation is the area of the surface times the electric field at the surface. The first term in the brackets is the droplet charge, the integral represents the total charge due to the electrons contained within the surface $-e\rho(r')$ is the charge per unit volume element. Using the relations where

$$eE = \text{Force} = \frac{dV(r)}{dr} \; ; \; \rho(r') = n_e = n_o \exp\left(\frac{eV(r')}{kT}\right)$$

eq. (8.24) becomes

$$r^2 \frac{d[-V(r)]}{dr} = -Ze^2 + 4\pi e^2 \int_0^r n_o \exp\left(-\frac{eV(r')}{kT}\right) r'^2 dr'$$

differentiating we get

$$\frac{1}{r^2}\frac{d}{dr}\left[r^2\frac{d[-V(r)]}{dr}\right] = 4\pi e^2 n_0 \exp - \frac{eV(r)}{kT}$$

After this step the above equation needs numerical methods for solution. Instead, if we could make use of its well known implication that Ref. (49)

$$V(r) \Rightarrow \frac{Ze^2}{r} \quad \text{as} \quad r \Rightarrow 0$$

and we assume that at the surface of the droplet the electrons will have fermi-levels of energy $\sim$ 4.6 eV and we further assume that at the edge of the cloud the electron energies will be that of the thermal energy of the vapour $\simeq$ .13eV forming a direct ratio

$$\frac{4.6}{0.13} \quad \alpha \quad \frac{\frac{Ze^2}{rd}}{\frac{Ze^2}{r_c}} \quad \alpha \quad \frac{r_c}{r_d}$$

where r_d is the radius of the droplet r_c is the radius of the electron cloud

$$r_c \quad \alpha \quad 35 \; r_d$$

This seems to be of the right order of magnitude to span the average distance calculated between the droplets in section (8.2.3).

8.2.9 Longini's model and the droplet hypothesis

In section 4.6, when reviewing the literature from the point of view of continuous transition from solid/liquid state to plasma, Longini's model was mentioned. In this model the matter in the cathodic

region was thought of as layers of positive ions with increasing lattice pitch in the direction of motion of the electrons. Furthermore the positive ions had the property of very slow motion, so that the individual electrons would see an almost static picture, which would facilitate application of the wave analysis. It was also stated that a form of recombination would also have to be introduced into the model to account for the fact that most of the departing material consisted of neutral atoms.

A rough analysis as presented in sections 8.2 - 8.2.8 shows that properties of charged droplets might be reconciled with such a model.

It must be emphasised that it is not the claim of this thesis that a new model is presented totally explaining the characteristics of cathode spots. Suggestions of this chapter are offered as possible explanations/ interpretations of the fact that mercury vapour conducts in a temperature and pressure regime in which it is generally assumed that should not conduct.

CONCLUSION

CONCLUSION

The primary purpose of this work was to investigate, the electrical behaviour of nearly saturated mercury vapour at medium pressures and low temperatures, which is believed to be present next to the cold-cathode spots in mercury arcs and, in particular,

a) to check the assumption made in many existing cold cathode theories that this vapour layer is electrically insulating, and,

b) to check the conclusion arrived at by, Endean and Christopoulos, following their work on caesium vapour under approximately similar conditions, that the ionization potential of the vapour is not too important a factor in determining the pre-breakdown electrical conductivity.

The present investigation has examined the dependence of mercury vapour's pre-breakdown electrical conductivity on the vapour pressure and temperature over ranges not previously investigated. The experiments were carried out within a pressure range corresponding to liquid temperatures of (300-600K) and a vapour temperature range of 600-900K, thus covering the temperatures and pressures estimated for the vapour clouds next to the mercury spot in an arc discharge.

The present experimental results have provided some evidence in support of the conclusion that the ionization potential of the vapour is not a pre dominantly important factor, and against the assumption that the vapour within these pressure and temperature ranges is an insulator.

It is possible to conclude from the experimental results that the pre-breakdown electrical conductivity within the experimental ranges depends very sensitively on the degree of saturation of the vapour, with two distinct regions of behaviour. Closer to full saturation, the conductivity

is pre dominantly dependent on pressure while further away from full saturation, after the 'switch-over point' ($10^3/T_l - 10^3/T_g \geq 1.05$), one observes Saha-type of behaviour, in that the conductivity is pre dominantly dependent on the vapour temperature, though radically different from it in quantitative terms, i.e., the apparent ionization potential is 1.9V as opposed to 10.4V.

After the first set of experiments, further measurements were carried out in which the discharge was driven still closer to the saturation, with different discharge tubes, i.e., similar dimension, the same interelectrode distance; and similar dimension, longer inter-electrode distance. The results of the new measurements confirmed the earlier results.

Theoretical predictions of electrical conductivity based on Saha's equation were many orders of magnitude lower than the experimental values. On the other hand it was possible to predict electrical conductivities of the right order of magnitude for super-critical mercury as determined by Franche and Hensel.

This present investigation has reviewed the literature dealing with arc discharges in general and cold-cathode mechanisms in particular. It appears that the formulae derived empirically from the present measurements cannot be reconciled with a simple theory based on equilibrium volume ionization, and moreover that the very sensitive dependence on the degree of saturation is a newly observed phenomenon, though not unique since similar behaviour was also observed in caesium vapour under similar conditions.

Possible interpretations of the results have been discussed in terms of their relevance to the existing cold-cathode theories. It was thought that the arguments were in favour of a metallic-type of behaviour in the dense vapour cloud when the vapour was very close to saturation. Although there seems to be no existing theory to explain the observed

experimental behaviour as a whole. On the other hand, the observed behaviour of cathode spots, in particular their apparently random motion, could be used to explain the present experimental results, since the extrapolation of the empirically derived formulae to full saturation predicts that the electrical conductivity varies from very low conductivities to metallic-type conductivities, with slight changes in the temperature and pressure of the vapour. Further suggestions were made for a new model in terms of liquid droplets. Possible approaches towards a new theory were discussed in conjunction with Longini's model. Further work is necessary to see if other metal-vapours behave in a similar way, to increase the accuracy of the temperature measurements, and to obtain corroborating spectroscopic evidence. It seems that the main difficulties are how to take into account dynamic and complex mechanisms at the microscopic level, and trying to derive a steady picture for the macroscopic quantities. Using the modern amenities, of vast data storage and automatic means of data recording, i.e., a data logger, continuous monitoring of the phenomena over prolonged periods of time to average out various uncontrollable factors should be possible and would facilitate a statistical approach.

As a result of the present investigation it is concluded that, contrary to the popular supposition that mercury vapour is a perfect insulator at low temperatures and medium pressures, it does in fact conduct. Moreover the ionization potential of the vapour is not too important a factor for the passage of the current and Saha's equation cannot be used indiscriminately for all temperature and pressure ranges for metal-vapours until a sound knowledge of what happens to the ionization potential under these circumstances is available.

LIST OF REFERENCES

1. DRUMMOND, J.E.

'Plasma Physics'
McGraw-Hill Book Company Inc., 1961

2. PAPOULAR, R.

'Electrical Pheonomena in Gases'
Iliffe Books Ltd., London 1965 (2nd Edition)

3. COBINE,

'Gaseous Conductors'
New York, Dover (1941) repr. (1958)

4. KOLTYPIN, E.A.,NASTYUKHA, A.J.,SMIRNOV, P.R.

'Rectification in a low-pressure arc with a Hollow Cathode.'
Sov.Phys.Tech.Phys.,Vol.15,No.10, (1971), p.1703-1708.

5. POKROVSKA, A.S.,SABOLAVA, Z.,KLYARFELD, B.N.

'Ignition of the High Voltage Discharge at Low Pressure.'
Sov.Phys.JETP,Vol.5, (1957), p.812

6. McCLURE, G.W.

'High Voltage Glow Discharges in D_2 Gas.I.Diagnostic Measurements'
Phys.Rew.,Vol.124, (1961), p. 969-982

7. ZAIDER, A.N.

'Local Thermodynamic Equilibrium.'
Sov.Phys.Tech.Phys.,Vol.22,No.3, (1977) p.401-402

8. HAWATSON, A.M.

'An Introduction to Gas Discharges.'
Pergomon Press, (1965)

9. HAYOUX, M.F.

'Arc Physics.'
Springer-Verlag, New York Inc., (1968)

10. SPITZER, L. Jr.

'Physics of Fully Ionised Gases.'
New York, Interscience Publishers Inc., (1956)

11. WOMACK, G.J.

'M.D.H. Power Generation.'
Chapman and Hall Ltd., (1969)

12. RICHTMYER, F.K.,KENNARD, E.A.,COOPER, J.N.

'Introduction to Modern Physics.'
McGraw-Hill, Book Company, 1969, (6th, ed.)

13. SEARS, F.S.,SALINGER, L.G.,

'Thermodynamics, Kinetic Theory and Statistical Thermodynamics.'
Addison-Wesley Publishing Company, 1975 (3rd ed.)

14. OSKAM, H.J.

'Microwave Investigation of Disintegrating Gaseous Plasmas.'
Utrecht University, Ph.D. Thesis, (1957) (Translated)

15. FLOOD, E.A.

'The Solid-Gas Interface.'
Edward Arnold (Publishers) Ltd., London, (1967)

16. ENDEAN, V.G.

'(Private Communication)'

17. PARKER, P.

'Electronics.'
Edward Arnold, (Publishers.), London, 1958 (5th ed.)

18. LABEDEV, A.M., et. al.,

'Excitation and Ionization in a Non-equilibrium Plasma.'
Sov.Phys.,Tech.Phys.,Vol.22,No.3, (1977),p. 339-344.

STAKHANOV, I.P,CHERKOVETS, V.E.

'Effects of Cathode Temperature on the Rate of Non-equilibrium Ionization.'
Sov.Phys.,Tech.Phys.,Vol.15,No.2, (1970) p. 215-219

RESHENOV, S.P.

'Non-equilibrium Ionization in the Cathode Region of a High Pressure Arc.'
Sov.Phys.,Tech.Phys.,Vol.19,No.8, (1975), p. 1073-1075

19. GRAKOV, V.E., et. al.

'Current Density in the Spot of an Electric Arc.'
Sov.Phys.,Tech.Phys.,Vol.15,No.10, (1971) p. 1664-1666

SANGER, C.C.,SECKER, P.E.

'Arc Cathode Current Density Measurements.'
J.Phys.D.,Vol.4, (1971), p. 1940-1945

20. ENGEL, V.

'Ionised Gases.'
Clarendon Press , Oxford (1955)

21. ASPEN, H.

'Electrodynamic Anomalies in Arc Discharge Pheonomena.'
IEE Transactions on Plasma Science,Vol.PS-5,No.3, (1977),
p. 159-163

22. SONNTAG, R.E.,WYLEN, G.J.V.

'Fundamentals of Statistical Thermodynamics'
John Wiley and Sons Inc., (1966)

23. DRUVESTEYN, M.J.

'Electron Emission of the Cathode of an Arc.'
Nature,Vol.137, (1936), p. 580.

DRUVESTEYN, M.J., PENNING, F.M.

'Mechanism of Electrical Dishcarges in Gases of Low Pressure.'
Rev.Mod.Phys.,Vol.12, (1940), p. 87-365.
See also Ref. (25)

24. LLEWELLYN JONES, F.

'Influence of Cathode Surface Layers on Minimum Sparking
Potential of Air and Hydrogen.'
Prc.Phys.Soc.B.,Vol.64, (1950), p. 397-404

25. MEEK, J.M.,CRAGGS,J.D.

'Electrical Breakdown of Gases.'
Clarendon Press, Oxford (1953)

26. GUILE, A.E. et. al.

'The Role of Surface Layers on Electron Emission, and
Cathode Root Motion of Cold Cathode Arcs.'

27. Mc.DONALD, J.E.

'Homogeneous Nucleation of Vapour Condensation,
I.Thermodynamic Aspects.'
Am.J.Appl.Phys.,Vol.30, (1962), p. 830-877

28 KRAT'KO, S.A.

'Existance of Threshold Arc Currents'
Sov.Phys.Tech.Phys.,Vol.21, (1976), p. 625-627

GOKBENBACH, E.

'Influence of Electrode Coating on the Breakdown Voltage of SF_6.'
IEE,5th Int.Conf. on Gas Discharges,No.165, (1978) p. 181-184

BERGER, S.

'Predischarge Currents in Compressed Air.'
IEE, 5th Int.Conf. on Gas Discharges, No.165, (1978) p. 173-176

LLEWELYN JONES, F.

'Incomplete Breakdown, a Cathode De-ionization Effect.'
Nature, Vol.157, (1946), p. 480
See also Ref. (25), Ref. (29), Ref. (30), Ref. (59).

29. I.E.E. CONFERENCE PUBLICATION

'Gas Discharges and Their Applications'
No. 189, Part I, (1981)

30. VLASTOS, E.,RUSCK, S.

'Influence of the Electrode Surface State on the Breakdown of Pressurized SF_6.'
IEE Conf. Publication, No. 189, (1981), p. 200-207.

31. GUILE, A.E.

'Stored Charges in Relatively Thin Oxide Films.'
J.Phys.D.,Vol.5., (1972), p. 1153-1156

32. HITCHCOCK, A.H.,GUILE, A.E.

'Effect of Copper Oxide Thickness on the Number and Size of Cathode Emitting Sites.'
Proc.IEE,Vol.124, (1977), p. 488-492

33. RAGEH, M.S.I. et. al.

'Initiation of Arc Cathode Emission in Cu_2O Films.'
Proc. IEE,Vol.125, (1978), p. 81-84

34. RAGEH, M.S.I. et. al.

'Charge Storage and Effect of Ultraviolet Radiation on Aluminium Oxide Films.'
J.Phys.D.,Vol.10, (1977), p. 2269-2275

35. LEE, T.H.

'Theory for the Cathode Mechanism in Metal Vapour Arcs.'
J.App.Phys.,Vol.32, (1961), p. 916-923

36. LEE, T.H.

'T-F Theory of Electron Emission in High Current Arcs.'
J.App.Phys.,Vo.30,(1959), p.166-171

37. ECKHARDT, G.

'Interpretation of Data on Cathode Erosion and Efflux from Cathode Sports of Vacuum Arcs.'
J.App.Phys.,Vol.46, (1975), p. 3282-3285

ECKHARDT, G.

'Velocity of Neutral Atoms Emanating from the Cathode of a Steady State Low Pressure Mercury Arc.'
J.App.Phys.Vol.44, (1973), p. 1146-1155

ECKHARDT, G.

'Efflux of Atoms from Cathode Spots of Low Pressure Mercury Arc.'
J.App.Phys.Vol.42, (1971), p. 5757-5760

38. FROOME, K.D.

'The Rate of Growth of Current and Behaviour of the Cathode Spot in Transient Arc Discharges.'
Proc.Phys.Soc.,Vol.60, (1948), p.424-435

FROOME, K.D.

'The Behaviour of Cathode Spot on an Undisturbed Liquid Surface of Low Work Function.'
Proc.Phys.Soc.B.,Vol.63, (1950), p. 377-385

39. COBINE, J.D.,GALLAGHER, C.J.

'Current Density of the Arc Spot.'
Phys.Rev.,Vol.74, (1948), p. 1524-1530

ROKHOVSKII, V.I.

'Experimental Study of Dynamics of Cathode Spot Development,'
IEE Transactions on Plasma Science, Vol.PS-4, (1976), p. 81-102

40. ECKER, G.

'Vacuum Arc Cathode - A Pheonomenon of Many Aspects.'
IEEE Transactions on Plasma Science, Vol. PS-4, (1976), p. 218

GRAY, E.W.

'On the Electrode Damage, and Current Densities of Carbon Arcs.'
IEEE Transactions on Plasma Science, Vol. PS-6, (1977), p 384.

ROTHSTEIN, J.
'On the Mechanism of Electron Emission at the cathode Spot of an Arc.'
Phys. Rev., Vol. 73, (1948) pg. 1214

41. McDONALD, J.E.

'Homogeneous Nucleation of Vapour Condensation, II. Kinetic Aspects.'
Am.J.App.Phys.,Vol.31, (1963), p. 31-41

42. HANGSTRUM, H.D.

'Theory of Auger Ejection of Electrons from Metals by Ions.'
Phys.Rev.,Vol.96, (1954), p. 336-365

43. KHRISTOV, N.N.

'Secondary Electron Emission with Charge Exchange'
Sov.Phys.Tech.Phys.,Vol.21, (1976), p. 464-467

44. MITTERAUER, J.

'Dynamic Field Emission (D.F. Emission): A New Model of Cathode Pheonomena in Cold Cathode Arcs.'
Int.IEE,Conf.Gas Discharges, (1972) p. 215-217

45. SHIKIN, V.B.

'Mobility of Charges in Liquid, Solid and Dense Gaseous Helium.'
Sov.Phys.Usp., Vol.20, (177),p.226-246

46. IAKUBOV, I.T.

'Positive Ions in Dense Gaseous Helium.'
Phys.Lett.,Vol.69A, (1978), p.45

47. BUBE, R.H.

'Electronic Properties of Crystalline Solids. (An Introduction to Fundementals.)
Academic Press (1974)

48. ZYKOVA, N.M. et. al.

'Cathode and Anode Regions in an Electric Arc., I. Cathode and Anode Region at Low Pressures and in Vacuum.'
Sov.Phys.Tech.Phys.,Vol.15, (1971), p. 1844-1849

49. EISBERG, R.M.

'Fundamentals of Modern Physics.'
Wiley International edition (1965) 2nd Ed.

50. HAYNES, J.R.

'The Production of High Velocity Vapour Jets by Spark Discharge.'
Phys.Rev.,Vol.73, (1948), p. 891-903

FINRELBURG, W.

'A Theory of the Production of Electrode Vapour Jets by Sparks and Arcs.'
Phys.Rev.,Vol.74, (1948), p. 1475-1479

51. WILLIAMS, G.C.,CRAGGS, J.D.,HOPWOOD, W.

'The Excitation and Transport of Metal Vapour in Short Spark in Air.'
Proc.Phys.Soc.B.,Vol. 62., (1949), p. 49-

52. FROOME, K.D.

'The Behaviour of the Cathode Sport on an Undisturbed Mercury Surface.'
Proc.Phys.Soc.,Vol.62.B., (1949), p. 805-812

CRAGGS, J.D.,HOPWOOD, W.

'Observation of Spectral Lines with Electron Multiplier Tubes.'
Nature, Vol. 158, (1946)., p. 618

53. AIREY, D.J.,SWIFT, J.D., GOZNA, C.F.

'Vapour Density Variation in a Pulsed Mercury Discharge.'
J.Phys.D.,App.Phys.,Vol.5, (1972) p. 2161-2169

54. HOLMES, A.J.T.,COZENS, J.R.

'The Abnormal Glow Discharge in Mecury Vapour.'
J.Phys.D.,App.Phys., Vol. 7, (1974), p. 1723-1739

55. ENDEAN, V.G.

'Pre-breakdown in Electrical Conductivity of Nearly Saturated Vapour Casium.'
IEE Proc.,Vol.127, (1980), p. 95-101

56. MITCHELL, P.,WILSON, M.

'A Note on Ionization Potentials of Mercury.'
Chem.Phys.Lett., Vol.3, (1969), p. 389-391

57. LEBEDEV., M.A.,GUS'KOV , Yu.K.

'Electrical Breakdown in Casium Vapour.'
Zh.Tek.Fiz.Vol.33.,(1963), p. 1462-1463

58. JONES, L.F.,GALLOWAY, W.R.

'The Sparking Potential of H_g Vapour.'
Proc. Phys.Soc., 50, (1938) ^{g}p. 207-212

HACKMAN, R.

'Breakdown Potentials of mercury Vapour in Uniform Electric Fields.'
Int.J.Electronics., Vol. 28, No. 3, (1970) p. 263-269

OVERTON, G.D.N.,SMITH, D.,DAVIES, D.E.

'A Deviation from Paschen's Law in Mercury Vapour.'
Brit.J.App.Phys., Vol. 16, (1965), p. 731-732

59. BORTNIK, I.M.

'Pre-breakdown Processes in High-Pressure Gases.'
Sov.Phys.Tech.Phys. 23(2), (1978), p. 156-160

60. NAKAMURA, Y., LUCAS., I.

'Electron Drift Velocity and Momentum Cross-Section in Mercury, Sodium and Thallium Vapours II Theoretical.'
J.Phys.D.App.Phys., Vol.11, (1978), p. 337-345

61. ENDEAN, V.G.

'Stable Cold Cathode Arc.'
Nature, Vol. 254, (1975), p. 131-132

62. YAKUBOV, I.T.

'Theory of the Enhanced Electrical Conductivity of Dense Metal Vapours Near Saturation.'
Sov.Phys.Dokl.,24(8), (1979), p. 634-636

63. HENSEL, F., FRANCK, E.U.

'Metal-Nonmetal transition in Dense Mercury Vapour.'
Rev.Mod.Phys. Vol.40., No. 4, p.697-703

64. FRANCK, E.U.,HENSEL, F.

'Metallic Conductance of Supercritical Mercury Gas at High Pressures.'
Phys.Rev.Vol. 147, No. 1, (1966), 109-110

65. RAKHOVSKII, V.I.

'Cathode Emission Mechanism in an Arc Discharge.'
Sov. Phys.Tech.Phys., Vol.10, No. 12, (1966), p. 1707-1709

67. SLEPIAN, J.

'Theory of Current Transference at the Cathode of an Arc.'
Phys.Rev., 27, 407 (1926).

68. HULL, A.W.

'Cathode Spot'
Phys.Rev. Vol. 126, No. 5, (1962), p. 1603-1610

69. MOTT, N.F.,DAVIS,E.A.

'Electronic Processes in Non-Crystalline Materials.'
Clarendon Press, Oxford, (1979) (2nd Ed).

70. RENKERT, Von.H.,HENSEL, F.,FRANCK, E.U.

'Elekrtische Leitfahigkeit Flussigen und Gasformigen Casiums Bis 2000°C und 1000 Bar.'
Ber.Bunsenges Phys.Chem.,Vol.137, (1971) p. (507-512.

continued over

APPENDIX I

ELECTRICAL CONDUCTIVITIES

Ion Mobility

Collision Cross-section

Mean Free Paths

Electron Mobility

Final Theoretical Expression for Conductivity

APPENDIX I

ELECTRICAL CONDUCTIVITIES

In a weakly ionised gas, a theoretical expression, for calculating the electrical conductivity could be derived from classical considerations, under a set of simplifying assumptions. Strict quantitative agreement between the theoretically calculated values and actual values is not to be expected, because of the nature of the assumptions, and the lack of basic data.

Nevertheless, given that the conditions set in the assumptions are fair approximations of the actual physical conditions. It should be possible to predict expected types of behaviour and approximate values; at least in terms of orders of magnitude.

A weakly ionised gas (vapour*) in thermal equilibrium should have an equal number of ions and electrons at low homegeneous concentrations. Therefore assume that the plasma number density n is

$$n \simeq n_i \simeq n_e \qquad (1)$$

and that externally applied low electric fields do not introduce severe disturbances is such an equilibrium.

---

* The terms vapour and gas are loosely used in the literature. Strictly speaking a gas which exists below its critical temperature is usually called a vapour, because it can condense.

The expression for the electrical conductivity of the gas, due to the motion of both charged particles, set in motion in this field E, could be derived as follows. From the definition of the total electric current density jt, :

$$jt = e\, n_i\, \bar{V}_{id} - e\, n_e\, \bar{V}_{ed} = enE\ (\mu_i + \mu_e) \qquad (2)$$

where $\bar{V}_{id} = \mu_i E$ and $\bar{V}_{ed} = \mu_e E$; e, n_i, n_e, $\bar{V}_{id}$, $\bar{V}_{ed}$, μ_i, μ_e are electron charge, ion number density, electron number density, average ion drift velocity, average electron drift velocity, ion mobility and electron mobility respectively. The electrical conductivity is defined as (from eq. (2)).

$$jt = \sigma E \ ; \text{ where} \qquad (3)$$

$$\sigma = en_o\ (\mu_i + \mu_e)$$

Ion Mobility

If ions could be thought of as forming a cloud, in which their velocity distribution is Maxwellian (equally distributed in all directions about a mean value), then an electric field acting on this cloud will move it bodily. The average speed with which the centre of this cloud moves, in the direction of and parallel to the field, is defined as the drift velocity. If this cloud was moving in its own gas, because of the low number density of the ions (compared to that of the neutrals), the frequency of ion-ion encounters would be negligibly low. That is to say ion-neutral encounters would dominate the physical processes. During the interval between two such consecutive collisions (which would be very short due to the high frequency of such

encounters), the ions would only receive very low levels of energy from the weak electric field. Therefore elastic collisions would dominate.

Having nearly equal masses, ions and neutrals will readily exchange most of their kinetic energies. After some time interval, this exchange of energy will lead to a quasi-steady state and ideally to a thermodynamic equilibrium. The equilibrium is thermodynamic only to a first approximation, since the drift velocities of the ions (though very small relative to the average random thermal velocities) is not zero.

In the following, perfect thermodynamic equilibrium, zero post-impact velocities and the hard-sphere model of the kinetic theory of gases will be assumed. It will be further assumed that, after such collisions, ions will proceed progressively in the direction and parallel to the field. Although this clearly cannot be true for each individual ion, considering that the random motion by itself cannot transfer the ions from one end of the plasma to the other, and within the spirit of the definition of the drift velocity, it should be, statistically at least, a safe assumption to make. Furthermore, the random thermal velocity of the individual ions will be assumed to be equal to the average random velocities of the neutrals, and all ions will be assumed to travel equal distances between two successive encounters. This in turn will be assumed to be equal to the mean free path of the ions in their gas.

With the above assumptions, the time interval between the collisions, would be

$$t = \lambda_{i/V_{th}} \tag{4}$$

The ion is accelerated by the field in this interval, and

$$F = m_i a = eE \tag{5}$$

F, m_i, a, e, E are the force experienced by the ion of mass m_i, acceleration of the ion, electron charge and the electric field respectively. Again from the laws of motion and neglecting time of impact, 's' the distance travelled, is

$$s = \tfrac{1}{2} at^2 = \tfrac{1}{2} \left(\frac{eE}{m_i} \right) t^2 \text{ and velocity } V = \frac{s}{t}$$

the ion drift velocity is

$$V_{id} = \tfrac{1}{2} \left(\frac{e}{m_i} \right) \left(\frac{\lambda i}{V_{th}} \right) E \tag{6}$$

Therefore, the ion mobility μ_i is

$$\mu_i = (\tfrac{1}{2}) \left(\frac{e}{m_i}\right) \left(\frac{\lambda_i}{V_{th}}\right) \tag{7}$$

A more rigorious treatment (taking into account the statistical distribution of mean free paths) would lead to

$$\mu_i = \left(\frac{e}{m_i} \right) \left(\frac{\lambda_i}{V_{th}} \right) \tag{8}$$

Collision Cross-section

When a particle is injected into a gas with velocity V_{th} the probability of collision of a given type to occur is,

$$c.p = nQ(V_{th})\, dx \tag{9}$$

where n is the number density of the target particle, dx is the distance travelled in the gas, $Q(V_{th})$ is a coefficient of proportionality dependent on the velocity and the nature of the reaction, or effective cross-section of the collision (in general, reaction). $Q(V_{th})$ also has a physical meaning, which is clear in the case of the hard-sphere model (since collision implies two particles touching each other).

$$Q(V_{th}) = \pi (R_1 + R_2)^2$$

where R_1 and R_2 are the radii of the two particles respectively. In the case of ion encounters since $r \cong r_i \cong r_a$

$$Q(V_{th}) = 4 \pi r^2 \qquad (10)$$

If the average velocity of the incident particles V_{th} is constant then from $dx = V_{th}\, dt$ and eq. (9) the probable number of collisions in time dt is

$$n\, Q(V_{th})\, dx = n\, Q(V_{th}) V_{th} dt \qquad (11)$$

Therefore the collisional frequency θ is

$$\theta = n\, V_{th}\, Q(V_{th}) \qquad (12)$$

Mean Free Paths

The mean free path of a particle is defined as the average distance it travels in between collisions. Since a particle will traverse a distance of $V_{th} dt$ in a time interval dt, it will undergo θdt

collisions, therefore

$$\lambda = \frac{V_{th}dt}{\theta dt} = \frac{1}{nQ(V_{th})} \qquad (13)$$

More rigorous treatment (taking into account the relative velocities of the colliding particles) would yield

$$\lambda = \frac{1}{\sqrt{2}} \left(\frac{1}{nQ(V_{th})}\right)$$

Because of their similar masses ions and neutrals will have nearly the same m.f.p. $\lambda \cong \lambda_i \cong \lambda_a$. The mean free path of the electrons could be expressed through the same relation since the size of the electron is very small and could be neglected

$$Q(V_{th}) = \pi r^2 \qquad \text{and therefore} \quad \lambda_e = \frac{1}{n\pi r_a^2} \qquad (14)$$

In the above discussion $Q(V_{th})$ has been assumed constant, that is, independent of the velocity. Experimental investigations have shown that it varies with the incident energy of the electron. This effect was first discovered by Ramsauer and Townsend Ref. (20), and is called after them. There is a marked minimum at low velocities of the order of $\sim$1eV , except in hydrogen and helium. Atoms from the same column in the periodic table behave on the whole in a similar manner. In every case, the effective cross-sections decrease regularly as the energy increases beyond $\sim$ 20eV and there is a marked maximum effective cross-section at a certain accelerating potential. (In between $\cong$ 1.5 - 4 eV for alkaline metals, which have higher cross-sections on the whole and $\cong$ 9 - 16eV for rare gases with lower cross-sections, see Fig. (A.I.1)(A.I.2)(A.I.3)(A.I.4).)

A theoretical explanation for this behaviour is provided by quantum wave mechanics. There is another way of predicting the Ramsauer-Townsend effect. It can be shown that, by the use of the uncertainty priciples, the classical collision between an electron and a molecule (atom becomes indefinite when their relative velocity is very small). Heisenberg's uncertainty principle is,

$$(\Delta mV)(\Delta x) \gtrsim h/2\pi$$

(where Δx is position coordinate and ΔmV is the linear momentum) for the classical concept to hold. Taking the uncertainty in position equal to the diameter of the atom $\Delta x \cong 10^{-8}$ cm and with $m \simeq 10^{-27}$gr, ΔV should be 10^{8}cm/sec or about 2.8eV, so electrons of energies of the order of $\lesssim$ 1eV moving in the gas are undetermined ($\Delta V \simeq V$) so far as atomic dimensions are concerned. Therefore for speeds of the order of $\lesssim$1eV the classical theory fails.

Electron Mobility

In Chapter two it has been mentioned that the electrons were the most serious violators of the thermodynamic equilibrium conditions. Therefore eq. (8) is not commonly applied to the electrons. Generally it becomes more feasible to apply these concepts when the gas pressure is some hundreds of mmHg and/or the gas temperatures are considerably higher.

However, with a change of emphasis in the concepts of the eq. (8), it could be re-written as

$$\mu_e = \frac{e}{m_e}\left[t_{(average)}\right] = \left(\frac{e}{m_e}\right)\left(\frac{1}{\theta_m}\right) \qquad (15)$$

where t (average) is the average time between collisions and θ_m is its reciprocal the collision frequency. The subscript signifies the assumption that an electron loses its momentum in the field direction in each collision. θ_m may be an effective collision rate, corresponding to the use of a cross-section for momentum transfer.

Therefore from eq. (3) and (8),(15)

$$\sigma = en_o \left(\frac{e\,\lambda i}{m_i V_{th(ions)}} + \frac{e}{m_e \theta_m} \right) \qquad (16)$$

In perfect equilibrium

$$\frac{e}{m_e \theta_m} >> \left(\frac{e}{m_i}\right) \left(\frac{\lambda_i}{V_{th(ions)}}\right) \qquad (17)$$

Therefore for a theoretical conductivity expression we would have

$$\sigma = \frac{n_o e^2}{n_a m_e \bar{Q}(V_{th}) V_{th}} \qquad (18)$$

Final Theoretical Expression for Conductivity

Finally to be able to calculate the theoretical electrical conductivity values, an expression for the plasma number density is needed. Although there is experimental evidence to support the calculations of the electrical conductivities using Saha's equation to calculate the plasma number densities at very high temperatures, no quantitative check has been done for the temperature and pressure regimes of this investigation.

Consider a cross-section at the boundary between the plasma and the sheath (near the wall). Again assume equilibrium and that the neutral number density does not change across the cross-section. Assume also

that the flux of the electrons into the volume of the gas from the wall is governed by Richardson's law of emission, and that flux of particles arriving at the cross-section is equal to the flux of the particles leaving the cross-section, and rebounding as ions from the wall. Then

$$n_e \langle V_{average} \rangle = n_F \exp\left(-\frac{e\psi}{kT}\right) \langle V_{average} \rangle \qquad (20)$$

$$n_i \langle V_{average} \rangle = n_a \exp\left(\frac{e\psi}{kT}\right) \langle V_{average} \rangle \qquad (21)$$

Now n_i and n_e may be written, from Boltzmann's relation,

$$n_i = n_o \exp\left(\frac{eV}{kT}\right) ; \; n_e = n_o \exp\left(-\frac{eV}{KT}\right) \qquad (22)$$

and the plasma number density n_o will be

$$n_o = (n_F \, n_a)^{\frac{1}{2}} \exp\left(-\frac{eV_e}{kT}\right) \qquad (23)$$

where n_F is the fermi-level number density.

$$n_F = [2(2\pi_m kT)^{3/2}]/h^3 \qquad \text{Ref. 49} \qquad (24)$$

in the above expression h is Planck's constant (6.62×10^{-34} J-H_z^{-1}) k is Boltzmann's constant (1.38×10^{-23} J-K^{-1}), and m_e is the mass of the electron (0.9×10^{-30} kg). Therefore

$$n_F = 4.7 \times 10^{21} \; T^{3/2} \; m^{-3} \qquad (25)$$

A similar equation can also be derived from thermodynamical

considerations, and is known as Saha's equation (see Chapter two). Combining eq. (18) and (23), the final expression for the electrical conductivity of a weakly ionised gas (vapour) is

$$\sigma = \frac{(n_a n_F)^{\frac{1}{2}} e^2 \exp\left(-\frac{eV_i}{2kT}\right)}{n_a m_e Q\,(V_{th})\, V_{th}} \qquad (26)$$

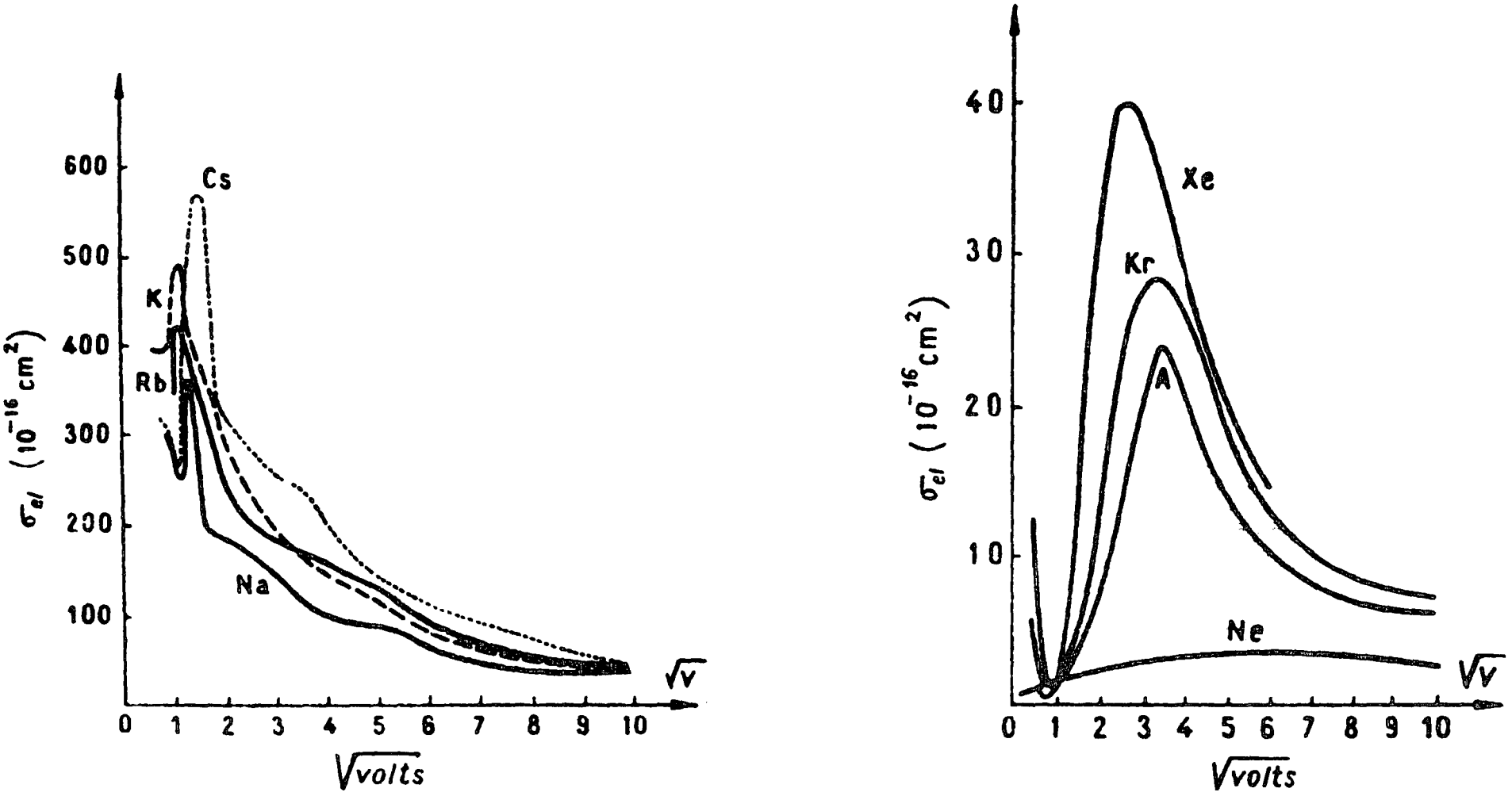
600
500
400
300
200
100
Cs
K
Rb
Na
σ_{el} (10^{-16} cm^2)
0 1 2 3 4 5 6 7 8 9 10
$\sqrt{V}$
$\sqrt{volts}$
40
30
20
10
Xe
Kr
A
Ne
σ_{el} (10^{-16} cm^2)
0 1 2 3 4 5 6 7 8 9 10
$\sqrt{V}$
$\sqrt{volts}$

FIG. AI-1

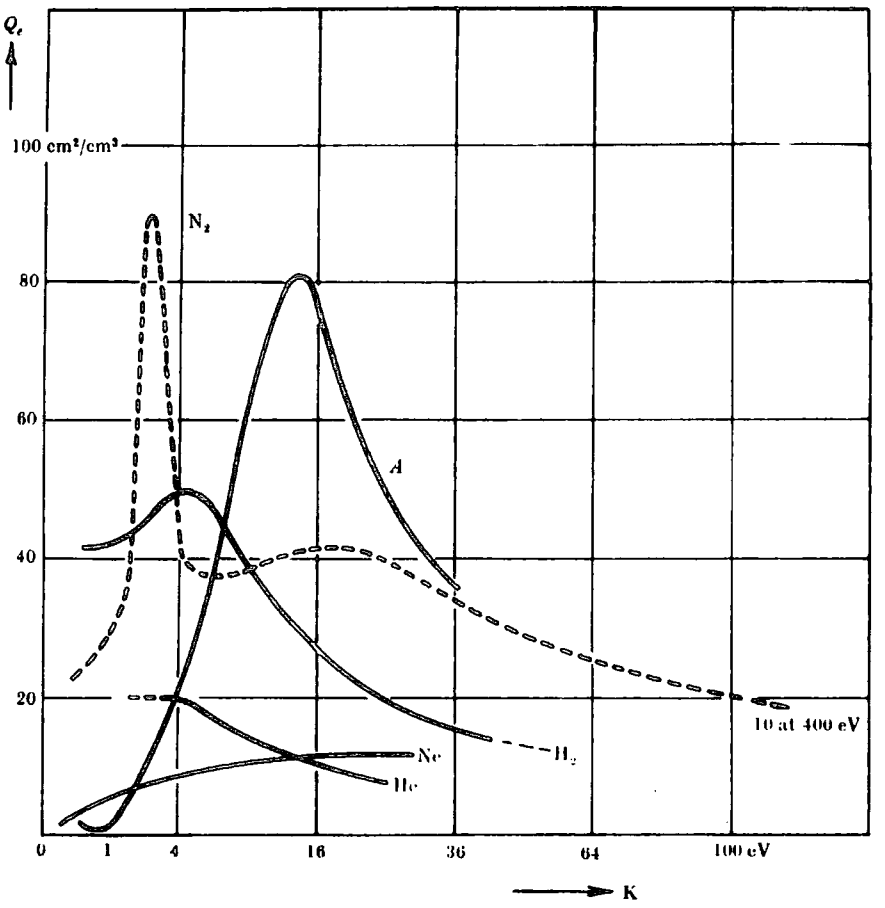

FIG. AI·2 Cross-section Q_e for collisions between electrons and molecules as a function of the electron energy K

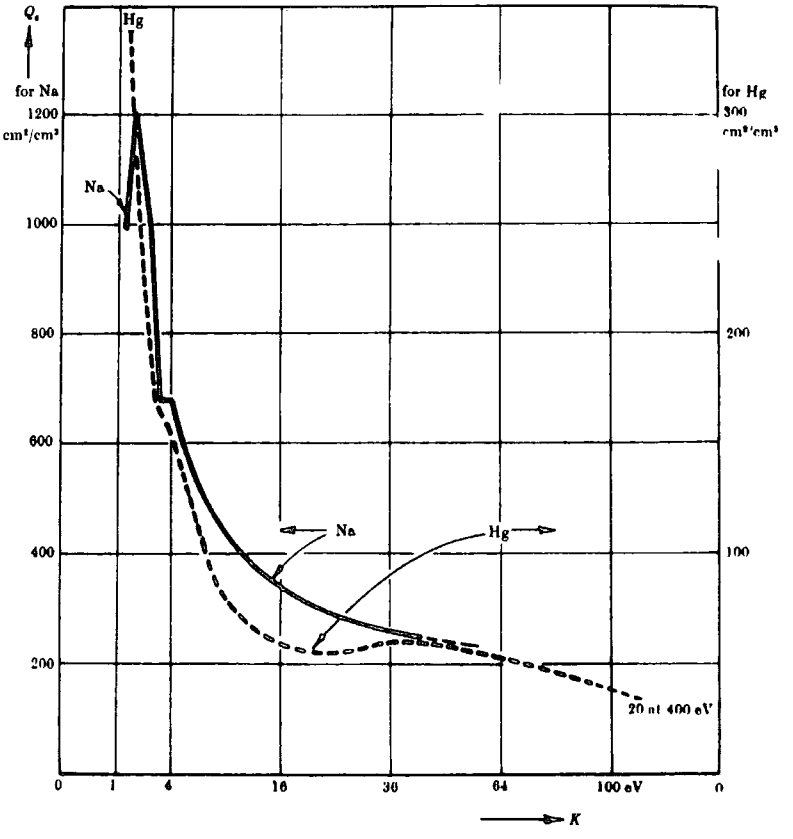

FIG. AI·3 Cross-section Q_e for collisions between electrons and atoms of vapours as a function of the electron energy K. Q_e for Cs about twice that for Na

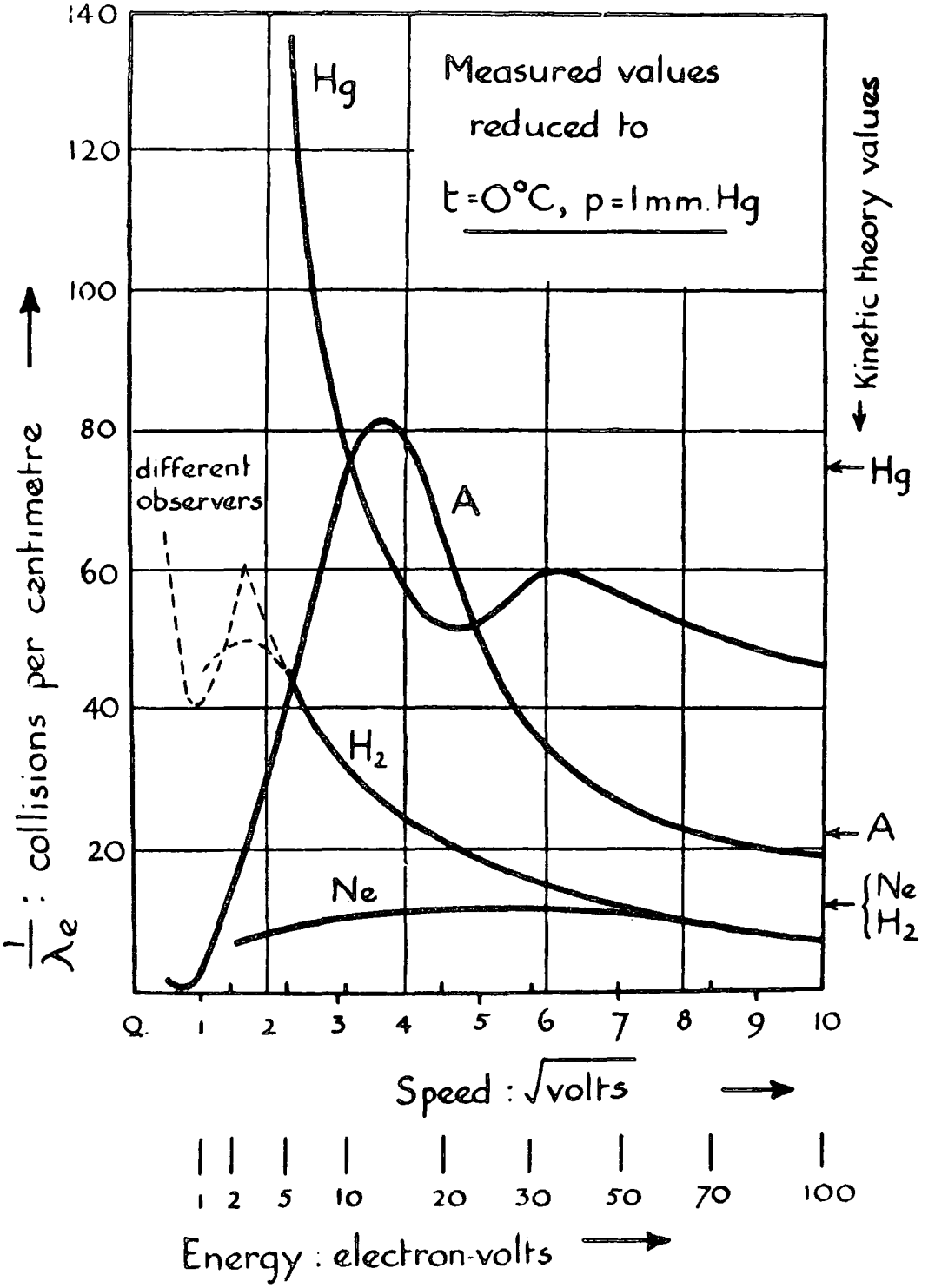

FIG. A I-4 Probability of collision for electrons in a gas, as a function of their speed.

APPENDIX II

Fluctuations

APPENDIX II

Fluctuations

In this appendix fluctuations will be considered in general. It must be stressed that they occur in all elastic systems, and are not due to effects such as unequal heating or non-uniform external pressures. They occur in all systems in thermal equilibrium and originate from certain aspects of the statistical theory.

When one talks about a gas being in thermal equilibrium (in the absence of electric fields) one talks about the density being uniform at all points; "on the average". However instantaneously this is not so. Obviously the density can fluctuate over a wide range if one concentrates on small volumes, in disordered systems.

One can very simply calculate the probability of finding a certain density near a given point in any fluid by fixing attention on a given number of molecules and calculating what volume they occupy.

Consider a fixed point x and n molecules which at any instant in time are to be found nearest to it, and assume that on the average they occupy a volume V_o such that V_o/n is equal to the mean number density averaged over the whole volume. But at any instant in time they may occupy a volume V greater or less than the volume V_o; of course the number density n/V will be less probable than n/V_o. Moreover it does not matter if one of the original molecules diffuses from the vicinity of x and is replaced by another molecule, since according to both classical and quantum theories of physics, molecules are identical to each other and cannot be distinguished from each other, and therefore we are safe in our treatment that V_o is always occupied by the same molecules.

We may then proceed to calculate the difference in the probabilities of these two states by calculating the energy difference between them

and then using the Boltzmann's factor. We first consider a volume V_o of fluid in equilibrium at a certain pressure and alter its volume by either compressing or expanding it.

The elastic moduli are all defined by equations of the type

change of pressure = modulus x fractional change of dimensions

The bulk modulus of a material (the reciprocal of the compressibility) is defined by

$$\text{(isothermal bulk modulus)} = K = -V \left(\frac{dP}{dV} \right)_T \qquad (1)$$

where V is the volume, which is decreased when a pressure P is exerted uniformly in all directions (it is assumed that the temperature is kept constant in compression). If the change of volume is not too great

$$K \cong -V_o \left(\frac{dP}{dV} \right)_T \qquad (2)$$

therefore

$$- \frac{\text{(bulk modulus) (change in volume)}}{V_o} = dP \qquad (3)$$

if volume increases from V_o to V

$$- \frac{K}{V_o} (V - V_o) = dP \qquad (4)$$

It is known that a compressed body can do work if pressure is released, that is a compressed body has potential energy. This energy is given by an equation of the form

(force)(distance) or (pressure)(volume)

the implication is that energy increases as volume decreases. Therefore we could write

$$dE = -dPdV \tag{5}$$

and

$$P = -\frac{dE}{dV} \tag{6}$$

pressure can usually be interpreted as energy density. It must be pointed out that the above relation assumes no heat flow during the compression. But it is also assumed that the thermal effects will be negligible at low temperatures. From the above consideration, we could state that the energy required to increase the volume further by dV is

$$-dE = -dPdV = +K\frac{(V - V_o)}{V_o}\,dV \tag{7}$$

so that the total energy required is

$$\Delta\bar{E} = \frac{K}{V_o}\int_{V_o}^{V}(V-V_o)\,dV = -\frac{K(V-V_o)^2}{2V_o} = \frac{1}{2}Ks^2V_o \tag{8}$$

where $s = (V-V_o)/V_o$ is the fractional change in volume.

The implication of eq (8) is that energy must be increased whenever it deviates from its equilibrium value because the squared term must be positive.

We could now calculate the probability of a volume fluctuation of magnitude s

$$\text{probability of volume fluctuation} = \frac{\text{probability of volume } V}{\text{probability of volume } V_o}$$

$$= \exp\left(\frac{\Delta\bar{E}}{kT}\right) = \exp - \left[\left(\frac{K V_o}{2kT}\right) s^2\right] \qquad (9)$$

Since the energy $\Delta\bar{E}$ is a squared term of exactly the same form of as the $\frac{1}{2} mv_x^2$ term in the kinetic energy of a single molecule, we could conclude that the compressibility of a volume V_o of any substance confers on it one degree of freedom. The theory of classical equipartition of energy states that every degree of freedom (that is every squared term in the energy; i.e., translational, rotational, oscillatory) contributes $\frac{1}{2}kT$ to the mean energy. An assembly of n particles each with f degrees of freedom has a mean energy per particle of $\frac{1}{2}fkT$, a total energy of $\frac{1}{2}fnkT$.

That is to say, if an assembly of molecules each capable of several sorts of motion (oscillation about a lattice point together with rotation about one or more axes for example or translation throughout a volume with one or more modes of internal oscillation of each molecule), then, according to the equipartition of energy theorem, in thermal equilibrium each possible mode of motion will be excited and the amount of energy in each mode is predictable if the temperature is known.

Therefore the mean square root of the fluctuation is given by

$$\frac{1}{2} KV_o s^2 = \frac{1}{2}kT \qquad (10)$$

$$\overline{s^2} = \left(\frac{V_o - V}{V_o}\right)^2 = \frac{kT}{KV_o} \qquad (11)$$

it is clear that if V_o is small the rms value of s is large, and this agrees with our previous statement that the fluctuations are larger the smaller the volume which is being considered.

From this result, we could derive the particular case discussed in the present investigations. From the ideal gas laws.

$$PV = RT \qquad (12)$$

and the relation

$$K = -V\left(\frac{\partial P}{\partial V}\right)_T \qquad (13)$$

$P = K$ (The isothermal bulk modulus is equal to pressure).

Thus

$$S = \frac{kT}{PV_o} \qquad (14)$$

where V_o is the mean value of the volume. Therfore $n/V_o = N/V$ where N_A is the Avogadro's number V is the molar volume at pressure P and temperature T. Hence

$$s = \frac{1}{\sqrt{n}} \qquad (15)$$

(This value of S is the rms fluctuations). This means that n molecules are contained in a volume V_o which fluctuates between the values

$$V_o\left(1 + \frac{1}{\sqrt{n}}\right) \quad \text{and} \quad V_o\left(1 - \frac{1}{\sqrt{n}}\right) \qquad (16)$$

in the sense that these limits define the rms fluctuation. Or alternatively, we can express this conclusion differently by calculating the number of molecules in a fixed volume of V_o.

If this number is n on the average, it fluctuates between probable limits

$$n\left(1 + \frac{1}{\sqrt{n}}\right) \qquad \text{and} \qquad n\left(1 - \frac{1}{\sqrt{n}}\right) \tag{17}$$